ELSEVIER

Catalysis Today 46 (1998) 233–316

CATALYSIS TODAY

Catalytic removal of NO

V.I. Pârvulescu[a,*], P. Grange[b], B. Delmon[b]

[a]*Department of Chemical Technology and Catalysis, Faculty of Chemistry, University of Bucharest, B-dul Republicii 13, Bucharest 70346, Romania*

[b]*Université Catholique de Louvain, Unité de catalyse et chimie des matériaux divisés, Place Croix du Sud 2/17 1348 , Louvain-la-Neuve, Belgium*

Abstract

The aim of this paper is to review the catalytic reactions for the removal of NO and, more particularly, to discuss the reduction of NO in the presence of NH_3, CO, H_2 or hydrocarbons as well as the decomposition of NO. The nature of the different active species, their formation due to dispersion and their interaction with different supports as well as the corresponding correlations with catalytic performance are also discussed. Another goal of this review is to explain the mechanism and kinetics of these reactions on different surfaces as well as the catalyst stability.

Keywords: Removal of NO; Decomposition of NO; Mechanism and kinetics

---

1. Introduction

The reduction of nitrogen oxide emissions has become one of the greatest challenges in environment protection. This is why it is being intensely studied by numerous groups from academic as well as industrial research laboratories. The interest in the subject is reflected in the number of papers, including a large number of reviews and patents, published each year. There is hardly an issue of a journal related to catalysis that does not contain contributions dealing with the elimination of NO.

The nature of the catalyst is another element giving weight to the topic. Virtually all known categories of catalysts have been tested: metal and metal-supported catalysts, monocrystals and mixed phases, oxides and mixed oxides (with either acidic or basic properties), zeolites and heteropolyacids, alloys and amorphous alloys, membrane and monolithic catalysts, etc.

Due to the extraordinary diversity of catalysts, this topic is always discussed at various conferences on catalysis. Each year, at least two conferences are entirely devoted to environmental catalysis, not to mention an additional periodic conference on automotive pollution control.

The use of such a large number of catalysts to eliminate NO is logically associated with different ways of reaction. It is possible to divide these ways into four categories or methods:

1. the selective catalytic reduction of NO with ammonia, typical of chemical industrial plants and stationary power stations;
2. the catalytic reduction of NO in the presence of CO and/or hydrogen, typical of automotive pollution control;

---

[*] Corresponding author.

0920-5861/98/$ – see front matter
PII: S0920-5861(98)00399-X

3. the selective catalytic reduction of NO in the presence of hydrocarbons and more particularly methane, a method which has not yet reached industrial use but can be applied both for automotive pollution control and in various industrial plants;
4. the direct decomposition of NO, which is a goal worth striving for since it eliminates the need for reductants, which in turn eventually eliminates the additional pollution associated with the other three methods.

All these methods have been extensively studied. The goal of this paper is to analyse the interaction of NO with different surfaces in the presence of various reductants or in the direct decomposition of NO. The paper intends to describe the effect of the different active species as well as the effect of their interaction and their dispersion with/on different supports on the catalytic performances of the catalysts. Explaining the mechanism and kinetics through which these reactions take place on different surfaces as well as the catalyst stability is another goal of this review.

2. NO pollution

NO is a major atmospheric pollutant. It has the ability to generate secondary contaminants through its interaction with other primary pollutants (like carbonyl corresponding molecules, alcohol radicals, etc.) also resulting from the combustion of fossil fuels in stationary sources such as industrial boilers, power plants, waste incinerators, and gasifiers, engines, and gas turbines or from the decomposition of a large number of organic products by light or micro-organisms.

$$\text{photochemical air pollution} = \frac{(\mathrm{NO}_x - \text{conc})(\text{organic conc})(\text{sunlight intensity})(\text{temperature})}{(\text{wind spread})(\text{inversion height})}.$$

NO plays a major role in the photochemistry of the troposphere and the stratosphere. It reacts with photochemical pollutants such as ozone, formaldehyde, organic hydroperoxides and peroxyacyl nitrates that all are very reactive and have a very short lifetime. This is a very fast reaction which generates more nitrogen oxides and organic nitrates. The formed NO_2 contributes substantially to so-called acid rains. Among the reactions involving ozone, the one with chlorofluorocarbons is very dangerous since it has a determining effect on the climate. The normal average content of ozone in the atmosphere is about 10^{-10} vol% and its interaction with NO also contributes to its diminution. The chemical depletion of ozone, in an important part due to nitrogen oxide species, is a prolonged phenomenon [2]. Carcinogenic products are also formed during these reactions.

Hydrocarbons in polluted air do not react among themselves under the action of sun radiations, not even to a very small extent, but show a high reactivity towards intermediate species such as peroxides RO_2 [1]. Such species react with the primary pollutants, NO, NO_2, O_3 and HC, according to a partially known mechanism. The photochemical complex $HC–NO_x–O_x$ is formed during the HC interactions in the photolytic cycle of NO; the mixture of products generated is called "photochemical smog" and contains O_3, CO, peroxyacetyl nitrates, alkyl nitrates, ketones, etc.

The photochemical cycle of nitrogen oxides initiates under sunlight (3000–4600 Å). NO_2 is initially decomposed as follows [3]:

$$NO_2 + h\nu\ (> 3.12\,\mathrm{eV}) \rightarrow NO + O \tag{1.1}$$

$$O + O_2 + M \rightarrow O_3 + M\ (\text{third body}) + 24.2\text{kcal} \tag{1.2}$$

$$O_3 + NO \rightarrow NO_2 + O_2 + 48.5\,\text{kcal} \tag{1.3}$$

until a dynamic equilibrium is reached:

$$NO_2 + O_2 \overset{h\nu}{\rightarrow} NO + O_3 \tag{1.4}$$

The overall dependence of photochemical air pollution on various factors may be written as [2]:

In the presence of oxygen, NO is oxidized very quickly to NO_2 which, as mentioned before, is partly responsible for the acid rains and the urban smog. They have very negative effects in agriculture, but may also predispose to respiratory diseases by weakening the ability of the bronchopulmonary structures to function properly [4].

Table 1
Values of the equilibrium constant, K_p, and the dissociation degree, α, corresponding to the thermal decomposition of NO_2 into NO and O_2 and N_2 and O_2, respectively

T (K)	$NO_2 \rightarrow NO + 1/2\ O_2$		$NO_2 \rightarrow 1/2\ N_2 + O_2$	
	K_p	α	K_p	α
298	7.23×10^{-7}	1.69×10^{-3}	9.14×10^{8}	6.3×10^{-8}
400	2.53×10^{-4}	3.15×10^{-2}	3.32×10^{7}	1.7×10^{-8}
500	8.00×10^{-3}	1.70×10^{-1}	4.65×10^{6}	1.2×10^{-7}
600	8.09×10^{-2}	4.87×10^{-1}	1.26×10^{6}	4.6×10^{-7}
700	4.22×10^{-1}	8.77×10^{-1}	4.90×10^{5}	1.2×10^{-6}
800	1.47	9.55×10^{-1}	2.50×10^{5}	2.3×10^{-6}

Table 2
Evolution of the thermodynamic parameters: entropy (S^0), enthalpy (ΔH_f^0), Gibbs free energy of NO (ΔG_f^0), and Gibbs free energy of the NO decomposition

T (K)	NO			NO reaction
	S^0 (cal mol K)	ΔH_f^0 (kcal mol^{-1})	ΔG_f^0 (kcal mol^{-1})	$(\Delta G_f^0)_r$ (kcal mol^{-1})
298	50.35	21.60	20.72	−2×20.72
300	50.40	21.60	20.71	−2×20.71
400	52.45	21.61	20.41	−2×20.41
500	54.06	21.62	20.11	−2×20.11
600	55.41	21.62	19.81	−2×19.81
700	56.57	21.62	19.51	−2×19.51
800	57.61	21.63	19.21	−2×19.21
900	58.54	21.63	18.91	−2×18.91
1000	59.39	21.64	18.60	−2×18.60

2.1. *Thermodynamic stability of nitrogen oxide*

The interconversion of nitrogen oxides is relatively easy. The values of K_p for $p=1$ atm corresponding to the thermal decomposition of NO_2 to NO and NO_2 to N_2 and O_2, respectively, are presented in Table 1.

According to these data, NO_2 is practically 100% decomposed in NO and O_2 above 800 K. It appears that there is no direct thermal decomposition of NO_2 to N_2 and O_2 because of the difference in K_p values.

Even though NO is an endothermic compound, no decomposition is observed at 825 K. The thermodynamic parameters (S^0, ΔH_f^0 and ΔG_f^0) corresponding to NO and the Gibbs free energy of the reaction are given in Table 2:

$$2NO \rightarrow N_2 + O_2 \qquad (1.5)$$

for a relatively broad range of temperatures [5].

From a thermodynamic point of view, as can been seen from Table 2, the NO molecule is unstable even at 298 K and 1 atm. This is due to the electronic structure of the bond in NO. The reaction is spin-forbidden, and NO is kinetically stable. Thus, the high thermal stability of nitric oxide is due to its high energy of dissociation (153.3 kcal mol^{-1}) and to corresponding extremely low decomposition rates.

The reaction is not sensitive to pressure variations (the variation of the stoichiometric number is 0) but reactions such as NO oxidation, its decomposition to N_2O and dimerization are. The evolution of the Gibbs free energy with temperature for the decomposition of NO to N_2O is presented in Table 3.

In the presence of a reductant, reactions lead to a strong decrease in the Gibbs free energy values. This explains that such reactions are used in practical applications. The Gibbs free energy values in the presence of the usual reductants in the catalytic reduction of NO are given in Table 4. The introduction of oxygen here leads to an additional reduction in the free energy. This point will not be discussed.

3. Selective catalytic reduction of nitric oxide with ammonia

General aspects. The catalytic reduction of nitrogen oxides in effluent residual gases from various industries, mainly nitric acid plants, can be carried out selectively using ammonia or urea. This is the so-called selective catalytic reduction (SCR) process. The reactions occur in a narrow temperature range; the main step is the reduction of NO or NO_2 to N_2. Generally, liquid ammonia is injected in the residual

Table 3
Evolution of the Gibbs free energy for the decomposition of NO to N_2O

T (K)	298	300	400	500	600	700	800	900	1000
ΔG_f^0	33.34	33.24	28.46	23.66	18.88	14.10	−9.36	−4.62	+0.12

Table 4
Values of the Gibbs free energy for the reduction of NO in the presence of various reductants

T (K)	$\Delta G^0_{\mathrm{f,r}}$ (kcal mol^{-1})								
	$+H_2$	+CO	$+NH_3$	$+CH_4$	$+C_2H_4$	$+C_2H_6$	$+C_3H_6$	$+C_3H_8$	$+C_4H_{10}$
298	−150.92	−164.34	−87.36	−134.26	−146.21	−144.38	−144.04	−140.59	−136.83
300	−150.66	−164.24	−87.34	−134.22	−146.11	−144.21	−144.01	−140.57	−136.79
400	−147.86	−159.46	−87.62	−132.19	−145.28	−141.58	−143.52	−140.47	−135.11
500	−144.94	−154.62	−87.92	−130.13	−144.28	−139.37	−143.04	−140.39	−133.43
600	−141.94	−149.80	−88.24	−128.06	−143.67	−139.14	−142.57	−140.32	−131.75
700	−138.86	−144.96	−88.56	−125.99	−142.86	−138.81	−142.10	−140.24	−130.06
800	−135.72	−140.14	−88.86	−123.93	−142.04	−138.69	−141.61	−140.15	−128.42
900	−132.54	−135.34	−89.17	−121.89	−141.23	−138.46	−141.13	−140.07	−126.76
1000	−129.28	−130.52	−89.45	−119.85	−140.38	−138.19	−140.62	−139.94	−125.11

gas before the catalytic reaction takes place, using a sophisticated system of distribution.

Bosch and Janssen [6] (and references herein) reviewed the catalysts used in the selective reduction of NO with NH_3 and showed that the most investigated and effective systems are oxides prepared by thermal decomposition of an appropriate precursor or by impregnation of the supports. Other extensively investigated catalysts are supported noble metals and metal zeolites. Recently, Janssen and Meijer [7] showed that more than a thousand catalyst compositions have been tested for application in this reaction up to now. This is the most used technique to control the emission of NO_x.

The main reactions that occur during SCR with ammonia are:

$$4NO + 4NH_3 + O_2 \rightarrow 4N_2 + 6H_2O \tag{2.1}$$

$$6NO + 4NH_3 \rightarrow 5N_2 + 6H_2O \tag{2.2}$$

$$6NO_2 + 8NH_3 \rightarrow 7N_2 + 12H_2O \tag{2.3}$$

$$2NO_2 + 4NH_3 + O_2 \rightarrow 3N_2 + 6H_2O \tag{2.4}$$

Unwanted secondary reactions can take place as a result of the catalyst nature, the oxygen content, the temperature or the presence of acid gases:

$$4NH_3 + 3O_2 \rightarrow 2N_2 + 6H_2O \tag{2.5}$$

$$4NH_3 + 5O_2 \rightarrow 4NO + 6H_2O \tag{2.6}$$

$$4NH_3 + 7O_2 \rightarrow 4NO_2 + 6H_2O \tag{2.7}$$

$$4NH_3 + 2O_2 \rightarrow N_2O + 3H_2O \tag{2.8}$$

$$2NH_3 + 8NO \rightarrow 5N_2O + 3H_2O \tag{2.9}$$

$$6NH_3 + 8NO_2 + 3O_2 \rightarrow 4N_2O + 6H_2O \tag{2.10}$$

$$4NH_3 + 4NO + 3O_2 \rightarrow 4N_2O + 6H_2O \tag{2.11}$$

$$16NH_3 + 12NO_2 + 7O_2 \rightarrow 4N_2O + 24H_2O \tag{2.12}$$

The presence of SO_2, CO_2 or HCl determines a consumption of NH_3 according to:

$$2SO_2 + O_2 \rightarrow 2SO_3 \tag{2.13}$$

$$NH_3 + SO_3 + H_2O \rightarrow NH_4HSO_4 \tag{2.14}$$

$$2NH_3 + SO_3 + H_2O \rightarrow (NH_4)_2SO_4 \tag{2.15}$$

$$2NH_4HSO_4 \rightarrow (NH_4)_2SO_4 + H_2SO_4 \tag{2.16}$$

$$NH_4HSO_4 + NH_3 \rightarrow (NH_4)_2SO_4 \tag{2.17}$$

$$NH_3 + HCl \rightarrow NH_4Cl \tag{2.18}$$

$$2NH_3 + CO_2 + O_2 \rightarrow (NH_4)_2CO_3 \tag{2.19}$$

The resulting products have corrosive properties and can therefore destroy the equipment.

In the absence of catalysts, the reduction of NO_x occurs with satisfactory conversion rates at temperatures in the range 1075–1175 K while the oxidation of NH_3 to NO_x (reactions (2.6)–(2.7)) takes place at temperatures above 1200 K (1325–1475 K) and the reduction rate decreases abruptly. The reaction rate is very low at temperatures below 1075–1175 K. In the presence of catalysts, the temperature of the reaction depends on the catalyst nature and can be in the 355–425 K range for the more active systems.

In the process, it is vital to ensure a NH_3 to NO_x ratio close to that required by stoichiometry (according to reaction (2.1)) [8]. An oxygen excess reduces the catalyst selectivity to N_2 and favours the formation of N_2O (reactions (2.9)–(2.12)) or even the oxidation of ammonia to NO or NO_2. However, no matter what the catalyst nature, the presence of oxygen is a very important factor and several authors stressed the fact that an increase in O_2 pressure enhances the reaction rate [6]. Thermodynamical analyses indicate that secondary products cannot be totally excluded. The degree of NO_x reduction as well as the amount of residual NH_3 in the effluent gases after the SCR could be controlled through an optimal NH_3-to-NO ratio. This also depends on the volume of the catalyst. Generally, the NH_3-to-NO ratio is about 40 mg NH_3 for 1 Nm^3 NO_x and corresponds to 1 vpm residual NH_3. Good results for the reduction of NO with ammonia could be obtained with higher residence times (i.e. a high volume of catalyst), a condition under which the residual NH_3 content is low, or with smaller residence times (i.e. a small volume of catalyst), but with a high residual NH_3 content (that can even reach 8 vol%). A high volume of catalyst implies higher pressure drops and therefore a high energy consumption. The use of monolith-integrated active components is often reported to avoid pressure falls for this reaction [9].

The SCR of NO with NH_3 can also be performed in multilayer reactors, using two or three layers of catalyst. In this case a significant reduction of NO occurs on the first layer and is favoured by a high NH_3 content. The residual NH_3 is then reduced on the second or third layer of the catalyst, where the NO_x reduction is negligible [1]. However, an optimal profile of the reactant distribution is very difficult to achieve even when using the NH_3 pulse technique, because the residual NH_3 increases in the zones in which the NO_x content is low. To have a simultaneous increase in NO_x reduction and a low NH_3 content in the effluent gases, some engineering systems like injecting NH_3 between the catalysts' layers, the use of a dynamic regime in compartment vibration chambers or the use of a periodic inversion of the direction of feed flow have also been considered [10,11–13]. The last method can achieve conversions above 99%.

A new approach is the use of non-permselective porous membranes [14]. It allows for a high conversion in the SCR of NO_x with ammonia, under fluctuating NO_x flow, and ensures a very low NH_3 content in the effluent gases. NH_3 and NO effluent gases are separated by a porous wall which contains the catalytically active materials. The diffusion occurs as a result of the concentration gradient between the two gases.

In the remainder of this section we will examine the main categories of catalysts used in this reaction, considering the influence of different additives as well as the nature of the support.

3.1. Base oxide catalysts

Bosch and Janssen [6] inventoried the base oxide catalysts active for the selective reduction of NO_x with ammonia: V_2O_5, Fe_2O_3, CuO, Cr_2O_3, Co_3O_4, NiO, CeO_2, La_2O_3, Pr_6O_{11}, Nd_2O_3, Gd_2O_3, Yb_2O_3. Catalytic tests performed with these oxides indicated vanadia oxide to be the most active and selective catalyst.

The deposition of vanadia as well as other oxides on supports leads to an increase in the catalytic activity. The nature of the support is also a very important factor [15]. Bauerle et al. [16] reported a very good activity for V_2O_5 supported on TiO_2 and Al_2O_3. Shikada et al. [17,18] were among the first to investigate more systematically the effect of the support, evidencing the promotional effect of TiO_2. They reported that the order of activity for supported vanadia is TiO_2–SiO_2>γ-Al_2O_3>SiO_2. At the same time, Pearson et al. [19] revealed that the anatase form is more active than the rutile-based catalyst.

A first explanation for the superior activity of titania-supported vanadia was given by Murakami et al. [20] who studied different supports: TiO_2, ZrO_2, SiO_2 and MgO, and suggested that this activity could be associated with a crystallographic concordance between the structures of the two components. In addition, Wachs et al. [21] conducted studies using ^{18}O. They indicated that the stability of the terminal V=O during the SCR reaction suggests that the bridging V–O support is involved in the rate-determining step. Other studies by Bond and Bruckman [22] and Wachs et al. [23] revealed that the optimal activity was achieved when approximately one monolayer of vanadia was dispersed on the anatase surface. Much attention has been given to vanadia–titania catalysts in recent years, because of their effectiveness in selectively reducing NO in the presence of ammonia. The conversion of NO and NH_3 on vanadia–titania catalysts with different vanadia contents is presented in Fig. 1.

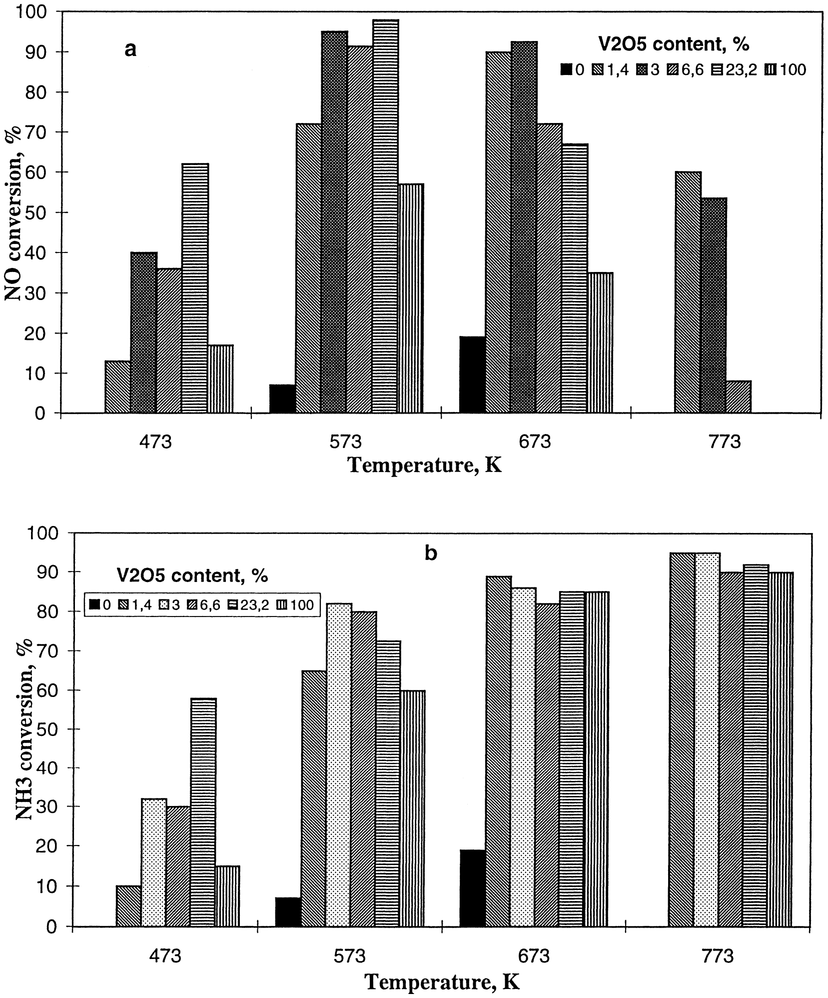

Fig. 1. NO (a) and NH_3 (b) conversion on vanadia–titania catalysts with different content of vanadia (50 mg catalyst; NH_3-to-NO ratio=1.38; O_2=3500 ppm).

Different techniques were used to characterize the structure of highly dispersed VO_x species on the anatase surface. Based on IR spectroscopy measurements, Busca et al. [24,25] showed that mainly monomeric vanadyl species are formed at low V_2O_5 concentration on the anatase surface. The presence of vanadyl species was confirmed by Bell et al. [26] and Wachs et al. [27], using Raman spectroscopy. If the vanadia loading increases, the monomeric species predominant at low vanadia loading react to form polymeric vanadates [28]. When the amount of V_2O_5 exceeds that corresponding to a full coverage of the TiO_2 support, V_2O_5 crystallites are formed [29]. After reduction with hydrogen, Raman spectroscopy reveals that part of the oxygen atoms from terminal V=O groups associated with monomeric and polymeric species are preferentially removed to make V–O–V bridging oxygens. Structural forms of vanadia-supported titania catalysts are presented in Scheme 1.

^{51}V NMR studies performed by Eckert and Wachs [30] offered additional information. They indicated the presence of monomeric species containing a fourfold coordinated vanadium with a symmetry greater than twofold. An increase of the vanadia loading leads to an increase in the vanadium coordination from fourfold to sixfold.

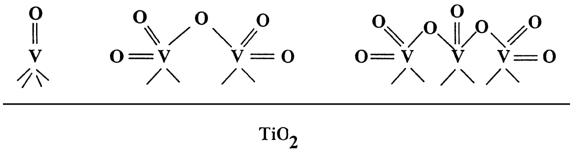

Scheme 1. Structural forms of vanadia-supported titania catalysts.

To improve the performance of this catalyst, different methods of preparation of TiO$_2$ were investigated. Generally, these methods correspond to different techniques for synthesizing the titania supports or to the deposition of precursors of a different chemical nature. Concerning the synthesis of the titania supports, the most investigated techniques involve the hydrolysis of TiCl$_4$ or titanium alkoxides or the precipitation of Ti(SO$_4$)$_2$ [6,31–35]. The sol–gel method was also investigated [36,37–39]. Recently, Ciambelli et al. [40] suggested a CO$_2$ laser pyrolysis of titanium alkoxides, indicating that monocrystalline TiO$_2$ powders with a uniform size could be obtained that way.

Different methods were also used for the deposition of vanadia. At the beginning, the usual method was the impregnation of titania using ammonium metavanadate in the presence of oxalic acid acting as a competitive, or regulative agent [6] or directly with vanadium oxalate, as Grange et al. [34] proposed. Watanabe et al. [41] suggested a sequential precipitation. Later, a selective grafting from non-aqueous solutions was proposed by Delmon et al. [35], Baiker et al. [42,43] and Bond and Tahir [44]. In the past, Baiker et al. [37,38,45] had stressed the performance of catalysts prepared using the sol–gel-solution method and subsequently removal of the solvent by supercritical drying.

SIMS and Raman spectroscopy results [38] showed that vanadia–titania aerogels contain active vanadium clusters in a relatively high degree of dispersion that differentiate them from traditional catalysts in which VO$_x$ clusters coexist with V$_2$O$_5$ crystallites. The SCR activity of these catalysts is very high and comparable to that of multiple grafted vanadia species.

It is now clear that polymeric species are 10 times more active than monomeric species [28,46]. Additional arguments were given by Lietti and Forzatti [47], based on temperature-programmed desorption, temperature-programmed surface reaction of adsorbed ammonia with gas phase NO and temperature-programmed reaction and steady-state reaction experiments in the presence and in the absence of oxygen on a series of V$_2$O$_5$/TiO$_2$ catalysts. These authors reported a higher reactivity of polymeric metavanadate species compared to isolated vanadyls, as well as a faster reduction by NH$_3$ and a faster reoxidation by gaseous oxygen of the polymeric metavanadate groups.

Vanadia/alumina and vanadia/silica were previously thought to have a lower catalytic activity than vanadia/titania. Shikada et al. [17,18] first observed the beneficial effects of adding titania to silica. Grange et al. [34,35,48] reported an improvement in the catalytic activity of vanadia supported on titania grafted on silica or alumina using selective grafting from non-aqueous solutions. Fig. 2 compares the NO conversion on mixed V$_2$O$_5$–TiO$_2$–SiO$_2$ (a) and V$_2$O$_5$–TiO$_2$–Al$_2$O$_3$ (b) with different percentages of TiO$_2$ and V$_2$O$_5$.

Lapina et al. [49–52] used the ^{51}V NMR technique to characterize supported vanadium catalysts. In the case of vanadia supported on titania grafted on silica surfaces [52], they suggested that V$_2$O$_5$ interacted both with SiO$_2$ and TiO$_2$. The structure of the V complexes depended on the sequence of the V and Ti deposition. The formation of several surface tetrahedral and octahedral complexes as well as two types of mixed triple V–Ti–Si complexes on the SiO$_2$ surface was mentioned.

Another way to promote the activity of vanadia–titania catalysts is by adding an other oxide species to vanadium oxide. The positive effect of WO$_3$ was reported by many groups [53–56]. The same effect was also evidenced for vanadia supported on alumina [57] or zirconia-promoted alumina supports [58]. Good results were also reported by Ross et al. [59] for zirconia-supported vanadia catalysts. It was shown that WO$_3$ increases the surface acidity by generating both Brønsted and Lewis sites. This was accompanied by an increased resistance towards deactivation by SO$_2$ or basic compounds like alkali metal or arsenious oxide. The catalytic activity concomitantly increased.

Other oxides like MoO$_3$, CeO$_2$, SnO$_2$ or ZrO$_2$ have a similar effect on V$_2$O$_5$/TiO$_2$ catalysts [60–63]. The corresponding catalysts are called "low temperature conversion catalysts", as the reaction can occur even at 393 K. However, this results in a relatively high

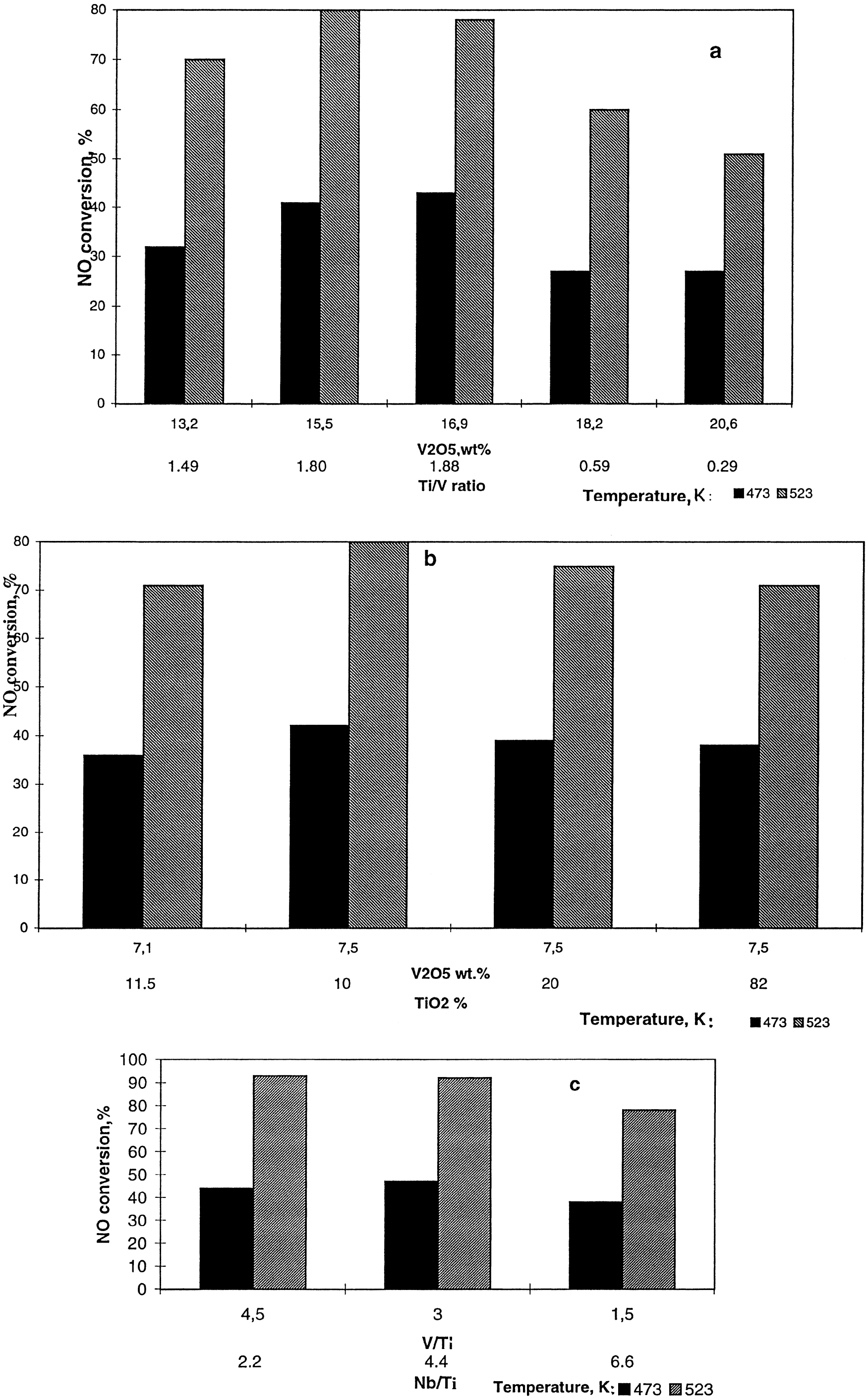

Fig. 2. NO conversion with NH_3 over V_2O_5–TiO_2–SiO_2 (a); V_2O_5–TiO_2–Al_2O_3 (b); V_2O_5–TiO_2–Nb_2O_3 (c) catalysts. (a) V_2O_5–TiO_2–SiO_2: NO=970 ppm; NH_3=12.40 ppm; O_2=3 vol%; 100 mg catalyst; flow rate=50 ml min^{-1}; (b) V_2O_5–TiO_2–Al_2O_3; NO=0.1 vol%; NH_3=0.106 vol%; O_2=3 vol%; 100 mg catalyst; flow rate=50 ml min^{-1}; (c) V_2O_5–TiO_2–Nb_2O_5: NO=0.4 vol%; NH_3=0.42 vol%; O_2=2 vol%; space velocity=58 000 h^{-1}.

NH_3 content in the effluent gases. Nb_2O_5 was reported to be another promising promoter for V_2O_5/TiO_2 catalysts [64,65] (Fig. 2(c)). Vikulov et al. [65] suggested that the promoting effect of niobia might be associated with the stabilization of the surface area of the catalyst. Another opinion is that of Wachs et al. [66] who showed that, in the frame of the general agreement that a dual site mechanism operates, the role of the promoter is to create a non-reducible oxide site adjacent to the surface vanadia site. Such a dual site created by tungsten, niobium or even sulphur generates a 5–10 fold increase in the SCR TOF. FT-IR and laser Raman studies [67] indicate that the promoter generates species similar to those generated by vanadia, i.e. monomeric and polymeric wolframyls and molybdyls, onto the titania surface. The effect of mixed deposition was also reported by Kasaoka et al. [68]. They showed that vanadium oxide supported on either active carbon or active carbon covered with titania is also a very active catalyst.

The presence of vitreous P_2O_5 was reported as another factor that could enhance the catalytic activity of vanadia/titania or V_2O_5–MO_3/TiO_2 catalysts [69]. Some $VOPO_4$ species are also formed in such cases.

Very recently, Wachs et al. [70] reported that titania-supported rhenium catalysts exhibit the same SCR activity as titania-supported vanadium catalysts but with a lower selectivity to N_2. They showed that the reaction on these catalysts requires the same dual site mechanism as vanadia.

Supported chromia catalyst systems are also much investigated in the SCR of NO. Niyama et al. [71,72] studied the behaviour of chromia–alumina catalysts with different compositions and reported good activities for lower chromia concentrations and for pure Cr_2O_3 oxide. The conversions were insignificant for intermediary amounts of deposited chromium. However, the conversions obtained with the active formulations were inferior to those obtained when using vanadia, and important quantities of N_2O were formed during the reaction. Later, Baiker et al. [73,74–82] showed that amorphous chromia exhibited interesting properties for low temperature SCR and selectively reduced NO to N_2. They showed that the selectivity and initial activity of titania-supported chromia catalysts depended markedly on the pretreatment. In a series of reductive pretreatments at temperatures below 720 K an improved selectivity to N_2 was reported at reaction temperatures up to 470 K. N_2 is therefore the major product below 470 K. The decrease in activity at higher temperatures was attributed to a partial crystallization of chromia, while the improved selectivity was attributed to the reduction of Cr(VI) and Cr(V) surface species. In fact, hydroxylated Cr(III) species formed during the reductive pretreatment constitute Brønsted sites, active for ammonia chemisorption. However, SCR tests indicate that a totally reduced surface is inactive and that the surface must be maintained in a partly oxidized state by the presence of oxygen in the feed in order to balance the partial reduction by NH_3. In the absence of oxygen the reaction between NO and NH_3 is much slower, but at higher temperatures (T>500 K) and in the presence of oxygen, the production of N_2O becomes significant [83]. Some oxidation of the ammonia to N_2 occurs in parallel to the SCR of NO. The variation of TOF with the chromia content on Cr_2O_3–TiO_2 is presented in Fig. 3.

Other oxide-supported catalysts were also studied. Experiments carried out by Grange et al. [84,85] indicated that molybdena–titania catalysts obtained by grafting from non-aqueous solutions were selective for the reduction of NO to N_2 with ammonia.

Fe_2O_3–Al_2O_3 catalysts exhibit a behaviour similar to that of chromia–alumina catalysts [71,72,86].

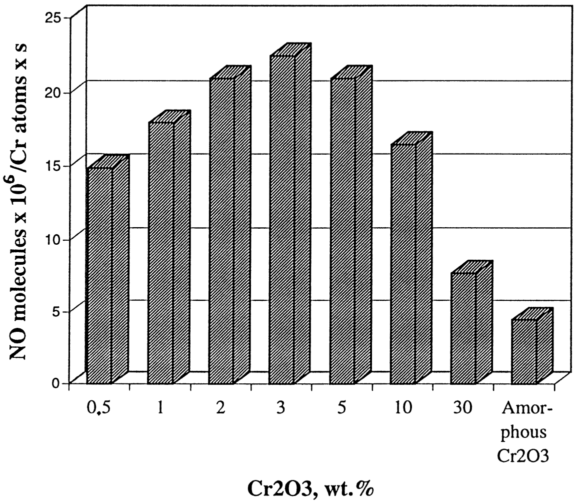

Fig. 3. Variation of TOF with the chromia content on Cr_2O_3–TiO_2 catalysts (NH_3-to-NO ratio=1, O_2=1.8 vol%, 100 mg catalyst, T=450 K).

Bosch and Janssen [6] made an inventory of a large number of catalysts, Fe_2O_3/TiO_2, $Fe_2O_3–WO_3/TiO_2$, $Fe_2O_3/TiO_2–ZrO_2$ (or SiO_2), and indicated that these catalysts were active in the 470–770 K range. Gryzbek and Papp [87,88] reported that carbon is also an effective support for iron oxides. In addition, these authors showed that low iron contents supported on active carbon are very active in the reduction of NO with ammonia at low temperatures. In that case, a good distribution of Fe^{3+} is only achieved after a controlled oxidation of the support surface.

Copper compounds are also effective catalysts in SCR with ammonia. Bosch and Janssen [6] reported the activity of copper oxide supported on titania, alumina and substituted alumina. However, many studies used $CuSO_4$ because copper oxide is transformed in copper sulphate in the presence of SO_2 and oxygen. Other studies by Nozaki et al. [89] or Moulijn et al. [90] stressed the fact that good conversions were obtained with copper oxide dispersed on a carbon support. Recently, Kiel et al. [91] investigated a series of $CuO/CuSO_4$ catalysts supported on silica, alumina and bauxite, and compared them with vanadia supported on titania or alumina. Experimental data clearly showed that the activity of all these catalysts was low compared with that of vanadia supported on titania.

Other investigated support-metal oxides are SnO_2, NiO, WO_3, Co_3O_4 [6,92]. Moulijn et al. [93] wrote a paper on the SCR of nitric oxide on alumina-supported manganese oxides. They showed that it is possible to achieve a high selectivity towards the formation of nitrogen, in addition to a good and stable activity, by properly choosing the loading or by adding tungsten. The SCR activity is strongly dependent on the oxygen partial pressure, whereas water inhibits it reversibly. The reaction stops in the absence of oxygen. Earlier, Wu and Chang also discussed the use of deep-sea manganese nodules in the reduction of NO with ammonia [94].

3.1.1. Stability

Vanadia–titania catalysts exhibit a very good stability over time, and are thus recommended for technical applications.

Water was found to adsorb more weakly than ammonia on the surface of vanadia–titania catalysts and does not inhibit the adsorption of ammonia on the vanadia surface [95,96]. Furthermore, water hydroxylates the surface, leading to an increase in Brønsted acid sites density, which interact with ammonia. An inhibition of the catalytic activity was observed only at temperatures below 663 K. In these conditions some authors reported a slight decrease [97] while others reported an approximately 40–50% decrease in the TOF [66]. However, an increase in the selectivity to N_2 was observed.

The beneficial effects of the supports and of the promoter in the presence of SO_2 have been demonstrated by Grange et al. [34,48] and Busca et al. [98,99] for the most active system, namely the vanadia–titania catalysts. It was also shown that the presence of SO_2 in the gas phase during SCR resulted in a significant increase of the TOF at low surface vanadyl coverages but had no effect when surface vanadia coverages exceeded half a monolayer [23]. At the increased vanadia coverages the adsorption of SO_2 is competitive with the adsorption of NH_3 on Lewis acid sites. The adsorption of SO_2 over $V_2O_5–WO_3–TiO_2$ catalysts at room temperature is fast and irreversible. The adsorption occurs over Lewis acid sites, leading to O-bonded molecular adsorbed species. Only at higher temperatures (450–600 K) does SO_2 react with surface oxide ions in a slow process, producing sulphite–sulphate species. In the presence of oxygen, only sulphate species that are stable on the surface up to about 600 K are formed, while SO_3 can be desorbed at higher temperatures. Therefore, under normal working conditions, the catalysts are expected to be partly sulphated and also to be active in the SO_2 to SO_3 catalytic conversion.

Hums and Spitznagel [100] showed that $TiO_2–V_2O_5–MoO_3$ catalysts obtained via a preformed V–Mo oxide phase exhibited an important increase in the resistance both to arsenic oxide deposition and to the SO_2/SO_3 conversion process. Interaction of arsenic oxides with conventional $TiO_2–V_2O_5–MoO_3$ generates different composite oxides ($As_xMo_yO_z$) and also $VO(AsO_3)_2$ after all the molybdenum species are consumed. The use of $V_9Mo_6O_{40}$ as precursor, at least in a first stage, suppressed these reactions. In addition the capacity to adsorb arsenic species was far higher for the same vanadium and molybdenum content. This behaviour could be attributed partly to a modification of surface tension in the presence of new species and partly to a different dispersion of the active species.

However, long exposure to the arsenic content emissions also leads to an important decrease in the activity [101,102]. Several attempts were made to elucidate the role of arsenic acid in the deactivation process. It was shown [103,104] that arsenate species are anchored in the vicinity of the non-reducible surface oxide site (W or Mo), suppressing the formation of Lewis acid sites where the adsorption of ammonia takes place.

The presence of oxide basic anions inhibits catalytic activity because these anions act as ligands for the vanadyl complexes [46]; the Lewis acidity is then strongly reduced. Experimental data indicated that alkali poisons adsorbed preferably by Lewis acid sites associated with vanadium rather than with Ti^{4+} ions. The concomitant reduction of NO suggests that these species are the active sites.

The activity of catalysts containing amorphous chromia indicated a time-dependent deactivation [72–82]. This behaviour was attributed to morphological changes in the structure of amorphous chromia.

3.1.2. Mechanism and kinetics

The above described catalysts exhibit a quite complex catalytic surface: both redox and acid–base sites coexist and it is difficult to assign the interaction of the reactants with the active sites to one group or to another. SCR of NO in the presence of NH_3 has been claimed to proceed according both to Langmuir–Hinshelwood and Eley–Rideal type mechanisms, irrespective of their chemical composition. Two systems elicited more interest, and our analysis shall focus on these: vanadia and chromia containing catalysts, respectively.

3.1.2.1. Vanadia containing catalysts

3.1.2.1.1. Eley–Rideal assumption mechanism

In unsupported vanadia, Murakami et al [105] suggested that ammonia was quickly adsorbed on Brønsted sites and reacted with NO according to an Eley–Rideal mechanism (Scheme 2). The regeneration of the active sites would occur in the presence of oxygen.

They showed that the differences in the equation rate of the NO–NH_3 reaction in the presence or in the absence of O_2 resulted not from the frequency factor but from the activation energy:

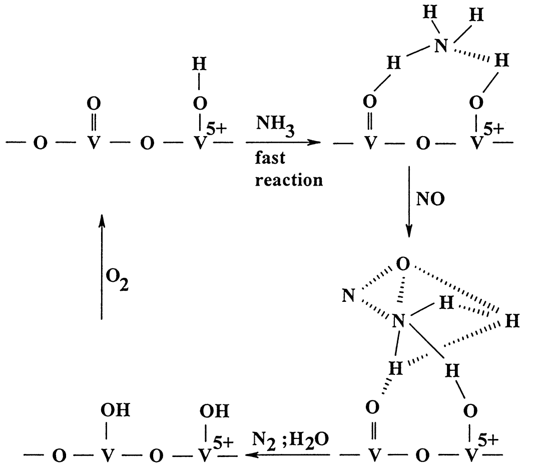

Scheme 2. Eley–Rideal mechanism for reduction of NO with NH_3.

$$r = 23.8\exp(-11600/RT)C_{\mathrm{NO}}C^{0}_{\mathrm{NH_3}}$$

in the presence of O_2

and

$$r = 32.4\exp(-16600/RT)C_{\mathrm{NO}}C^{0}_{\mathrm{NH_3}}$$

in the absence of O_2.

Concerning the SCR of NO on vanadia–titania catalysts, Bosch and Janssen [6] (and references herein) reviewed the proposed mechanisms, and based on experiments using the stable ^{15}N isotope, suggested that the reduction of NO to N_2 also occurred according to an Eley–Rideal type mechanism:

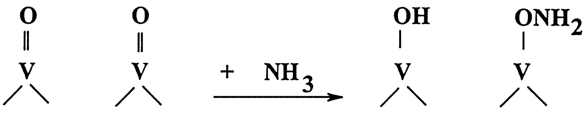

(2.20)

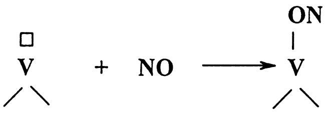

(2.21)

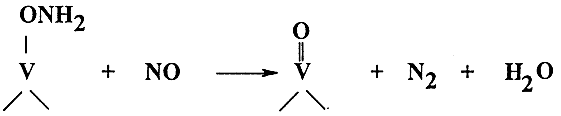

(2.22)

whereas the production of N_2O proceeded via a dual site mechanism:

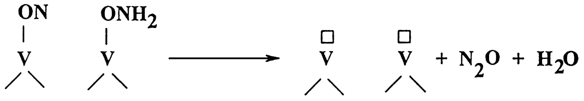

(2.23)

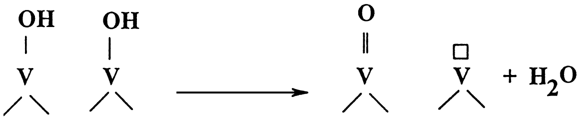

(2.24)

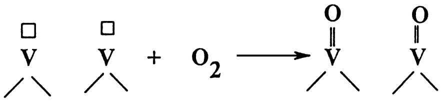

(2.25)

where □ represents the reduced surface site.

The adsorption of NH_3 as NH_4^+-like species on Brønsted acid sites and as NH_x-like species (x=1–3) on Lewis acid sites is now very well demonstrated [106–110]. Studies carried out later, using very sophisticated techniques, indicated that the interaction of the reactants with the catalytic active sites could occur according to almost all possible structures. The high dispersion of vanadia and its cluster structure favours these multiple interactions.

Odriozola et al. [111,112], based on investigations using different techniques such as thermal desorption spectroscopy, Auger electron spectroscopy, electron spin resonance or XPS, suggested that the production of N_2 also occurred according to an Eley–Rideal type mechanism but following other routes:

$$V_2O_5 + x/2\,NH_3 \rightarrow V_2O_{5-x} + x/4\,N_2O + 3x/4\,H_2O \tag{2.26}$$

$$V_2O_{5-x} + xN_2O \rightarrow V_2O_5 + xN_2 \tag{2.27}$$

$$V_2O_{5-x} + NO \rightarrow V_2O_5 + x/2\,N_2 \tag{2.28}$$

The NO adsorption occurs only on reduced sites. In the presence of oxygen a competitive reaction was suggested:

$$V_2O_{5-x} + x/2\,O_2 \rightarrow V_2O_5 \tag{2.29}$$

In addition, to explain the presence of strongly adsorbed ammonia species, the authors considered that NH_3 molecules could dissociate on the surface of the reduced V_2O_5 samples

$$V_2O_{5-x} + xNH_3 \rightarrow V_2O_{(5-3x/2)}(NH_2)_x + x/2\,H_2O \tag{2.30}$$

In the presence of oxygen the original V_2O_5 surface would be restored according to

$$V_2O_{(5-3x/2)}(NH_2)_x + xO_2 \rightarrow V_2O_{5-x} + x/2\,N_2O + H_2O \tag{2.31}$$

At the same time, at high temperatures, the titania support also contributes to further oxidation of ammonia

$$TiO_2 + xNH_3 \rightarrow x/2\,N_2O + 3x/2\,H_2O + TiO_{2-2x} \tag{2.32}$$

Later, numerous studies using labelling by stable isotopes such as ^{15}N or ^{18}O [113,114] or positron-emitting ^{13}NO molecules [115] were carried out. The latter technique allows to perform kinetic studies at very low pressures of the reactants (more than 11 orders of magnitude lower than usual). This technique brought out additional arguments to establish a real mechanism. So, based on this kind of experimental data, Duffi et al. [113] suggested that steps 1, 5 and 6 proposed by Bosch and Janssen [6] were correct, but proposed two different routes for the formation of N_2 and N_2O:

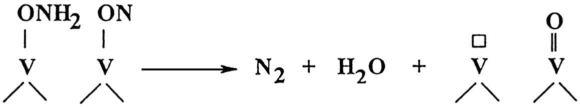

(2.33)

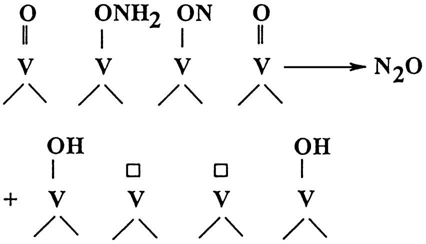

(2.34)

To explain the higher formation rate of N_2O at high temperatures or on catalysts with a high V_2O_5 content, they suggested that the catalysts having a larger number of V=O groups favoured the dissociation of NH_2 to NH in a process similar to (2.20), followed by a reaction between NH and NO:

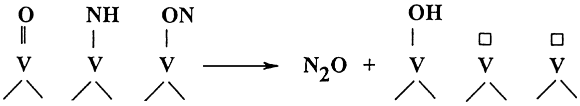

(2.35)

The decrease of N_2O in the presence of water was explained by a shift to the left of the reaction equilibrium (2.24). Consequently, a decrease in the number of V=O groups and of vacancies on the surface occurs and the dissociation of NH_3 is delayed. A similar proposal was also made by Odenbrand et al. [95] for step (2.24). In addition, these authors considered that the oxidation of N_2O to NO could also explain the decrease in the NO conversion at temperatures above 673 K.

Based on the same isotopic labelling studies and TPR/TPD data, Ozkan et al. [114,116] suggested that, in the first step, NH_3 interacted with different Lewis acid sites forming different species:

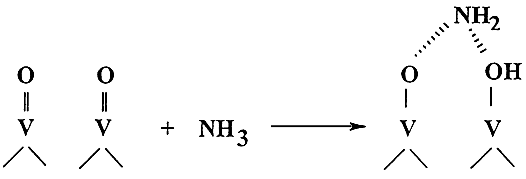

(2.36)

and respectively

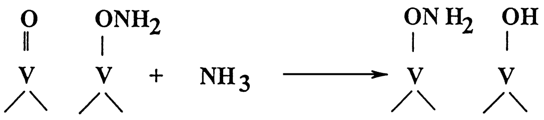

(2.37)

or with Brønsted acid sites, forming NH_4 species

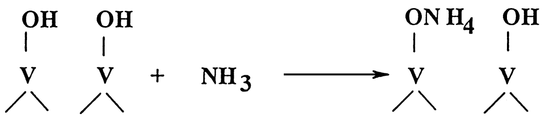

(2.38)

The interaction of NO also occurs as an Eley–Rideal mechanism, but with the generation of different products depending on the nature of the adsorbed species:

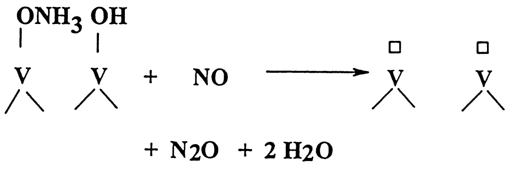

(2.39)

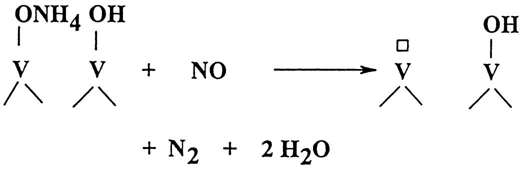

(2.40)

In addition, N_2 and N_2O could result from the oxidation of –ONH_3 and –ONH_4 adsorbed species:

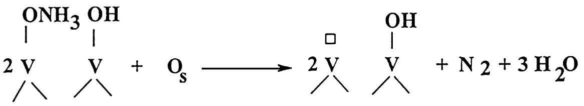

(2.41)

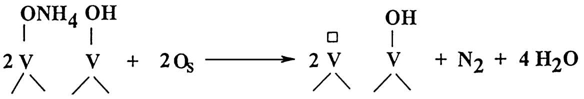

(2.42)

Recent studies by Baiker et al. [117], based on an in situ diffuse reflectance FT-IR study and transient experiments, confirmed that vanadia Brønsted sites are very much involved in the SCR of NO with ammonia, and that NO is not kept in significant concentration on the surface of the catalysts. These findings are additional arguments in favour of an Eley–Rideal type mechanism.

3.1.2.1.2. Langmuir–Hinshelwood assumption mechanism

Other authors suggested a Langmuir–Hinshelwood mechanism for this reaction. Tamaru et al. [118–120] first suggested that NO is oxidized by the ambient O_2 and is then adsorbed as NO_2:

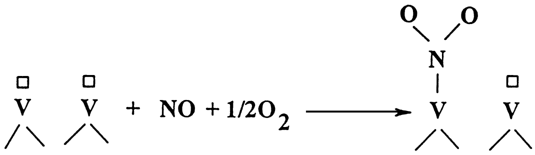

(2.43)

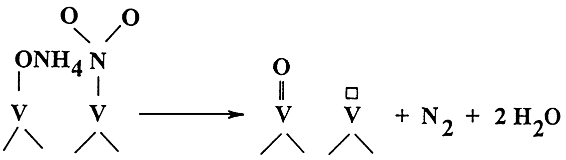

(2.44)

and the Brønsted sites are regenerated in the presence of water:

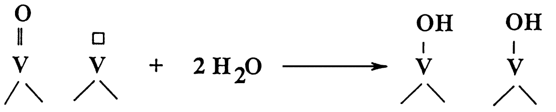

$$\overset{\overset{O}{\|}}{V}\;\overset{\square}{V} + 2\,H_2O \longrightarrow \overset{OH}{V}\;\overset{OH}{V} \quad (2.45)$$

A Langmuir–Hinshelwood mechanism was also proposed by Bell et al. [26,27,28] who neglected to name the superficial sites involved in the SCR:

$$M + NH_3 \rightarrow M{-}NH_3 \quad (2.46)$$

$$M + NO \rightarrow M{-}NO \quad (2.47)$$

$$NH_3 + V_mO_{2.5m} \rightarrow N_2 + H_2O + V_mO_{(2.5-x/2)} \quad (2.48)$$

$$M{-}NH_2 + M{-}NO \rightarrow N_2 + H_2O + 2M \quad (2.49)$$

$$M{-}NH_2 + M{-}NO + V_mO_{2.5m} \rightarrow N_2O + H_2O + V_mO_{(2.5m-1)} + 2M \quad (2.50)$$

$$M{-}NO + V_mO_{(2.5-1)} \rightarrow M{-}N + V_mO_{2.5m} \quad (2.51)$$

$$1/2\,O_2 + V_mO_{(2.5m-1)} \rightarrow V_mO_{2.5m} \quad (2.52)$$

3.1.2.1.3. Dual Eley–Rideal Langmuir–Hinshelwood assumption mechanism

Topsoe et al. [96,108,109,121–124], based on temperature-programmed desorption/reaction and in situ spectroscopic studies, suggested that both mechanisms are possible but that NO more likely reacts as a weakly adsorbed species. They considered that vanadia–titania catalysts exhibit two separate catalytic functions, i.e. acid and redox functions. Scheme 3 exemplifies the last version they proposed for the catalytic cycle [125]. Turco et al. [126,127] also agree with this scheme.

Kinetic equations suggested for this reaction account for the different types of reaction mechanism (Langmuir–Hinshelwood or Eley–Rideal) and for the numerous equilibria even though not all discussed equilibria (about 32) were considered. This means that evidently not all the proposed equilibria are important in this mechanism. For the SCR, considering only an Eley–Rideal mechanism, Prins and Nuninga [128] proposed the following expression for the reaction rate:

$$r = \frac{kk_{20}\cdot k_{-20}^{-1}\cdot p_{NH_3}\cdot p_{NO}}{k_{20}\cdot k_{-20}^{-1}\cdot k_{22,39,40}\cdot k_d^{-1}\cdot p_{NH_3}\cdot p_{NO} + k_{20}\cdot k_{-20}^{-1}(1+k\cdot k_d^{-1})\cdot p_{NH_3} + k\cdot k_{-20}^{-1}\cdot p_{NO} + (1+k\cdot k_d^{-1})}, \quad (2.53)$$

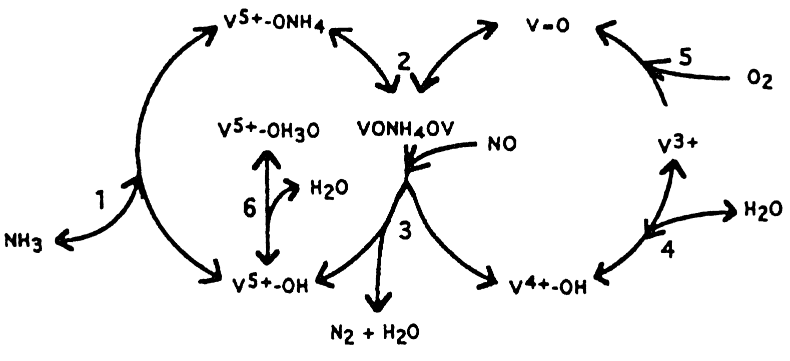

Acid-Base Interaction **Redox Interaction**

Scheme 3. An integrated mechanism for reduction of NO with NH_3 [125].

where k_i is the constant associated with step i; and k_d is the constant of desorption.

If the reaction rate is not fast, compared to the adsorption and the desorption, the expression becomes

$$r = \frac{k \cdot k_1 \cdot k_{-1}^{-1} \cdot p_{NH_3} \cdot p_{NO}}{k \cdot k_1^{-1} \cdot p_{NH_3} + 1}. \tag{2.54}$$

However, the fact that the partial pressures of NO and NH_3 appear at the denominator indicates that these species are relatively strongly chemisorbed.

This expression agrees with the expression previously proposed by Bosch and Janssen [6], but differs from the expression proposed by Dumesic et al. [129], who in addition considered the contribution of a Langmuir–Hinshelwood type mechanism:

$$r = k \cdot p_{NO} \frac{k \cdot p_{NH_3} \cdot p_{NO}^{-1}}{1 + k \cdot p_{NH_3} \cdot p_{NO}^{-1} + k_2 \cdot p_{NO}^{-1} + K_{NH_3} \cdot P_{NH_3}}, \tag{2.55}$$

where $k_1 = k^* k_{NH_3}/k^*, k^*, k^*$ and $k_2 = k^*_{-2}/k_3$ are the constants of step i from Scheme 3. K_{NH_3} is the equilibrium constant of step 1 from the same scheme.

These authors [124] recently refined this equation, giving an expression that describes the kinetics of the SCR under a wide range of reaction conditions. According to the above scheme the catalytic cycle involves an acid site (V^{5+}–OH), the activation of adsorbed ammonia by the interaction with redox sites (V=O), the reaction of activated ammonia with gaseous or weakly adsorbed NO and the recombination of surface hydroxyl groups:

$$r = \frac{\alpha^2}{\beta}[\gamma - (\gamma^2 + \beta S/a)^{1/2}]^2, \tag{2.56}$$

where

$$\alpha = \frac{k_2 k_3 p_{NO} K_1 p_{NH_3}}{(k_{-2} + k_3 p_{NO})(1 + K_6 p_{H_2O} + K_1 p_{NH_3} + k_2 k_1 p_{NH_3})}, \tag{2.57}$$

where k_i and K_i are the constants of step i in Scheme 3.

$$\beta = 16 k_4 k_5 p_{O_2}, \tag{2.58}$$

$$\gamma = (2 k_5 p_{O_2})^{1/2} + (k_4)^{1/2} \tag{2.59}$$

and S is the ratio of V=O to V^{5+}–OH sites on the fully oxidized surface.

Using the same model of reaction as Topsøe, Turco et al. [115] reported an inhibiting effect of water on the reaction rate.

All these models are valid if one supposes that the number of active sites is constant. However, there is a modification of the number of these sites during the reaction, and in the presence of inhibitors like SO_2 or H_2O, this process is accentuated. On the other hand, it is still not clear in which proportion different active sites account for a redox behaviour or for an acid–base interaction. For species such as vanadia as well as molybdenum or tungsten oxides, the barrier between these states is very fragile.

3.1.2.2. Chromia containing catalysts. The low catalytic performances of chromia compared to vanadia led to a decreased interest in this system. However, some similarities have been evidenced by research that followed a similar path.

Using isotope labelling on crystalline chromia, Niyama et al. [72] proposed a Langmuir–Hinshelwood type mechanism in which the role of the active sites could be described by the following steps:

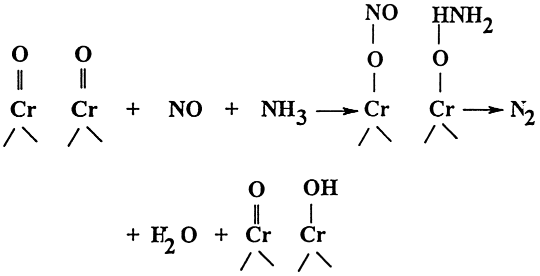

(2.60)

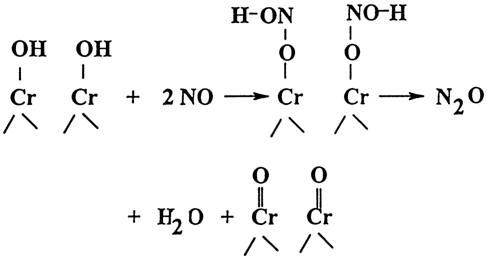

(2.61)

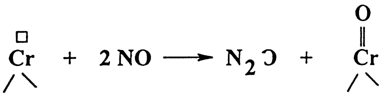

(2.62)

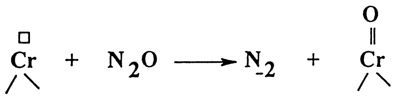

$$\overset{\square}{\underset{/\backslash}{\mathrm{Cr}}} + N_2O \longrightarrow N_2 + \overset{\overset{O}{\|}}{\underset{/\backslash}{\mathrm{Cr}}} \qquad (2.63)$$

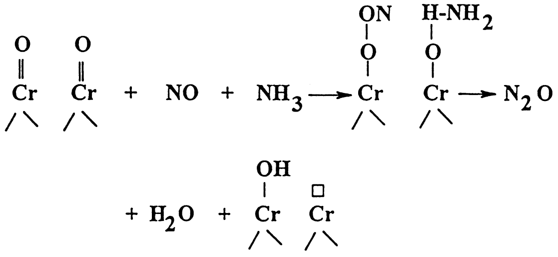

$$\overset{\overset{O}{\|}}{\underset{/\backslash}{\mathrm{Cr}}}\ \overset{\overset{O}{\|}}{\underset{/\backslash}{\mathrm{Cr}}} + NO + NH_3 \longrightarrow \overset{\overset{ON}{|}}{\overset{\overset{O}{|}}{\underset{/\backslash}{\mathrm{Cr}}}}\ \overset{\overset{H\text{-}NH_2}{|}}{\overset{\overset{O}{|}}{\underset{/\backslash}{\mathrm{Cr}}}} \longrightarrow N_2O + H_2O + \overset{\overset{OH}{|}}{\underset{/\backslash}{\mathrm{Cr}}}\ \overset{\square}{\underset{/\backslash}{\mathrm{Cr}}} \qquad (2.64)$$

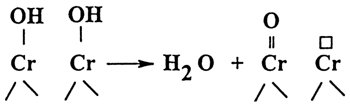

$$\overset{\overset{OH}{|}}{\underset{/\backslash}{\mathrm{Cr}}}\ \overset{\overset{OH}{|}}{\underset{/\backslash}{\mathrm{Cr}}} \longrightarrow H_2O + \overset{\overset{O}{\|}}{\underset{/\backslash}{\mathrm{Cr}}}\ \overset{\square}{\underset{/\backslash}{\mathrm{Cr}}} \qquad (2.65)$$

They established power rate expressions for the SCR of NO with NH_3 on chromia–alumina and chromia oxide catalysts:

$$r = k \cdot p_{\mathrm{NO}} \cdot p_{\mathrm{NH_3}} \quad \text{on } Cr_2O_3-Al_2O_3 \quad \text{and}$$
$$r = k' \cdot p_{\mathrm{NO}}^{0.7} \cdot p_{\mathrm{NH_3}}^{0.2} \quad \text{on } Cr_2O_3. \qquad (2.66)$$

These expressions are based on a very weak adsorption of the reactants, because the contribution of the partial pressures of NO and NH_3 are rather low, 0.7 and 0.2, respectively.

Using ^{15}N labelling in amorphous chromia–titania, Curry-Hyde et al. [83] suggested a mechanism very close to the one suggested by Topsoe [122] for vanadia–titania catalysts. In addition, they considered that the production of N_2O could also result from structures like

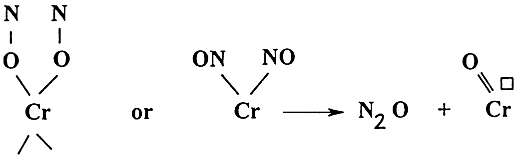

$$\overset{\overset{N\quad N}{|\quad\ |}}{\overset{O\quad O}{\underset{/\backslash}{\overset{\backslash\,/}{\mathrm{Cr}}}}} \quad \text{or} \quad \overset{ON\quad NO}{\overset{\backslash\,/}{\mathrm{Cr}}} \longrightarrow N_2O + \overset{O}{\overset{\backslash\backslash\,\square}{\mathrm{Cr}}} \qquad (2.67)$$

Because these amorphous catalysts do not exhibit an important activity, no additional investigation about the mechanism or kinetics was performed.

3.2. Metal zeolites

Metal zeolites represent another group of catalysts much investigated in this reaction.

Seiyama et al. [130] first investigated the SCR of NO with NH_3 over a large number of M-Y zeolites. In monoexchanged catalysts, the activity order was: Co(II)-Y>Cu(II)-Y>Pt(II)-Y>Pd(II)-Y≫Fe(III)-Y>-Ni(II)-Y>Co(III)-Y. For copper, the catalytic activity was detectable at temperatures as low as 323 K, with a maximum at about 393 K. At this temperature, the selectivity to N_2 was about 70%. The activity of different copper-exchanged zeolites was Y>X>A. This difference was attributed to the difference in the molecular diffusibility within the zeolites (Fig. 4).

Seiyama et al. [130] suggested that, at low temperatures, NH_3 was adsorbed on Cu-exchanged zeolites to form a square planar complex $Cu(NH_3)_4^{2+}$ in the supercage. The complete removal of NH_3 from the complex would result in the migration of Cu(II) ions from the supercage to the β-cage. A linear dependence between NO conversion and the exchange level was found to be in the range from 7% to 79%.

When a second metal is introduced, the ranking of specific activity per Cu(II) is: Cu–Co>Cu–Pd>Cu–Fe>Cu–Ni. This order is parallel with the ranking of the redox potential of M^{n+}/M^{p+} ($p>n$) of the second element. These data suggest that the second metal ion participates in the catalysis as a redox system to alter the Cu(II) to Cu(I) ratio.

Brandin et al. [131] and Choi et al. [132] reported that Cu-exchanged mordenite was also an effective catalyst for the SCR of NO with ammonia. Recently, Yashima et al. [133] investigated Cu-exchanged ZSM-5 zeolites and reported very good activities and selectivities. They suggested that diatomic copper was the active site. They reported the same positive effect of the exchange level upon the specific activity as that previously reported by Iwamoto et al. [134]. To explain the decrease in the activity for an exchange level higher than 200% they considered that the excess of Cu(II) ions might form aggregates such as small particles of CuO and that such aggregates were inactive or much less active than the Cu(II) present as a counter anion. In addition, such CuO species may block the pores of ZSM-5, which may also result in a decrease in the activity.

The Si/Al ratio is another factor found to affect the activity of Cu-ZSM-5 catalysts. For the same exchange level, a lower Si/Al ratio allows for a higher specific activity. In such conditions copper is merely implanted in position close to aluminium. Therefore,

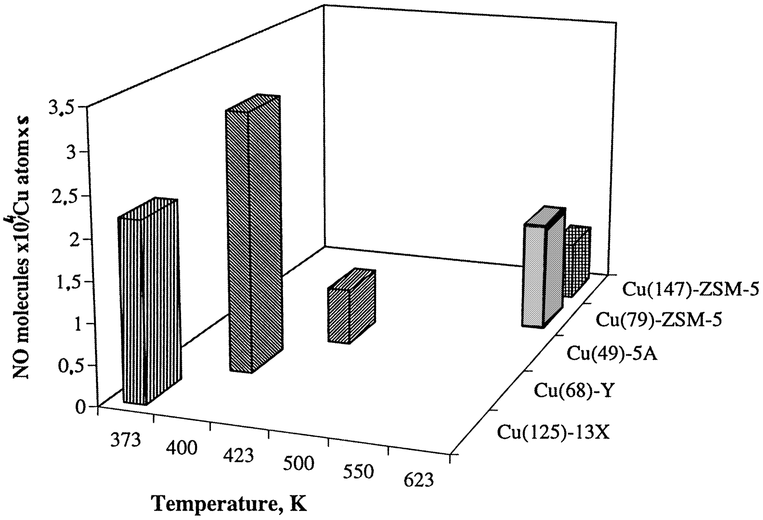

Fig. 4. Variation of TOF for reduction of NO with NH_3 on different Cu-zeolites (for Cu-X, Cu-Y and Cu-A zeolites: space velocities: 2.77×10^{-4} h cm^{-3}, NH_3=1.2%, NO=1.8%, O_2=2%; for Cu-ZSM-5 zeolites: space velocities: 3.3×10^{-6} h cm^{-3}, NH_3=0.1%, NO=0.1%, O_2=2%).

because a lower Si/Al ratio corresponds to a higher aluminium content, these elements represent an additional factor supporting the positive effect of the dispersion. The zeolite lattice also plays an important role in this mechanism [134]. A comparison of Cu-ZSM-5, Cu-Y and Cu-mordenite indicates that, at low temperatures, i.e. below 473 K, Cu-Y exhibits a certain activity whereas Cu-ZSM-5 and Cu-mordenite are inactive. However, in this range, the conversions are too small to present any interest. At higher temperatures, i.e. above 573 K, Cu-ZSM-5 and Cu-mordenite exhibit activities higher than the ones obtained for Cu-Y.

In addition, Wang and Hwang [135] showed that pretreating catalysts is also important. At the optimal temperature, the activity of Cu-Y after dehydration is higher than that of hydrated Cu-Y. Furthermore, in the same conditions, the oxidation or ammonia treatment of catalysts tested in NO–NH_3 reactions leads to a higher activity than that observed on dehydrated Cu-Y. Conversely, the reduction of catalysts at high temperatures leads to a low activity.

Very recently, the use of oxides supported on pillared clays was also reported [136,137]. In fact, these systems increase the dispersion both of titania (as pillars) and of the active phase. The latter could be a consequence of the combination of the TiO_2 pillars with the tetrahedral SiO_2 surface. Thus, it was shown that deposition of Fe_2O_3 on dealuminated titania-pillared clay catalysts leads to an SCR activity higher than that of commercial type tungsten-promoted V_2O_5/TiO_2 and also higher than that of undealuminated pillared clay or supported Fe_2O_3 catalysts. The deposition of mixed Fe_2O_3 and Cr_2O_3 on the same titania-pillared clays support leads to a supplementary increase in the activity. Thus, compared with the same commercial catalysts, the activity of supported pillared clay catalysts is twice as high under H_2O and SO_2 free conditions and approximately 40% higher in the presence of H_2O and SO_2.

3.2.1. *Stability*

The stability of metal zeolites is discussed in the section on the reduction of NO in the presence of hydrocarbons. Concerning the SCR of NO with ammonia, it must be pointed out that the presence of oxygen enhances the activity, while H_2O and SO_2 have poisoning effects.

3.2.2. *Mechanism and kinetics*

Seiyama et al. [130,138] suggested that the SCR of NO with ammonia on Cu-Y zeolites could be analysed in terms of a Langmuir–Hinshelwood type mechanism, considering the participation of strongly adsorbed

NH_3 and weakly adsorbed NO. The surface of these catalysts is more homogeneous than that exhibited by vanadia–titania catalysts. Cu-zeolites contain copper which is very well dispersed (interacting merely with NO) and zeolite acid sites (interacting merely with NH_3). This allows to avoid a high number of the equilibria determined in the case of vanadia.

$$\mathrm{Cu(II)\text{-}Y + NH_3 \rightarrow Cu(II)(NH_3)_{\mathit{n}}\text{-}Y} \qquad (2.68)$$

$$\mathrm{Cu(II)(NH_3)_{\mathit{n}}\text{-}Y + NO \rightarrow [Cu(II)(NH_3)_{\mathit{n}}(NO)\text{-}Y] \rightarrow} \qquad (2.69)$$

$$\mathrm{Cu(I)(NH_3)_{\mathit{m}}\text{-}Y + N_2 + H_2O + (\mathit{n} - \mathit{m} - 1) + H^+\text{-}Y}$$

$$\mathrm{H^+\text{-}Y + NH_3 \rightarrow NH_4^+\text{-}Y} \qquad (2.70)$$

$$\mathrm{Cu(I)(NH_3)_{\mathit{m}}\text{-}Y + 3NO \rightarrow Cu(II)(NH_3)_{\mathit{m}}NO_2^-\text{-}Y + N_2O} \qquad (2.71)$$

$$\mathrm{Cu(II)(NH_3)_{\mathit{m}}NO_2^-\text{-}Y + NH_4^+\text{-}Y \rightarrow Cu(II)(NH_3)_{\mathit{m}} + N_2 + 2H_2O} \qquad (2.72)$$

$$\mathrm{Cu(II)(NH_3)_{\mathit{m}}\text{-}Y + (\mathit{n} - \mathit{m})NH_3 \rightarrow Cu(II)(NH_3)_{\mathit{n}}} \qquad (2.73)$$

Based on this mechanism the following expression of the reaction rate was proposed:

$$r = \frac{k \cdot K_{\mathrm{NO}} \cdot K_{\mathrm{NH_3}} p_{\mathrm{NO}} \cdot p_{\mathrm{NH_3}}}{\left(1 + K_{\mathrm{NO}} p_{\mathrm{NO}} + K_{\mathrm{NH_3}} p_{\mathrm{NH_3}}\right)^2}, \qquad (2.74)$$

where k is the rate constant, $K_{\mathrm{NH_3}}$ the adsorption equilibrium constant (step 2.68) of NH_3 and K_{NO} is the adsorption equilibrium constant (step 2.69) of NO. This relation (2.74) is typical of a Langmuir–Hinshelwood mechanism.

Yashima et al. [133] analysed a series of Cu zeolites, in which the copper exchange level, the Si/Al ratio of ZSM-5 and the nature of the zeolites (ZSM-5, Y or mordenite) were changed. They concluded that the active centres are copper dimers and proposed the steps included in Scheme 4 as the reaction mechanism.

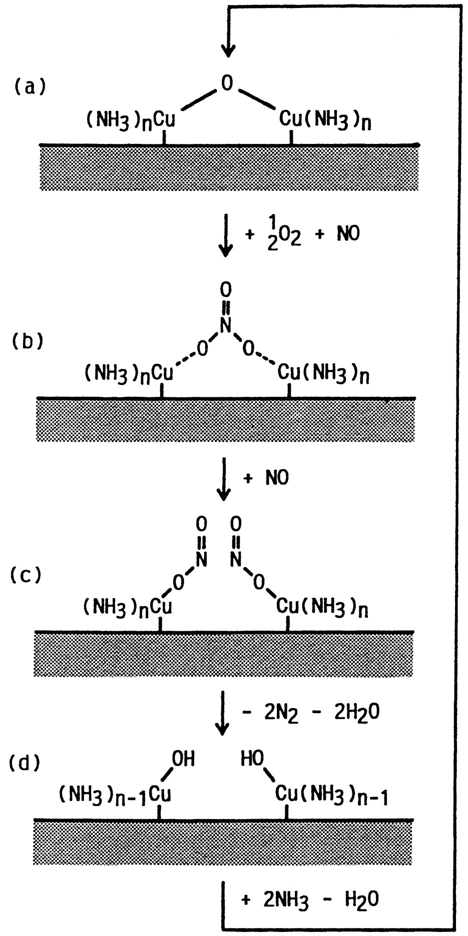

Scheme 4. Reaction scheme of SCR of nitric oxide with ammonia on Cu-ZSM-5 [133].

3.3. Noble metals

Generally, the reduction of NO with NH_3 is used in industrial plants where high sulphur concentrations are present. Even though the conversions are good [139] the use of noble metals is not effective in this process because of their low stability in the presence of sulphur. However, from a theoretical point of view, the reaction of NO with NH_3 could offer some important information about oscillatory kinetics. A detailed understanding of the oscillatory mechanism needs to account for the individual reaction steps and to look for the effects which can either promote or inhibit the overall reaction.

Lombardo et al. [140] reported that on a Pt(1 0 0) monocrystal surface the dynamical behaviour of the reaction of NO with NH_3 is similar to that of NO with H_2 (see the section about the reduction of NO with hydrogen). The decrease in the rates of N_2 and H_2O production above 500 K coincides with the occurrence of a 1×1→hex reconstruction. The reduction in activity at the higher temperatures is attributable to the low dissociation probability of NO on a well-formed hex phase. As the surface is modified the reaction remains low until the hex→1×1 phase transition occurs. This corresponds to the restoring of a high catalytic level activity. Apparently, NO controls the phase transitions in both directions. The explanation of oscillatory behaviour appears to be that the inhibition coverage of the "surface explosion" is 0.5 and is identical with the local NO coverage in the growing 1×1 islands through which the hex→1×1 phase transition proceeds [141].

Similar results were indicated by Nieuwenhuys et al. [142], who showed that all the recorded partial pressures (of N_2O, H_2O, NH_3, NO and N_2, respectively) varied in an oscillatory manner. The amplitude and the period of the oscillations increase with the increase of the NO-to-NH_3 ratio. Self-sustained oscillations in the reaction of NH_3 with NO were also evidenced on polycrystalline platinum by Takoudis and Schmidt [143] and Somorjai et al. [144]. The effect of oxygen in these experiments corresponded to contradictory observations. Somorjai et al. [144] reported that the introduction of a very small amount of oxygen suppressed the oscillations whereas Nieuwenhuys et al. [142] indicated that the system showed reaction rate oscillations even if the total amount of oxygen was about 66%.

3.4. *Activated carbon catalysts*

The selective reduction of NO in the presence of activated carbon was also investigated [6]. An important advantage of these catalysts is that they are very cheap. The results obtained by dispersing different oxides on the activated carbon surface were mentioned.

Moulijn et al. [145] reported that activated carbon also exhibited very good performances. The properties of activated carbon depend on several factors, such as the preparation procedure, a porous texture and surface chemistry. The presence of heteroatoms like oxygen and nitrogen also influences the SCR activity and there is therefore a relation between the nature of the carbon and the catalytic behaviour. The SCR of NO over activated carbon is most selective at temperatures below 450 K and requires an NO-to-NH_3 stoichiometric ratio of 1:1. The NH_3 oxidation starts at high temperatures and carbon is degraded simultaneously with a production of CO_2. The presence of O_2 is always necessary. Steam also activates the carbon but no explanation of this effect was given.

3.5. *Other investigated catalysts*

The occurrence of SCR of NO in the presence of NH_3 was also reported for polysulphomolybdates [146]: $M_XMo_6S_{8-Y}$ and $M_XMoS_{8-Y}O_Z$, M=Ni, Fe, Mn, Cu, Zr, Cr; Al_2O_3-supported coordinative complexes [147] of the type: $M''(M''(CN)_6Fe)$, M=Mn, Fe, Ce, Ni, Cu or M-sulpho-phthalocyanines [148,149], M=Cu, Ni, CO.

3.6. *Honeycomb catalysts*

Two kinds of honeycomb catalysts were investigated: monoliths obtained by extruding a paste-like catalytic material and plate catalysts obtained by depositing the catalytic material onto a stainless steel net or a perforated metal plate [67]. The catalysts in the first type are only used in dust-free conditions while those of the second type can be used in the presence of dust.

The advantages of these catalysts are an increase in the SCR activity obtained by improving the geometric surface area and a reduced SO_2 conversion obtained by a kinetically controlled reaction that decreases the thickness of the metal.

Summary. Up to now, tungsten or molybdenum promoted vanadia–titania catalysts exhibit the best catalytic activities in this reaction and these catalysts have already been industrialized for some time. However, they are sensitive to different poisons and additional work is still necessary to improve their stability. In this respect, studies concerning the mechanisms of deactivation are scarce and could be very useful. The redox and acid-basic behaviour ratio is also not very clearly defined and this could also be useful to improve these catalysts. All other investigated catalysts were either less active or more sensitive to the presence of the poisons. However, supported carbon as well as titania-pillared clay catalysts could also represent potential solutions.

On the other hand, ammonia is an expensive reductant and, within certain limits, is a pollutant itself. Therefore, the interest for other reductants, cheaper and less polluting, is justified.

4. Catalytic reduction of NO in the presence of CO or H_2

General aspects. The use of CO or H_2 for catalytic reduction was one of the first possibilities investigated in view of eliminating NO from automotive exhaust gas [150–153]. The reaction of NO with CO:

$$NO + CO \rightarrow CO_2 + 1/2\,N_2 \tag{3.1}$$

is one of the most important reactions occurring in automotive catalytic converters, where both reactants are undesirable pollutants. Because of the presence of some hydrogen in the exhaust gases, the following reaction also occurs:

$$NO + H_2 \rightarrow N_2 \text{ (or } NH_3, N_2O) + H_2O \tag{3.2}$$

Neither the reduction of NO with CO nor that with hydrogen can be considered as selective because, in addition to nitrogen, other undesired compounds like N_2O or NH_3 (in the case of hydrogen) are generated. Oxygen is always present in the exhaust gases. The oxygen excess achieved by lean carburization or addition of air in the exhaust stream prevents the reduction of NO and causes the concomitant oxidation of CO or H_2 by O_2 and NO.

Few categories of catalysts have been investigated: base metal oxides and mixed metal oxide compounds like perovskites, supported metal catalysts, metal zeolites and alloys. New categories have also been considered recently. In spite of the considerable research work carried out on these important reactions, the existence of these side reactions and the difficulty to achieve long-term stability of the catalysts in the presence of H_2O, SO_2 and heavy metals make that only few systems can be used in practice. The reduction by CO and H_2 will be examined separately.

Let us note that establishing the reaction mechanism and kinetics for the catalytic reduction of NO using CO or even H_2 is easier because the IR spectra of NO and CO gases adsorbed on different surfaces exhibit very well assigned bands. This was well described in the initial paper [154] and summarized in numerous reviews [155–160]. Because CO and NO are frequently used as probe molecules to investigate different chemisorption properties of the surfaces, other techniques such as ESR (especially for NO) [161,162], NMR (especially for CO) [163,164] and XPS are also available.

4.1. *Catalytic reduction of NO by CO*

As mentioned above different materials and many elements were investigated in this reaction. However, special attention focused on copper that was investigated both as base metal oxide catalysts and as metal supported or in perovskite compositions. Irrespective of the material type, copper is active in this reaction in the oxidation (II) state. However, in order to respect the presentation scheme, the catalyst types will be considered, thus evidencing its particularities in different chemical environments.

4.1.1. *Base metal oxide catalysts*

Base metal oxide catalysts were the first investigated in the oxidation of CO in the presence of O_2 and NO [153,157,165–170]. Using different transitional metal oxides supported on 95 wt% alumina–5 wt% silica, Shelef and Kummer [171] showed that there was a difference between the activities of the following oxides in a CO–O_2 and a CO–NO reaction, respectively.

For CO reduction the following reactivity order was found: Fe_2O_3>$CuCr_2O_4$>Cu_2O>Cr_2O_3>NiO>Pt>-Co_3O_4>Al_2O_3 (5% SiO_2)>MnO>V_2O_5 (Fig. 5). These experiments showed a good selectivity to N_2 and CO_2 for Fe_2O_3 and Cr_2O_3-supported catalysts. Above 575 K, the N_2O content was very low, but a dependence on the NO-to-CO ratio at inlet was evidenced. In the presence of other oxides the reaction between CO and O_2 was faster than the reaction between CO and NO. The apparent selectivity of Cr_2O_3 was explained by the poisoning effects of oxygen on the active surface of this oxide. The activity of Al_2O_3 (5% SiO_2) catalysts could be explained by the low silica content or by the presence of impurities. Good activities for the NO with CO reaction in the absence of water over α-Cr_2O_3 and Fe_2O_3 were also found by Kobylinski and Taylor [172].

Later, much attention was focused on copper oxide as well as on alumina-supported copper oxide. Gandhi and Shelef [170] compared the adsorption and oxidation rates of a reduced Cu_2O sample and a CuO sample and showed that the rate of adsorption of NO on the more oxidized oxide was higher than on the reduced sample at lower temperatures. This behaviour was different from that observed on other metal oxides [167,169]. Moreover, the equilibrium uptake of NO on

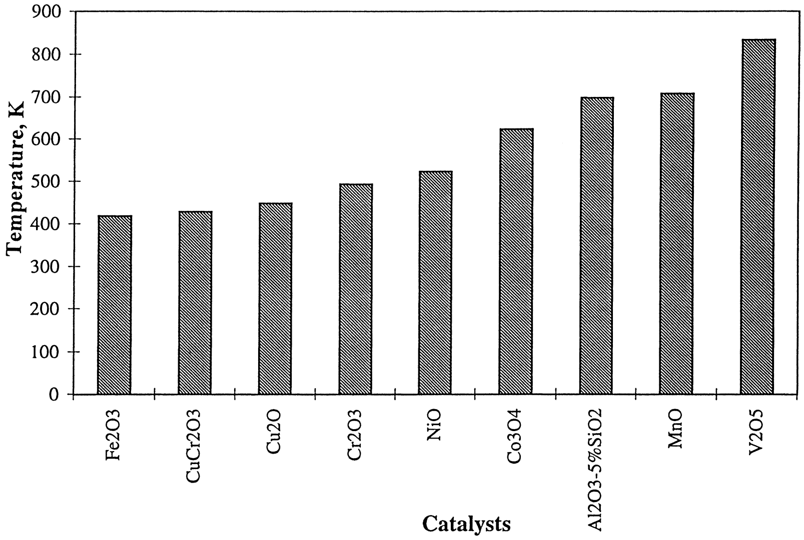

Fig. 5. Reactivity of different Al_2O_3–SiO_2 supported transitional metal oxides in the reduction of NO with CO (NO – 2.0 vol%; CO – 1.2 vol%; space velocities – 17.5 min^{-1}; ~10 wt% metal).

Cu–Al_2O_3 was somewhat higher than on CuO, even though the surface concentration of copper atoms is lower.

Mixed (10 wt%) copper–chromium oxides supported on alumina were reported by Stegenga et al. [173] to be very effective in this reaction, even in the presence of O_2. N_2O is predominantly formed at low NO conversions. At higher conversion levels, the N_2O formation reaches a maximum and only N_2 is observed at the higher temperatures. Roughly the same behaviour was reported by Stegenga et al. [174,175] for carbon-supported Cu–Co catalysts. These catalysts are very active at temperatures above 800 K where only N_2 and CO_2 are produced.

4.1.1.1. Stability. The stability of these catalysts is rather low. The presence of excess CO or of a relatively large quantity of oxygen strongly diminishes the CO reduction activity. Kobylinski and Taylor [172] reported a poisoning of the supported oxides in the presence of water vapour. Since water vapour is always present in exhaust gases (up to 15 wt%) the stability of catalysts under these conditions is a very important factor. The above authors suggested that H_2O and NO competed for the active sites and allowed for the possibility of a dissociative adsorption of water as H^+ and OH^-. In this case the proton would get associated with the coordinatively unsaturated (cus) O^{2-} site and the hydroxyl with the (cus) cation site. The initial activity could be restored only after regeneration at high temperatures.

Dispersion of the active species as well as the nature of the support play an important role in increasing the stability of catalysts. Stegenga et al. [174] reported the same inhibition of activity in the case of carbon-supported mixed Cu–Cr oxide catalysts but found that this inhibition was reversible. Furthermore, a better resistance towards SO_2 poisoning [175] than in the case of unsupported oxides was evidenced.

4.1.1.2. Reaction mechanism and kinetics. In a first attempt to explain the oxidation of CO in the presence of O_2 and NO, Shelef and Kummer [171] assumed that on most metal oxide catalysts, there was a parallelism between the oxidation of CO and the oxidation of the catalyst reduced surface sites. Cu(II) sites chemisorb NO faster than Cu(I) ones. The reduction of NO in the presence of CO could proceed in two steps, first a partial reduction of NO to N_2O, and second a subsequent reduction of N_2O to N_2. Each of these steps corresponds to the oxidation of a reduced site and therefore, the majority of oxygen contained by NO is liberated as metal oxide. If the second step is slow, part of the N_2O would be evacuated from the catalyst surface before it is converted to N_2.

$$2NO + \text{cus Cu(II)} \rightarrow \text{Cu(II)O} + N_2O \quad (3.3)$$

$$N_2O + \text{cus Cu(II)} \rightarrow \text{Cu(II)O} + N_2 \quad (3.4)$$

$$\text{Cu(II)O} + CO \rightarrow \text{cus Cu(II)} + CO_2 \quad (3.5)$$

In consequence, NO dissociation occurs only in the regions where empty sites are accessible. This behaviour concerning chemisorption of released oxygen by cus cationic sites and then reduction of these sites by CO do not exclude a surface rearrangement due to the oxygen atom of the NO molecule in contact with the surface, as was suggested by Yates and Madey [176].

Later, Force and Ayen [177] reported that the activity of copper chromite catalysts was consistent with a single site mechanism in which the rate-limiting step was the reaction between the adsorbed carbon monoxide and nitric oxide. Unfortunately, this mechanism cannot explain the formation of nitrous oxide evidenced on all investigated oxides [172].

Gravimetric studies of the chemisorption of NO on copper oxides [178], chromia [167], iron oxides [169], nickel oxides [170], manganese oxides [179] and cobalt oxides [180] showed isotherms of the Freundlich type and the rate closely corresponded to the Elovich equation. When the chemisorption of NO and CO on the same adsorbent was compared [170,180] it was found that NO was adsorbed more strongly than CO. As we already mentioned, the adsorption of NO depends on the reduction state of the oxides [155]. On chromia, iron oxides or manganese oxides the adsorption is much faster on the reduced surface whereas for copper it is much faster on the oxidized surface.

Physico-chemical investigations concerning copper catalysts support the main conclusions of the kinetic measurements. In order to explain the mechanism of nitrogen oxide reduction on copper catalysts and to find a rate equation, London and Bell [154,181] performed a very rigorous IR investigation of the interaction between the CO and NO molecules using a CuO/SiO_2 catalyst. The bands observed and the assignments of these bands [181] on CuO/SiO_2 are presented in Table 5. Later, IR spectroscopy became a very important tool to investigate the chemisorption of CO and NO molecules and much effort was put into the structural characterization of supported metals and metal catalysts. The excellent review by Fierro [182] concerning the application of IR spectroscopy to characterize the chemisorption of CO and NO should be mentioned here.

The reaction mechanism proposed by London and Bell [154,181] takes into account nine elementary steps:

$$Cu + NO \rightleftarrows Cu{-}NO \quad (3.6)$$

$$Cu{-}NO + Cu^+ \rightarrow Cu{-}N + Cu^{2+}O^- \quad (3.7)$$

or

$$Cu{-}NO + Cu{-}CO \rightarrow Cu{-}N + Cu + CO_2 \quad (3.8)$$

$$Cu{-}N + NO \rightarrow Cu + N_2O \quad (3.9)$$

$$Cu^+ + CO \rightleftarrows Cu^+{-}CO \quad (3.10)$$

$$Cu + N_2O \rightleftarrows Cu{-}ONN \quad (3.11)$$

$$Cu{-}ONN \rightarrow Cu^+O^- + N_2 \quad (3.12)$$

$$Cu^{2+}O^- + CO \rightarrow Cu^+ + CO_2 \quad (3.13)$$

$$Cu^+O^- + CO \rightarrow Cu + CO_2 \quad (3.14)$$

$$Cu{-}N + CO \rightleftarrows Cu^+NCO^- \quad (3.15)$$

There are other alternatives for the formation of N_2O:

$$M{-}NO + M{-}NO \rightarrow M^+O^- + N_2O + M \quad (3.16)$$

$$M{-}N + M{-}NO \rightarrow N_2O + 2M \quad (3.17)$$

and for the formation of N_2:

$$M{-}ONN + M{-}CO \rightarrow N_2 + CO_2 + 2M \quad (3.18)$$

$$M{-}N + M{-}N \rightarrow N_2 + 2M \quad (3.19)$$

These studies confirm that activity towards the reduction of NO is enhanced when the catalyst surface is partially reduced. In the IR spectra no carbonates or nitrate bands were evidenced when the catalyst was active. As suggested by step (3.12), N_2O also appears to be an intermediate. The mechanism proposed by London and Bell [181] is a double site mechanism. They suggest that only NO dissociates. The Cu(II) ions act as NO adsorption sites while Cu(I) ions act as recipients of the O atoms produced through the dissociation. Therefore, it ensures an inhibition of the reduction of NO by increased CO partial pressures, due to the adsorption of CO on these sites.

Based on this mechanism, London and Bell [181] proposed an expression of the rate of NO consumption of the type

Table 5
Vibrational frequencies for adsorbed N_xO_y and CO_z

Frequency, cm^{-1}	Structure	Frequency, cm^{-1}	Structure
2220	M - NNO or M - ONN	2170	$M^- - CO^+$
2136	M - NO_2	2140	M - CO
1989	M - $(NO)^-$	1675	$M^+ - OCO_2^{2-}$
1890 - 1898	$M^{n+} = NO^+$ or $M^{n+} : NO^+$	1565 - 1585	$M^+ - CO_2^-$
1883	M - N_2O_3	1350	$M^+ - OCO_2^-$
1827	asymmetric 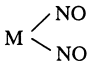		
1812	M - N_2O_3		
1740	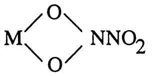		
1734	symmetric 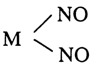		
1705	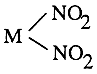		
1649	M - NO_2		
1605	M - ONO_2 or M- ONO		
1589	M - N_2O_3		
1575 - 1585	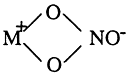		
1510 - 1520	$M^+ - ONO_2^-$		
1310 - 1313	M - NO_2		
1265	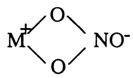		
745	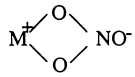		

Fig..

$$-1/2\, r_{NO} = \frac{b_1 \cdot b_2 \cdot c_{NO}}{(1 + b_2 \cdot c_{NO} + b_3 \cdot c_{N_2O})(1 + b_4 \cdot c_{CO})}, \qquad (3.20)$$

where $b_1 = k_7 \cdot K_6 \cdot c_{Cu} \cdot c_{Cu^+}/Q$; $b_2 = K_6 Q$; $b_3 = k_{12} \cdot K_{11}/Q$; $b_4 = K_{10}$; $Q = 1 + K_{15} \cdot k_7 \cdot K_6 \cdot c_{Cu^+}/k_9 \cdot K_{10}$; k_i=the rate constant of reaction i; K_i=the equilibrium constant of reaction i; c_x=the concentration of the components in the gas phase; c_{Cu}=the concentration of Cu sites.

This equation takes into account an important role of the reaction intermediates. The negative order related to CO is thought to be the result of the formation of isocyanate at elevated CO pressure. The isocyanate ions would coordinate onto the metal ions and block the site [183].

More recently, Fu et al. [183] revealed additional arguments in favour of the presence of two active sites on the CuO surface. They reported a selective adsorption of NO and CO on the CuO/Al_2O_3 catalyst surface and suggested that Cu(I), which has a 3d electron that is easier to donate, acted as an active site for the CO molecule whereas Cu(II) acted as an active site for NO, possibly through the transfer of an active electron from a π^* orbital of NO to a 3d orbital of Cu(II).

Knozinger et al. [184] also investigated the NO chemisorption on an alumina with a high copper content (about 10%) and many of their conclusions agree with the previous ones. In addition, they suggested that superficial sites could interact with one another. A transformation of nitrite into nitrate complexes with the evolution of NO was therefore suggested:

$$2\mathrm{Cu}^+{-}\mathrm{ONO} \rightarrow \mathrm{Cu}^+{-}\mathrm{ONO}_2^- + \mathrm{Cu}^0 + \mathrm{NO}_{\mathrm{gas}} \tag{3.21}$$

and at 685 K:

$$\mathrm{Cu}^+{-}\mathrm{ONO}_2^- \rightarrow \mathrm{Cu}^0 + \mathrm{NO}_{\mathrm{gas}} + \mathrm{O}_{\mathrm{gas}} \tag{3.22}$$

Cu^0 atoms are reoxidized by superficial Cu^{2+}:

$$\mathrm{Cu}^0 + \mathrm{Cu}^{2+} \rightarrow 2\mathrm{Cu}^+ \tag{3.23}$$

To a certain extent, these conclusions might apply to complex catalysts containing copper. In the case of carbon-supported Cu–Cr catalysts, Stegenga et al. [174] showed that the reaction of NO with CO occurred according to a first-order in nitric oxide and a zero-order in carbon monoxide in the presence of excess carbon monoxide. They observed that CO and NO could inhibit the reaction by reversible competitive adsorption, whereas carbon dioxide could not. Instead, oxygen completely inhibited the reduction of NO due to a more rapid reoxidation of the catalytic sites compared to nitric oxide. The formation of N_2O followed by its reduction to N_2 was thought to occur according to the following reactions:

$$2\mathrm{NO} + \mathrm{CO} \rightarrow \mathrm{CO}_2 + \mathrm{N}_2\mathrm{O} \tag{3.24}$$

$$\mathrm{N}_2\mathrm{O} + \mathrm{CO} \rightarrow \mathrm{CO}_2 + \mathrm{N}_2 \tag{3.25}$$

However, we can remark that these reactions were included in the mechanism suggested by London and Bell.

4.1.2. Metal-supported catalysts

4.1.2.1. Non-platinum supported catalysts. As is the case for oxides, copper, as a metal, is the most investigated element. It is very clear that at high dispersions (in small clusters or very small crystallites) copper can interact with and activate the NO molecules. A catalyst containing a low amount of deposited copper exhibits particular properties compared to copper oxide or highly loaded supported catalysts. The characteristics of low-loading copper catalysts seem to be closer to those of metallic copper.

Rewick and Wise [185] reported activity data in a CO–NO reaction over Cu/SiO_2 and $Cu/CuAl_2O_4$ catalysts, showing that the activity decreases in the order $Cu/SiO_2 > Cu/CuAl_2O_4 > Cu$. They suggested that the mechanism is similar for all three catalysts because the activation energy values are the same.

Recently, Geus et al. [186–189], using XPS and IR techniques, reinvestigated the interaction of NO with different copper single crystals (the Cu(1 0 0) and Cu(1 1 0) faces, as well as stepped Cu(7 1 1) and Cu(7 1 0) surfaces) and Cu/SiO_2 and the subsequent reduction with CO. They reported that the general features were the same for all surfaces. NO desorbs dissociatively by generating superficial oxygen and nitrogen atoms. At low pressure, no molecularly adsorbed species were detected on the single crystal surfaces. The saturation of the surface coverage was followed by the penetration of oxygen atoms into subsurface layers. Nitrogen atoms do not accumulate at the surface and desorb. Weakly adsorbed nitrogen atoms, originating from the dissociation of NO, react with CO to form isocyanate (found to be present on the support) and with NO to form N_2O. It was shown that the exposure to NO led to the rapid oxidation of Cu^0 to Cu(I) and subsequently, to a much lower extent, to oxidation to Cu(II); nitrite and nitrate species were also present on the surface. Upon prolonged exposure of equimolar amounts of NO and CO to reduced catalysts, the copper particles were only slightly oxidized. The formation of CO_2, N_2O, and isocyanate indicated that surface reactions already occurred at room temperature. Wee et al. [190] reported an SIMS and XPS study of the NO and CO interaction on Cu(1 0 0) and Cu(2 1 0) surfaces. Their results about the behaviour of dissociated O atoms agree with those of Geus et al. [186–189]. Concerning dissociated nitrogen adatoms, they indicated a stronger chemisorption on Cu(2 1 0). These adatoms formed a stable nitride species upon heating at higher temperatures.

Using a TiO_2 support, Boccuzzi et al. [191,192] showed that strongly reduced samples are more active in the CO–NO reaction than moderately reduced ones and suggested that in this case, the catalytic performances of copper catalysts were similar to those of platinum catalysts. The electron microscopy characterization of Cu/TiO_2 samples indicated that the average particle size decreased with an increase of the reduction temperature. However, an analysis of the reaction data revealed that, in this case, the activity measurements are only meaningful after 15 min. During this time, as previously thought by London and Bell [181], part of the copper could be oxidized. Actually, it is more likely that the dispersion of the active phase plays a very important part, and that the interface between the active phase and the support also contributes greatly. A negative contribution of sintering was mentioned by Rewick and Wise [185] and a $Cu–TiO_x$ interdispersed phase was reported by Boccuzzi et al. [191,192].

Based on an FT-IR study of the surface of copper oxide, Busca [193] showed that bulk CuO cannot be present, even in mild reducing conditions, since it is transformed into the metal. Therefore, the decrease in particle size observed by Boccuzzi et al. [191,192] could also be associated with an increase in activity. This assumption is supported by experiments done by Knozinger et al. [184] on samples of hydrogen-reduced copper supported on alumina. During the reduction, copper sinters to form small Cu^0 crystallites but coordinatively unsaturated Cu^+ sites are still exposed on the catalyst surface. In FT-IR, the presence of NO generates a band assigned to Cu^0–NO adsorbed species which, particularly at high temperatures, decreases with time concomitantly with the generation and the increase of a Cu^{2+}–NO complex band. Thermal desorption spectra obtained by the same authors offered some evidence on a CuN phase decomposing at high temperatures as

$$2CuN \rightarrow 2Cu^0 + N_{2,gas} \qquad (3.26)$$

Another non-platinum system was investigated by Guglielminotti [194,195]. This is Fe/ZrO_2 obtained by reducing monoclinic ZrO_2 impregnated with iron nitrate with hydrogen. On these catalysts, NO partially dissociates, already at room temperature, on the reduced and coordinatively unsaturated iron sites, with the formation of more oxidized $Fe^{(3-x)+}$ sites. Subsequently, NO can adsorb on these sites, producing mononitrosylic species. Dinitrosylic species could also be detected. Even at room temperature, NO displaces CO adsorbed on the Fe^{2+} sites but does not displace CO adsorbed as carbonylic species on Fe^0. At 475 K, the reaction of CO with NO is complete, producing mainly N_2 and carbonates.

4.1.2.1.1. Stability

Rewick and Wise [185] showed that Cu/SiO_2 exhibited a higher stability than $Cu/CuAl_2O_4$ or the metal under reaction conditions. In the case of $Cu/CuAl_2O_4$ the decrease in the activity was attributed to a sintering process.

The addition of water vapour (3 vol%) to the reactant stream results in the formation of significant amounts of NH_3 without modification of the degree of NO conversion. On the contrary, the addition of oxygen to the reactant mixture has an important effect and the NO conversion decreases to nearly 0 when the O_2 concentration approaches the stoichiometric amount required for CO oxidation. A good stability was also reported for Cu/TiO_2 catalysts in the absence of oxygen [196].

4.1.2.1.2. Reaction mechanism and kinetics

Deposition of copper as metal does not change its behaviour in this reaction. NO dissociation also requires the presence of acceptor oxygen sites and the release of oxygen occurs through metal oxide intermediates. Therefore, the data reported on the reaction mechanism and kinetics in the case of copper metal-supported catalysts are very close to those presented in Section 4.1.1.2.

Based on chemisorption and activity data, Rewick and Wise [185] suggested a reaction mechanism involving the presence of reduced sites. According to this mechanism, the main step is also NO decomposition.

$$\mathrm{NO} + 2\mathrm{M} \rightarrow \mathrm{M{-}N} + \mathrm{M{-}O} \quad (3.27)$$

$$\mathrm{M{-}O} + \mathrm{CO} \rightarrow \mathrm{CO_2} + \mathrm{M} \quad (3.28)$$

$$\mathrm{M{-}N} + \mathrm{NO} \rightarrow \mathrm{N_2} + \mathrm{M{-}O} \quad (3.29)$$

$$\mathrm{M{-}N} + \mathrm{CO} \rightarrow \mathrm{M{-}NCO} \quad (3.30)$$

$$\mathrm{M{-}CO} \rightarrow \mathrm{M{-}CO} \quad (3.31)$$

The rate of consumption of NO reveals a strong chemisorption of NO and CO:

$$-r_{\mathrm{NO}} = k_{27}(\mathrm{NO})\{1 + k_{29}(\mathrm{NO})/[k_{29}(\mathrm{NO}) + k_{30}(\mathrm{CO})]\} \quad (3.32)$$

This mechanism does not account for the N_2O formation during the reaction.

Recently, Boccuzzi et al. [191,192], using IR data, suggested a mechanism which considers a dissociation of NO determined by an electron transfer from the reduced surface to an antibonding orbital of the NO molecule:

$$\mathrm{NO} + \mathrm{M} \rightarrow \mathrm{M{-}NO} \quad (3.33)$$

$$\mathrm{CO} + \mathrm{M} \rightarrow \mathrm{M{-}CO} \quad (3.34)$$

$$\mathrm{M{-}NO} + \mathrm{e^-} + \mathrm{M} \rightarrow \mathrm{M{-}N} + \mathrm{M{-}O^-} \quad (3.35)$$

$$\mathrm{M{-}N} + \mathrm{M{-}NO} \rightarrow \mathrm{N_2O} + 2\mathrm{M} \quad (3.36)$$

$$\mathrm{M{-}NO} + \mathrm{M{-}NO} \rightarrow [\mathrm{M{-}(NO)_2}] + \mathrm{e^-} + \mathrm{M} \rightarrow \mathrm{N_2O} + \mathrm{M{-}O^-}$$

$$\mathrm{M{-}CO} + \mathrm{O^-} \rightarrow \mathrm{CO_2} + \mathrm{e^-} \quad (3.38)$$

$$\mathrm{CO{+}M{-}O^-} \rightarrow \mathrm{M{-}[CO_2]{+}O^{2-}}\ \mathrm{ret} \rightarrow \mathrm{M{-}CO_3^{2-}} + \mathrm{e^-} \quad (3.39)$$

$$\mathrm{N_2O} + \mathrm{e^-} \rightarrow \mathrm{N_2} + \mathrm{M{-}O^-} \quad (3.40)$$

In addition to these steps, Knozinger et al. [184] and Geus et al. [189] considered the possibility of an interaction between two M–N species, leading to an evolution of N_2:

$$2\mathrm{M{-}N} \rightarrow 2\mathrm{M} + \mathrm{N_2} \quad (3.41)$$

The copper nitride on the catalyst surface could also act as a promoter in this reaction. This species was found by Higgs and Pritchard [197] after reducing Cu/SiO_2 catalysts prepared by copper nitrate impregnation. Recently, Wee et al. [190] also evidenced this species using SIMS and XPS techniques.

4.1.2.2. Supported noble metal catalysts. The low stability of metal oxides in the reduction of NO by CO led the investigation on supported noble metals. In an extensive review, Shelef and Graham [198] (and references herein) very convincingly argued in favour of the use of rhodium in automotive three-way catalysts. They showed that other metals (Pt or Pd) are less able to dissociate NO than Rh, even though NO is largely dissociated on the Pt(1 0 0) surface. This conclusion was reached after considerable work in all the investigations aiming at the improvement of the catalytic activity of other noble metals. Much information on this subject can be found in the literature. The following sections constitute an attempt to extract the main findings from the corresponding publications. The principal factor that controls NO reduction in the presence of CO is the nature of the noble metal and the support, but the size of the supported metal and the reaction temperature are two other very important parameters.

Concerning the influence of the catalyst nature, Kobilynski and Taylor [199] were the first to indicate ruthenium as the most active metal (% NO conversion was total for temperatures below 523 K). They tested the catalytic activity in the reduction of NO with CO over 0.5 wt% alumina-supported noble metals (Ru, Rh, Pt, Pd). The order of activity was Ru>Rh>Pd>Pt (Fig. 6). As a consequence of these results, ruthenium

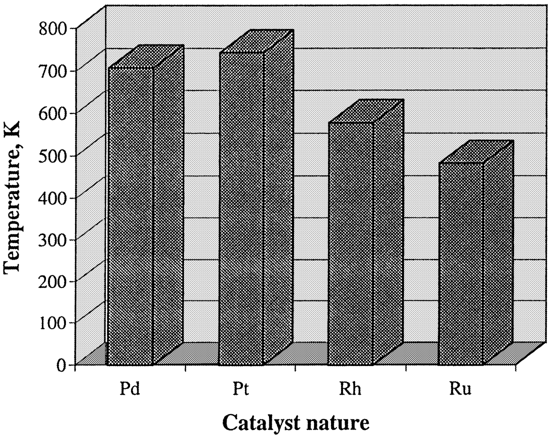

Fig. 6. Influence of the catalyst nature upon the temperature at which is removed 80% NO in a flow containing 0.5 wt% NO and 2 vol% CO (metal content: 0.5 wt%; space velocities: 24 000 GHSV).

catalysts were further investigated [200–204]. Unfortunately, small amounts of oxygen are detrimental to ruthenium [199,204–206].

Shelef and Gandhi [201] showed that certain base metal oxides could stabilize supported ruthenium against oxidation. One initially promising method was based on the stabilization of ruthenium via the formation of non-volatile ruthenates by the reaction with basic oxides of barium and lanthanum. Clausen and Good [207] analysed these catalysts using Mossbauer spectroscopy. They reported that there is a significant loss in the ruthenium stabilization when the catalyst is treated in an atmosphere of composition between that of a net reducing exhaust mixture and a net oxidizing exhaust mixture. This loss was attributed to a segregation of the ruthenium from the barium phase.

The interest therefore focused on other noble metals, especially rhodium, which was second in the activity order. Schlatter and Taylor [208,209] reported data on alumina-supported rhodium catalysts in conditions of feed gas simulating the exhaust composition. Hydrogen is always present in the exhaust composition. The particularities of the reduction of NO with hydrogen shall be discussed in a separate section, but we only note here that these catalysts had adequate activity for converting NO to N_2 but not for oxidizing CO and H_2. The addition of platinum or palladium to a rhodium catalyst not only improved its oxidation performance but also increased the amount of ammonia formed. However, the deposition of platinum or palladium on pellets distinct from those with rhodium enhanced the oxidation activity without jeopardizing the activity or selectivity in the reduction of NO to N_2. This allows to suppose that the main function of rhodium will be to control the emission of nitrogen oxides [210].

Later, investigating a series of alumina-supported noble metals (Ir, Rh, Pd, Pt) in the same conditions, Taylor and Schlatter [211] reported a high ability of Ir/Al_2O_3 catalysts to promote the NO–CO reaction in the presence of low CO concentrations and high O_2/CO ratios. These data agree with those obtained by Tauster and Murell [212]. The high conversions obtained on Ir/Al_2O_3 compared with Rh/Al_2O_3 denote a high ability of Ir to adsorb and dissociate NO in the presence of excess oxygen.

Mechanistic and kinetic studies [209,210,213–216] dealt with the formation of N_2O during the catalytic reduction of NO with CO. McCabe and Wong [216] showed that, at temperatures above 550 K, N_2O reacted with CO during the reaction of NO with CO and that CO_2 and N_2 were the only detectable products. The selectivity to the formation of N_2O was not dependent on gas space velocity and only weakly dependent on the reactant concentration and temperature [217], which suggested that both N_2 and N_2O were formed via common paths.

NO reduction with CO over noble metals is also sensitive to the oxidation state of the active sites. Studies made using preoxidized and prereduced Rh/SiO_2 catalysts [217] evidenced that preoxidized samples exhibit a higher activity. The strength with which the metal is anchored on the support could also be an important factor controlling the activity of these catalysts. Ward et al. [218] investigated the influence of the support (γ-Al_2O_3) upon Rh, Pd and Pt in relation to their interaction with NO. They considered the metal–support interface, and concluded that the support may be more than an inert component. Aluminium–metal and oxygen–metal interfaces are predicted to be stable on both Pd or Pt, and therefore bare species are formed. For rhodium, the strength is not so high and therefore the oxygen–metal interface is particularly favourable for generation of cus species. These sites are therefore accessible both for the dissociative adsorption of NO and for generation of gem-dinitrosyl $(NO)_2$ species.

An effect of the catalyst surface state and the reaction conditions was recently shown by Srinivas et al. [219,220] who performed an in situ IR study of the reactivity of adsorbed NO and CO on Rh/SiO_2 and Rh/CeO_2–SiO_2 catalysts. Adsorbed CO on reduced Rh/SiO_2 and $Rh//CeO_2$–SiO_2 cannot react with gaseous NO to form CO_2. The presence of both CO and NO gases led to the increase in the coverage of NO^- and adsorbed CO on Rh^{2+} sites and promoted CO_2 formation. The surface state of the active catalyst catalysing the formation of CO_2 is different from that of the catalyst chemisorbing the individual reactants.

The dimension of the size of the supported metal particle was considered earlier as another factor influencing the reduction of NO by CO. Hecker and Breneman [221] showed that on Rh/SiO_2 catalysts the increase of supported rhodium particles size could

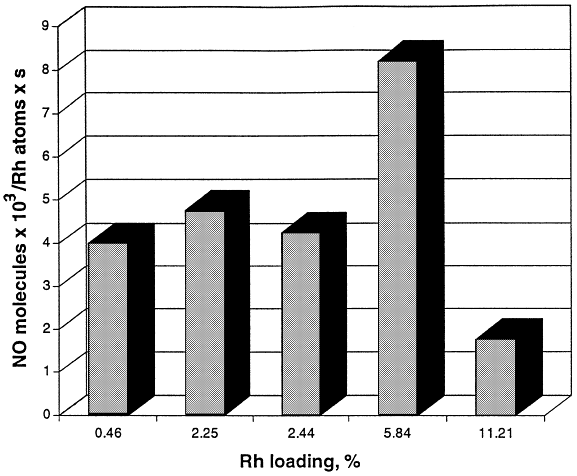

Fig. 7. Variation of the NO turnover frequency as a function of Rh loading on Al_2O_3 support (temperature: 503 K, 3 vol% CO, 1 vol% NO, space velocities: 300 000 h^{-1}).

lead to a small increase in the reaction rate. Later, Oh and Eickel [222] reported a 50-fold increase in the turnover frequency when the dispersion of a Rh/Al_2O_3 catalyst was decreased from 100% to 1.7%. The variation of the turnover frequency for Rh using catalysts with contents varying from 0.4 to 11.2 wt% is presented in Fig. 7. It appears that there is a certain limit to the effect. Actually, an increase of the Rh loading from 5.84 to 11.21 causes a strong decrease in the turnover frequency. Recently, Kaspar et al. [223] reported that for particles of intermediate dispersion (25–95%) the reaction rate was enhanced by an increase in the size of the rhodium particles, and that this effect was strongly dependent on the reaction temperature.

The temperature plays a very important role in this process. Yates et al. [224,225] showed that below 775 K, CO induces an oxidative disruption of the rhodium particles, and it is therefore very important to stabilize the rhodium dispersion in the catalytic conditions.

In a low pressure range (10^{-8}–10^{-4}), over the Rh surface, NO interacts selectively with CO even in the presence of oxygen, but Pt can also give high selectivities under certain conditions. Under moderate pressures, rhodium is also a very effective catalyst for this reaction.

Xu and Goodman [226] also analysed the effects of the particle size and temperature in silica-supported palladium catalysts. They reported that the reaction rate increases with the catalyst temperature, reaching a maximum at about 580 K, then declined. During the steady-state reaction of a 1:1 mixture of NO and CO, on large palladium particles the maximum rate of N_2O evolution was at 570 K, whereas N_2O was not evidenced on small particles. They concluded that the reaction pathway for the formation of N_2O is not available on small particles (<50 Å) and that the formation of N_2O requires the simultaneous presence of adsorbed NO and atomic nitrogen at sufficient coverage. In spite of these data, Valden et al. [227] recently showed that palladium clusters obtained by impregnating γ-Al_2O_3 are highly active towards the dissociation of NO and indicated the possibility of reducing NO to N_2 by CO at a rate higher than half of the CO/O_2 reaction.

Another possibility mentioned to increase the activity of palladium was to promote it with other metals. Sigg and Wicke [228] observed that Pd–Ag–Fe–Al_2O_3 catalysts are considerably active for reducing NO in the presence of excess oxygen. Hamadaoui et al. [229] indicated that silver alone had an unfavourable effect since only CO and NO are evolved on Pd–Ag. These data were attributed to a large silver migration to the surface of the catalyst. On the contrary, chromium promotes the dissociation of NO compared to pure palladium. Under static conditions, the behaviour of this catalyst is close to that of Rh. It was suggested that this behaviour was due to the influence of this element on the electronic properties of palladium.

Halasz et al. [230–233] prepared PdO–MoO_3/γ-Al_2O_3 catalysts using different methods. The catalytic activity and selectivity of these catalysts were found to be superior to PdO/γ-Al_2O_3 in slightly oxidizing conditions and at temperatures ranging from 575 to 775 K. Moreover, the selectivity to N_2 and N_2O was somewhat higher than on the commercial Pt–Rh catalyst. As in the case of chromium, these results indicate a probable interaction between Pd and Mo leading to improved yields compared with a monometallic palladium catalyst. A 10-fold excess of molybdenum oxide compared to palladium was required to reach an activity comparable to that of rhodium catalysts. Very recently, Hoost et al. [234] showed that the use of organometallic bicomponent precursors such as $[Pd_2Mo_2(C_p)_2(CO)_6(PPh_3)_2]$ (C_q – cyclopentadienyl) (Ph – phenyl) led to the same catalytic performances. A catalyst containing a very small amount of molybdenum oxide exhibits a higher selectivity to N_2 than one prepared from a monometallic precursor, but it lacks stability under the reaction conditions generally used.

A positive effect of adding a second 6 d transitional group was also reported for platinum by Regalbuto and Wolf [235]. They found that the addition of WO_3 to a Pt/SiO_2 catalyst increased its activity towards the NO+CO reaction. Kinetic experiments indicated that WO_3 serves to decrease the CO surface coverage at CO partial pressures where CO coverage on Pt is high and inhibits the access of NO. However, the rate of NO dissociation over Pt on the tungsten-promoted catalyst was slow. An explanation for this might be reduction of the number of the adjacent sites required for the dissociation of NO, caused by the patches of WO_x decorating the platinum surface ($x>3$). It was also suggested that new sites for NO dissociation could be created at the interface of the decorating WO_x patches on Pt crystallites, i.e. ''adlineation'' or ''boundary'' sites, but these are not sufficient to improve the reaction rate. Similar results were reported by Megler et al. [236,237] for Pt/SiO_2.

The addition of cobalt as CoO_x or manganese as MnO_x was found to have several effects: (a) an increased ability to dissociate NO at low temperatures compared with pure Pt. This leads to a lower onset temperature for the reaction of NO with CO; and (b) at high CO coverages, part of CO chemisorbed on the Pt surface spills over to the oxidic decorating patches, thus keeping a certain active metal surface for chemisorption of NO. An oxidation pretreatment causes a shift to higher temperatures for the conversion of NO. CoO_x/SiO_2 catalysts exhibit low conversions and low selectivity to N_2 whereas manganese oxide exhibits some activity, according to previous data [179].

Investigations using different crystallite faces seem to offer some indications about the reaction of NO with CO even though the information in the literature is sometimes contradictory. These contradictions mainly concern the formation of N_2O. Campbell and White [238] and Root et al. [239,240] did not observe the formation of N_2O neither on polycrystalline Rh wire nor on Rh(1 1 1). Castner and Somorjai [241] observed a significant amount of N_2O formation in the NO–CO reaction on Rh(s)-[6(1 1 1)×(1 0 0)]. Belton and Schmieg [242] reexamined the reaction of NO and CO over an Rh(1 1 1) surface at pressures between 2 and 120 torr and reported that N_2O was always produced for a CO:NO pressure ratio between 10:1 and 1:5 and in the temperature range 525–675 K. The selectivity for N_2O is not sensitive to the reaction temperature, overall conversion and reactant pressure and a comparison with Rh/SiO_2 catalysts shows that Rh(1 1 1) gives results very similar to those of conventional catalysts. Additional data from Permana et al. [243] confirm that the NO surface coverage plays a key role in determining the activity and selectivity of these catalysts. For coverage degrees above 0.5, the reaction is of zero-order and the selectivities are not sensitive to the reaction temperature. Conversely, for coverage degrees below 0.5, the kinetics changed from zero-order to positive order in NO and negative order in CO and the selectivities are temperature-sensitive [245]. These data prove that on Rh catalysts N_2O and N_2 are formed following parallel paths. Microkinetic data indicate no differences between Rh/SiO_2 and Rh/Al_2O_3 catalysts. DeLouise and Winograd [244] showed that, on an Rh(1 1 1) surface, more than half of the NO adsorbed to saturation desorbs as N_2 at 470–500 K. However, the question remains open as to whether the formation of N_2O is connected with certain surfaces, or to specific reaction conditions.

Graham et al. [245] investigated the oxidation of CO over Pd(1 0 0) and revealed major differences between the reaction rate of CO with NO and of CO with O_2 (about two orders of magnitude). They showed that, in contrast with Rh(1 1 1), the addition of NO to the $CO+O_2$ mixture reduces the rate of the CO_2 formation. This behaviour can also be compared to the unusual adsorption site occupation sequence of NO on Pd(1 1 2), diametrically opposed to that on Pt(1 1 2), as well as to the behaviour of other adsorbates on stepped transitional surfaces, as was recently evidenced by Yates et al. [246]. At high NO coverages, step sites are occupied, producing chemisorbed NO with their molecular axis oriented downward.

Other information about the behaviour of these metals was gathered from quantum-mechanic considerations. In recent computations using extended Huckel methods, Ward et al. [247] compared various configurations of NO adsorbed on Rh, Pt and Pd using the (1 0 0) surface as a model. The two main conclusions were that: (i) the dissociative chemisorption of NO is favoured by the Rh surface as a consequence of

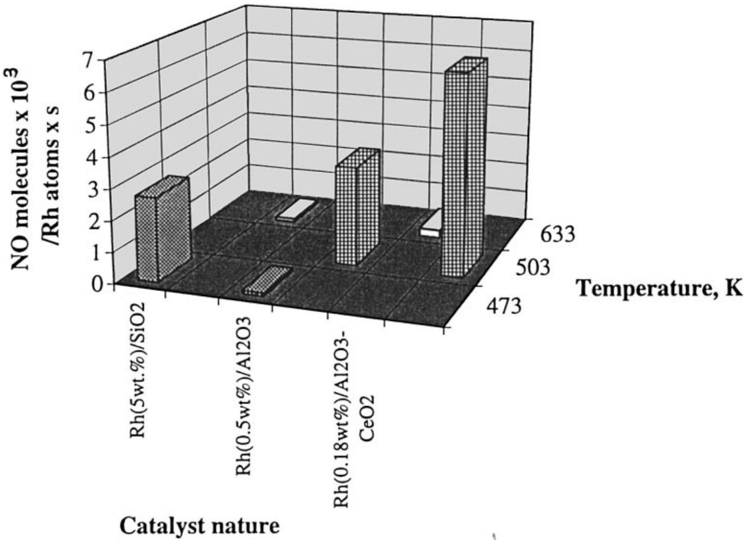

Fig. 8. Variation of the turnover of NO on different Rh loading supported on common oxides used in NO reduction with CO.

a concordance of Fermi levels of the metal with those of the adsorbed NO; (ii) it is possible to form $(NO)_2$ species from different linearly adsorbed NO. This new species gives rise to a strong N–N bond and a weakened N–O bond compared to that of single NO adsorbed molecules.

4.1.2.2.3. Effect of the support

Data reflecting the general behaviour of different supported Rh catalysts are presented in Fig. 8. This reflects the general agreement of scientists that the supports have a crucial effect upon the activity and selectivity of supported noble metal catalysts in the reduction of NO in the presence of CO [218]. In particular, several contributions in the 1970s showed that, in the presence of oxygen, cerium acted as an "oxygen storage" compound and enhanced the stability of the catalysts. In addition, because of its thermal stability, cerium stabilizes the dispersion of noble metals [248–255]. However, it seems that the effect of cerium is observed mainly in mixed oxides without noble metals. Yao and Yao [256] investigated CeO_2 and CeO_2/Al_2O_3 catalysts and showed that the deposition of CeO_2 increased the oxygen storage capacity, compared to pure CeO_2 oxide. After impregnation with noble metals, this capacity decreased in the order Pd>Rh>Pt. At the same time, the activation energy for the formation of CO_2 decreased by more than 10 kcal mol^{-1} [257,258]. The remark of Rao et al. [259] that the promoting effect of cerium in the reduction of nitrogen oxide can be attributed to the redox couple Ce^{3+}<->Ce^{4+} is logical. However, the situation seems more complex.

The effect of cerium was extensively analysed during the Second International Symposium on Catalysis and Automotive Pollution Control held in Amsterdam in 1991. It was clearly shown [260] that cerium plays a double role: one, known previously, is to stabilize the metal dispersion (i.e. Pt or Rh) and the other is to promote an enhanced activity for the reduction of NO. This enhancement seems to be associated with ionized vacancies in the CeO_2 lattice [261] located near the noble metal crystallites. Loof et al. [262], based on TPD spectra of NO and CO, indicated the presence of a significant noble metal–cerium interaction for Pt, Rh and Pt+Rh supported on Al_2O_3. The long-term stable capacity to dissociate NO from cerium containing catalysts was attributed to an oxygen spillover from the noble metal to the oxygen vacancies in the reduced cerium. Rhodium surfaces, as Zafiris and Gorte [263,264] suggested, are partially covered with cerium after heating and this could also be the case in the case of lanthanum. If oxide species could partially spread onto the metal, oxygen could migrate through these entities and create a larger interface between the oxide and the metal. CO could react with NO at this interface or border.

On Pt/Al_2O_3 the positive effect of cerium can be detected at low temperatures. The conversion of NO then gives mainly dinitrogen oxide. Leclercq et al. [255] showed that the addition of cerium promoted the reaction because of its affinity for atomic oxygen. On Pt/Al_2O_3 catalysts with or without cerium, in the presence of oxygen, the conversion of NO is low until the oxygen disappears from the gas phase. This behaviour is due to a weak adsorption of NO compared to that of oxygen. The adsorption of NO is less depressed in the presence of rhodium, as was mentioned before.

Other positive effects of cerium were reported by Cho et al. [265,266] who indicated that the nature of the support had an influence on the selectivity to N_2O. On Rh/Al_2O_3 the conversion of both NO and N_2O is favoured in the temperature range 475–525 K, whereas on Rh/CeO_2–Al_2O_3 and Rh/CeO_2 it is favoured at about 675 K. The contribution of cerium in the suppression of N_2O formation was also stressed by Oh [267].

The oxygen storage and transport characteristics of cerium oxide doped with gadolinia compared to alumina are even higher than for pure CeO_2 (one order of magnitude greater). This modification is consistent with a significant enhancement of the transient catalytic activity of supported rhodium in the NO with CO reaction under cycled feedstream conditions.

A positive effect of the support was also reported for lanthanum. Schaper et al. [268,269] and Bettman et al. [270] indicated that the main effect of lanthanum is to prevent the sintering of alumina. Recently, Shelef et al. [198,271] gave additional arguments in favour of the idea that, even though it is valence-invariant (i.e. does not act as an oxygen storage), lanthanum is very effective for the support stability. Some modern versions of automotive catalysts contain significant amounts of this oxide. The presence of lanthanum or neodymia is consistent with a diminution of the surface area loss at high temperatures but the activity of the catalysts is lower compared to that of Rh/Al_2O_3 [272].

Some additional evidence on the effect of the support was given by Kudo et al. [273] for platinum catalysts. The experiments carried out both in the absence and the presence of water revealed that the activity strongly depends on the nature of the support (in the order $TiO_2 > Nb_2O_5 > SrTiO_3 > Al_2O_3 > SiO_2$) and on the reduction pretreatment temperature. An SMSI effect was also mentioned.

This review shows that the effect of the support is very complex. Nevertheless, it seems that two main favourable effects can be expected from supports, especially supports modified by Ce or other rare earth oxides, namely to improve both the oxygen storage and the stability of the noble metals. This is the key to the development of improved catalysts.

4.1.2.2.4. Catalyst stability

Formation of NCO groups on the catalysts. Lorimer and Bell [274] mentioned that, under reducing conditions, noble metal catalysts suffer a decline in NO reduction and simultaneously, that CO_2 production is higher than the stoichiometric amount expected for the NO with CO reaction. Under these conditions, IR spectra revealed a strong NCO band and a weaker CN band. Experimental data indicated that part of the NO (less than 5%) is consumed for the generation of these groups. It seems that the NCO species are formed on the metal surface and NCO then migrates to the support surface. However, NCO species on the metal surfaces resulted from the interaction of adsorbed N atoms and gaseous CO molecules exhibit a very low stability and were detected only with experimental precautions. Contrarily, Al–NCO or Si–NCO are rather stable and easily detectable in the IR spectra. The Si–CN bond was thought to thermally decompose Si–NCO.

Apparently, the low stability of NCO species on the metal surfaces and the catalyst deactivation seem contradictory. Other experiments performed by Hecker and Bell [276] on Rh/SiO_2 catalysts clearly demonstrate that the rates of formation and decomposition of Rh–NCO and Si–NCO differ substantially. A possible explanation for the contribution of these species to catalyst deactivation is given by Lorimer and Bell [274]. They assumed that the presence of NCO species resulted from migration of those preformed on the metal particles or even by

$$Si + NO + 2CO \rightarrow Si{-}NCO + CO_2 \qquad (3.42)$$

can determine a change in the local electronegativity of the support that could cause a charge transfer from the metal to the support and a decrease in the availability of noble metal electrons for interaction with the adsorbent.

Niiyama et al. [275], who used Pt/Al_2O_3 catalysts, proposed an alternative mechanism in which NCO species are primarily formed on the support surfaces and then migrate onto the metal crystallites where they avoid the interaction of NO with the surface. However, the above mentioned differences between the stability of NCO on the metals and support surfaces does not sustain such an idea.

In oxidation conditions, i.e. in the presence of an excess of NO, the CO coverages are reduced and in consequence the formation of NCO is very limited.

Sintering and formation of noble metal oxides. Important changes in the physical characteristics of the catalysts can result from the atmosphere in which the catalysts were pretreated [277]. For both Rh and Pt, the dispersion is not severely damaged in the reductive conditions, even at high temperatures. Conversely, the treatment of these catalysts in an oxidizing environment causes a rapid oxidation of supported Rh and its subsequent dissolution into the support. In an oxidizing environment [272], the rise of temperature increases the rate of this process. Unlike Pt, supported Rh can easily be reduced and/or oxidized under relatively mild conditions. The reduction of oxidized Rh allows only a partial recovery of its initial state, partly as sintered particles. However, low dispersions of Rh seem to have a positive effect because for CO oxidation highly dispersed Rh are less active than large ones. Inactive oxygen species are formed on highly dispersed catalysts because of a higher percentage of edges and steps where O_2 dissociation occurs preferentially. Therefore, sintering of catalysts may lead to a decrease of such inactive oxygen species. Furthermore, CO itself can disrupt or disperse relatively small Rh particles into isolated Rh(I) species. The oxidation of Rh particles can be limited by increasing the rate of alternate oxidizing/reducing conditions.

Investigations of rhodium supported on different supports: CeO_2 and SiO_2 [278,279], Al_2O_3 [280], CeO_2–SiO_2 [281], CeO_2–Al_2O_3 [257], using elaborated techniques (TEM, HREM, EELS and XPS), allowed Schmidt et al. [278,279] to reach useful conclusions about the influence of the support on the catalyst stability. Highly dispersed silica-supported Rh loose the metal in mixture of NO and CO at relatively low temperatures. NO contributes to the dispersion of the Rh particles whereas CO favours the volatilization of dispersed Rh, although heating in CO alone has no effect on dispersed Rh. Preoxidation increases the volatilization of Rh and this should be correlated with the capacity of CO to disrupt small metal particles. The addition of cerium was found to hinder the loss of Rh. On alumina only an insignificant loss of Rh was evidenced even though NO has the same dispersing effect upon supported particles.

Other studies made by Mergler and Nieuwenhuys [282] investigating the influence of CeO_x upon Pt/Al_2O_3 showed that the beneficial effect of cerium against Pt deactivation is due to the fact it controls less platinum oxide formation. Platinum oxidized species form with CO relatively stable Pt^{n+}–CO structures up to 400°C. Using CeO_x modified Al_2O_3 support, the main inhibitor species (CO) are slowly removed with oxygen generated by the dissociation of NO on CeO_x or by the lattice oxygen of CeO_x.

Lee et al. [283] also observed morphological transformations of Pt particles resulting from the aggregation of irregular small clusters to uniform and polyhedral shapes in the presence of NO–CO gases on Pt deposited on highly oriented pyrolytic graphite. A possible explanation for the shape transformations of Pt particles is the adsorption of gaseous species. At high temperatures, the NO–CO reaction causes a modification of the graphite pore structure, when Pt particles attack the edges and step off the based plane of graphite.

In a recent review on nitric oxide catalysts in automotive exhaust systems, Taylor [284] (and references herein) described the effect of sulphur dioxide on the activity of the catalysts. In the presence of SO_2 resulting from combustion processes, much of the activity of these catalysts is deteriorated. Sulphur dioxide interacts both with the noble metal and with the support. On the support, sulphur is stored as sulphates and sulphites. The sulphur can easily be removed by a treatment in reducing conditions at high temperatures (975 K). In the presence of cerium, the activity is recovered more quickly. Noble metals exhibit an opposite effect: sulphur is retained under reducing conditions and can be removed in an oxidizing atmosphere. Pt and Rh can rapidly recover their activity whereas Pd cannot.

4.1.2.2.5. Mechanism and kinetics

The mechanisms suggested for the reduction of NO in the presence of CO over supported noble metals are not essentially different from those discussed in the case of oxides. However, the reaction is more complex because these metals participate to the reaction with different faces with different activities and because of the strong influence of the metal dispersion.

A first attempt to understand the mechanism of the catalytic reduction of NO in the presence of CO on alumina-supported noble metal catalysts is due by Unland [287,288], using the method commonly used in such studies, namely IR spectroscopy [274,285–288]. The IR spectra recorded by Unland in the presence of all potential active noble metals: Ru, Rh, Pd, Pt and Ir, indicated that, all catalysts with the exception of ruthenium which presented the weakest band for freshly prepared catalysts, presented a very intense band located at 2264 cm^{-1}. This led the authors to point to NCO species as intermediates in the reaction. However, numerous later studies [289–293] clearly established that this band was due to the isocyanate species bound to the alumina support and not to the metal. A similar Si–NCO band was also identified on Pt/SiO_2 catalyst surfaces [274]. Instead, on Rh/SiO_2 catalysts, Solymosi and Sarkany [286] identified another very weak band at 2195 cm^{-1} which was assigned to Rh–NCO. Other evidence of the formation of M–NCO intermediates on VIIIth group metal catalysts was then reported in [294–296] for Ru and Ni supported on silica, for Pt/SiO_2 [276,297], Ru/ZnO [298] as well as for MO_x (M=Co, Mn, Ce) modified Pt/SiO_2 or Pt/Al_2O_3 catalysts [237,282].

Lorimer and Bell [274] considered the following steps for the reaction of NO with CO, also based on IR investigations:

$$CO + M \rightarrow M{-}CO \tag{3.43}$$

$$NO + M \rightarrow M{-}NO \tag{3.44}$$

$$M + M{-}NO \rightarrow M{-}N + M{-}O \tag{3.45}$$

$$M{-}N + M{-}N \rightarrow N_2 + 2M \tag{3.46}$$

$$M{-}N + M{-}NO \rightarrow N_2O + 2M \tag{3.47}$$

$$M{-}N + NO \rightarrow N_2O + M \tag{3.48}$$

$$M{-}O + CO \rightarrow CO_2 + M \tag{3.49}$$

$$M{-}N + CO \rightleftarrows M{-}NCO \tag{3.50}$$

Under reducing conditions, they assumed that the rate of the NO disappearance can be expressed as

$$r_{NO} = \frac{k_{45} \cdot K_{44} \cdot p_{NO}}{(1 + K_{43} \cdot p_{CO} + K_{44} \cdot p_{NO})^2}, \tag{3.51}$$

where k_i and K_i represent the rate coefficient and equilibrium constant for reaction i, respectively. Other experiments on Rh/SiO_2 catalysts, carried out by Hecker and Bell [276], concluded to the same steps but, instead of Eq. (3.46), Hecker and Bell suggested

$$M{-}NO + M{-}N \rightleftarrows N_2 + M{-}O + M \tag{3.52}$$

In those conditions a new expression of the rate of the NO disappearance was considered:

$$r_{NO} = \frac{k_{45} \cdot K_{44} \cdot p_{NO}}{1 + K_{44} \cdot p_{NO} + [K_{43} + K_{50} \cdot k_{45}/(k_{52} + k_{47})] \cdot p_{CO}} \tag{3.53}$$

This equation takes into account the contribution of the additional steps ((3.47) and (3.52)) and equilibria ((3.50) and (3.52)). Both expressions stress the fact that chemisorption of NO and CO on the noble metal surfaces is strong.

On Rh/Al_2O_3 and Rh/CeO_2 catalysts using transient isotopic cycling and steady-state experiments, Cho et al. [265] identified the same elementary surface processes as Hecker and Bell [276] and a few additional processes:

$$M{-}N_2O \rightarrow N_2O + M \tag{3.54}$$

$$M{-}N_2O \rightarrow N_2 + M{-}O \tag{3.55}$$

$$M{-}O + M{-}CO \rightarrow CO_2 + 2M \tag{3.56}$$

The reason why N_2O was generally not observed at temperatures of about 675 K on Rh/CeO_2 or Rh/CeO_2–Al_2O_3 is not the absence of N_2O formation but its fast reaction with CO [267]. This means that an additional step, the rate of which is as fast as or even faster than the rate of the overall NO with CO reaction, must be considered in the reaction mechanism

$$M{-}N_2O + M{-}CO \rightarrow 2M + CO_2 + N_2 \tag{3.57}$$

According to these data, the rate of the steady-state reaction of N_2O with CO is limited primarily by the rate of N_2O adsorption. No special contribution of the supports, namely of CeO_2 modified ones, was reported. The steps facilitated by its presence, from a kinetics point of view, are mainly connected to atomic oxygen species and are frequent enough to be limitative.

Recent IR-pulse transient studies on Rh/SiO_2 catalysts by Chuang et al. [299–301] showed that the mechanism of the reduction of NO by CO eventually corresponds to an oxidation–reduction mechanism at the surface of the noble metal. The adsorption of NO on the reduced Rh was found to result in the formation of an Rh^+ site that then chemisorbs either NO or gem-dicarbonyl.

$$NO_g + Rh^0{-}CO \rightarrow Rh^0{-}NO^- + CO_g \tag{3.58}$$

$$Rh^0{-}NO^- + 2Rh^0 \rightarrow (O^{2-})2Rh^+{-}NO + Rh^0{-}N \tag{3.59}$$

$$Rh^+ + NO_g \rightarrow Rh{-}NO^+ \tag{3.60}$$

$$Rh{-}NO^+ + 2CO_g \rightarrow Rh^+{-}(CO)_2 + NO_g \tag{3.61}$$

$$Rh^+ + 2CO_g \rightarrow Rh^+{-}(CO)_2 \tag{3.62}$$

The formation of the Rh^+–$(CO)_2$ gem-dicarbonyl is a key step in this reaction because this species can either undergo reduction to form aggregates of Rh^0–CO and CO_2:

$$2Rh^+(CO)_2 + O^{2-} \rightarrow Rh^0{-}(CO)\ (\text{linear}) + CO_2 + CO \tag{3.63}$$

or rapidly react with oxygen from dissociated NO to produce CO_2:

$$Rh^+(CO)_2 + 2O_{ad} \rightarrow 2Rh^+ + 2CO_2 \tag{3.64}$$

The formation of N_2O occurs on reduced Rh^0 sites as follows:

$$Rh^0{-}NO^- + Rh^0{-}N \rightarrow 2Rh^0 + N_2O \tag{3.65}$$

whereas the formation of N_2 occurs as follows:

$$Rh^0{-}N + Rh^0{-}N \rightarrow 2Rh^0 + N_2 \tag{3.66}$$

In addition to these data Belton et al. [302] showed that the formation of N_2 from atomically adsorbed species is at least 50 times faster than the other steps, indicating that the N atom recombination is not the rate-limiting step in this reaction. These data led to the conclusion that the NCO species is not directly involved in the formation of CO_2.

Goodman et al. [303], considering results obtained by Schwartz et al. [304], Peden et al. [305] and Bowker et al. [306], also concluded that step (3.49) on the Rh surface is a Langmuir–Hinshelwood reaction and occurs rapidly with a relatively low activation energy. This reaction is structure-sensitive in a low CO and high oxygen coverage regime, whereas it is structure-insensitive on a higher CO coverage.

Pt/Al_2O_3 was also kinetically investigated in this reaction. Using TAP experiments, Burch et al. [307] suggested a very simple mechanism:

$$2Pt + NO \rightarrow Pt{-}N + Pt{-}O \tag{3.67}$$

$$2Pt{-}N \rightarrow Pt + N_2 \tag{3.68}$$

$$Pt{-}O + CO \rightarrow Pt + CO_2 \tag{3.69}$$

Recently, Kostov et al. [287] (and references herein) investigated the NO with CO reaction on the surface of Ru(0 0 1) and showed that the presence of adsorbed O is a necessary condition for step (3.50). Two mechanisms were proposed to explain these results: one, considering the influence of the O induced dipoles as "external" field on N_{ad} and CO_{ad}, similar to step (3.47) on Pt(1 1 1) in a high electric field; and the other, considering O induced changes of the adsorption properties of Ru(0 0 1) leading to new more favourable sites for step (3.52).

The investigation of monocrystal surfaces also offered very useful information. Lambert and Comrie [308] investigated the catalytic reduction of NO with CO on Pt(1 1 1) and (1 1 0) surfaces and proposed the dissociation of NO as the rate-limiting step. Evidence of the dissociation of NO was given by numerous techniques: field electron microscopy, LEED, UPS, XPS, and Auger electron spectroscopy [309,310]. Sawabe and Matsumoto [315] reported an oxygen-exchange reaction between O_2 and NO coadsorbed on a Pt(1 1 1) surface. This constitutes an additional argument in favour of an NO dissociation. Nitrogen was shown to be formed by the recombination of adsorbed nitrogen atoms whereas N_2O was formed by one of these atoms reacting with adsorbed NO [316,317].

Studies done on Pt(1 0 0) [311–316] indicated that the catalytic reaction of NO with CO occurred according to a different path: NO and CO co-adsorbed on the surface react with sharp desorption peaks of the reaction products at temperatures below 375 K, and CO_2 exhibits a kinetic oscillation under steady flow conditions. Slin'ko and Jaeger [317] (and references herein) showed that both phenomena could be attributed to a phase transition on the Pt(1 0 0) surface (from hex to a 1×1 structure of the catalyst surface). The reaction mechanism includes the step previously presented. Kinetic oscillations were also observed during the reaction of CO and NO on an Rh(1 1 0) single crystal surface for CO rich mixtures and in an unusually high temperature range (above 900 K), but the mechanism responsible in this case is not clear [317].

For polycrystalline Pt, an oscillatory behaviour [313] in the CO with NO reaction was observed at low pressures (about 10^{-4} torr), but the introduction of oxygen led to the disappearance of the effects. This effect was also reported on Pt/SiO_2 (5 wt%).

Surface-enhanced Raman spectroscopy as an in situ time probe of catalytic mechanisms carried out at atmospheric pressures by Williams et al. [318,319] offered additional information concerning the dissociation of NO on Rh, Pt or Pd films. The findings suggested that the higher the ability to dissociate NO, the lower the selectivity toward N_2O. Under a Pd surface under similar conditions, the NO dissociation products blocked the adsorption of CO whereas significant quantities of CO were detected over Pt.

A more general treatment of the kinetic phase transition in a three-component NO–CO–O_2 heterogeneous catalytic reaction was given by Yaldram et al. [320,321], using a Monte-Carlo simulation. From these simulations they concluded that the catalytic surface is more efficient in giving a steady reactive state in the case of three components than in the respective NO–CO two-component reactions.

4.1.3. *Metal zeolites*

Recently, metal zeolites were investigated for the reduction of NO by CO, but their activities and selectivities are inferior to those of noble metal catalysts. Therefore, no special effort was made to obtain information about the reaction mechanism and the catalysts were not characterized in detail. In particular, the position of the noble metal, as small particles on or in the zeolite crystallites, or on amorphous part of the zeolites was not determined. Tzou et al. [322] studied the activity of Pt–Rh/Na-Y catalysts. They reported that alloy particles of Pt–Rh_2 included in Na-Y zeolites are more active than monometallic components in the reduction of NO with CO. Kato et al. [323] reported high activities for zeolite-supported noble metals (Rh, Pt or Pd) promoted with Ti, Mo, V, Cr or W oxides. Later, Ichikawa et al. [324–327] investigated the activity of high load Au-ZSM-5 and Au–Na-Y obtained by the interaction of ZSM-5 with gaseous $AuCl_3$ and reductive carbonylation. In situ IR studies of the reaction showed a reduction of NO to N_2O, an undesirable product. They associated the formation of different intermediates formed on Au–Na-Y ($Au(N_2O_3)$) and Au-ZSM-5 ($Au(NO)_2$ and $Au(NO_2)$) with the different acidic properties of these zeolites. Other studies using CuO/mordenites [328] or Cu supported on faujasite-type zeolites obtained from fly ash [329] were also made. However, this latter paper relates a rather surprising support considering the nature of the precursor in its synthesis.

Iron-clusters obtained by exchange were used by Okamoto et al. [330] in the same reaction. They reported that ($FeO_{1.5}$)–Na-Y catalysts exhibit some activity in the reaction of NO with CO (about 60% NO conversion to N_2) at temperatures above 550 K. Fe-mordenite [331] and Fe–Al_2O_3 catalysts show a very low activity in the same conditions. Sidamonidze et al. [332] proposed a Cu-clinoptilolite catalyst for the same reaction.

4.1.4. *Perovskites*

Perovskites have been extensively investigated in catalysis in the last few years. Recently, two reviews reviewed the activity of these catalysts; one by Viswanathan [333] concerned the oxidation of CO by NO and the other, more general, by Tejuca et al. [334], included considerations about this reaction.

It has been shown above (see 2.1.2) that the introduction of lanthanum leads to an increase in the catalytic properties and especially the stability of this reaction, even though lanthanum oxide does not possess oxygen storage capacities. In fact, one may speculate that the beneficial role of lanthanum would be to form mixed oxides with the general formula ABO_3 (A being the cation with larger radius), named perovskites, with transitional metals. Perovskites are believed to constitute excellent matrixes for catalyticals. The interest first stemmed from studies that showed that the perovskite structure could stabilize the noble metals and should thus increase their thermal stability. Ruthenium was shown to have the highest activity among the noble metals in this reaction but, unfortunately, a very low stability. Shelef et al.

[335,336] suggested to increase the stability of ruthenium by including Ru^{3+} or Ru^{4+} ions in a perovskite structure. Another reason for using perovskites is that nearly all the experiments with NO carried out until now in environmental catalysis indicated that the bottleneck was the capacity of the catalysts to eliminate oxygen at the temperature of reaction. The variable oxygen stoichiometry of the perovskite structure gave rise to great expectations in that direction. It was expected with these catalysts to eliminate noble metals and to use base metal oxides as active catalysts for the elimination of NO.

Perovskites containing lanthanum and, more recently, yttrium were mainly investigated. The first studies by Voorhoeve et al. [337–341] and Yao [342] used $LaCoO_3$ and $LaMnO_3$ perovskites. Later, Mizuno et al. [343] reported results obtained on $LaCuO_4$ perovskites whereas Tascon et al. [344] obtained their results on $LaCrO_3$, $LaFeO_3$, $LaMnO_3$, $LaCoO_3$ and $LaNiO_3$ perovskites.

The data obtained in these studies indicated that the specific activity of these catalysts could vary considerably depending on the method of preparation. Generally, these catalysts exhibit a good activity for NO reduction and CO oxidation at temperatures above 475 K but the selectivity to N_2 is not always very good. On La_2CuO_4 the selectivity is lower than 20%, whereas the selectivity to N_2 reaches 100% on $LaMnO_3$ [334]. At higher temperatures, the kinetic parameters for CO oxidation over the most active $LaCoO_3$ change because the reaction is controlled by the rate of diffusion of the reactant or the product molecules between the gas phase and the catalyst surface. The maximum NO conversion on $LaCoO_3$ perovskites is approximately 95% and up to 85% for CO [334]. However, recent studies by Simonot et al. [345] indicated that this perovskite is inferior to Co_3O_4 for which the global activities are considered.

The conversion of CO in the presence of NO on different rare earth perovskites is presented in Fig. 9.

A large amount of substituted perovskites was also investigated. Bismuth, e.g. was intensively studied [334]. $(La_{0.85}Bi_{0.08}K_{0.07})$ MnO_3 exhibits a high activity but a poor stability because of the presence of low melting-point components. La_{2-x} Sr_xNiO_4 also exhibits good activities but an important part of the NO is transformed into N_2O [346]. Mizuno et al. [347] reported that completely substituted $Bi_2Sr_2CaCu_2O_4$ shows some catalytic activity for the reaction between NO and CO, and that the valence of copper is close to two (2) in these catalysts. $LaCrO_3$-substituted perovskites like $La_{0.7}Sr_{0.3}CrO_3$, $LaCo_{0.5}Cr_{0.5}O_3$ or $La_{0.7}Sr_{0.3}Cr_{0.95}Ru_{0.05}O_3$ have been shown to be effective catalysts for this reaction, the conversion being higher (over 80%) than the conversions of both reactants combined [348]. Several superconducting lanthanide mixed oxides containing yttrium also exhibit some activity in this reaction. Mizuno et al. [349] reported that $YBa_2Cu_3O_y$ has a good activity and a good selectivity to N_2 (about 95%). Shelef et al. [350] and Lin et al. [351] also reported on the activity of these catalysts.

The deposition of these perovskites modifies their catalytic behaviour. La_2CuO_4 supported on ZrO_2 showed a low selectivity to N_2 (12% N_2 and 88% N_2O) [352] whereas only N_2 was evidenced on $LaNiO_4$ supported on Al_2O_3 or ZrO_2 [334]. La_2NiO_4 perovskites supported on ZrO_2 prestabilized by adding

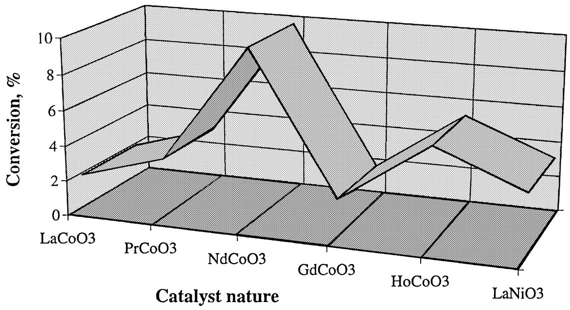

Fig. 9. CO conversion in the presence of NO on different perovskites (NO 2.0 vol%, CO 1.4 vol%, space velocities: 1400 h^{-1}, temperature: 450 K).

La_2O_3 exhibited more activity than $LaNiO_3/Al_2O_3$ [353]. An explanation of this behaviour was that the Ni^{2+} contained in La_2NiO_4 is more active than the Ni^{3+} contained in $LaNiO_3$. Ni^{2+} was thought to diminish the adsorption strength of oxygen, whereas Ni^{3+} would favour a strong adsorption of oxygen. A comparison with unsupported La_2NiO_4 indicates an activity nearly five times higher than the supported perovskite. There is an important yield of N_2O on supported perovskites up to 800 K but it decreases at higher temperatures. Studies performed by Lin et al. [351] using XPS and FT-IR techniques evidenced a strong modification of the catalyst surfaces with the generation of nitride, nitrite and nitrate groups.

Up to now the reported data indicate that perovskite catalysts are inferior to noble metals.

4.1.4.1. Catalyst stability. Yao [342] investigated the stability of a few perovskites ($LaCoO_3$, $LaMnO_3$) and substituted perovskites (La_{1-x} Pb_x MnO_3) in the presence of water and SO_2. These experiments revealed that the introduction of water caused an immediate decrease in the activity, the specific activity being comparable to that of Co_3O_4 at low temperatures. Conversely, the introduction of 0.1 vol% SO_2 determined an increase in the activity of substituted perovskites containing 300 ppm of Pt. However, the effect of SO_2 is generally to depress, rather than to increase activity. On perovskites containing lanthanum, the total amount of SO_2 needed to cause a more than 90% reduction in the reaction rate was found to be approximately that of a monolayer. Tejuca et al. [334] suggested that the poisoning effect of SO_2 on perovskites is due to the adsorption on B sites (the cations with smaller radius) or oxygen anions, which are the centres responsible for the catalytic action. SO_2 may also interact with cations in position A, but this process does not result in the deactivation of the catalysts. A good stability of the perovskites against lead poisoning was also reported [344]. These data seem to indicate a superior resistance of perovskites to contaminants other than metal oxides of other structure.

4.1.4.2. Mechanism and kinetics. Ladavos and Pomonis [353] consider that the reaction between nitric oxide and carbon monoxide on perovskite surfaces corresponds to the following sequence of elementary surface processes:

$$NO \rightarrow NO_{ads} \tag{3.70}$$

$$NO_{ads} \rightarrow N_{ads} + O_{ads} \tag{3.71}$$

$$CO \rightarrow CO_{ads} \tag{3.72}$$

$$CO_{ads} + O_{ads} \rightarrow CO_2 \tag{3.73}$$

$$2N_{ads} \rightarrow N_2 \tag{3.74}$$

$$N_{ads} + NO_{ads} \rightarrow N_2O_{ads} \tag{3.75}$$

$$N_2O_{ads} \rightarrow N_2O \tag{3.76}$$

$$N_2O_{ads} \rightarrow N_2 + O_{ads} \tag{3.77}$$

$$2O_{ads} \rightarrow O_2 \tag{3.78}$$

They suggested that, at low temperatures, the reaction was controlled by the oxygen generated through the decomposition of nitric oxide. This oxygen keeps the surface oxidized competing with NO for the active site

$$r_{NO} = k_{71}\theta, \tag{3.79}$$

where θ is the oxygen surface coverage and k_i is the constant rate of step i, while at high temperatures the reaction is controlled by the oxygen-scavenging process through the reaction between CO_{ads} and O_{ads}:

$$r_{NO} = k_{71}\theta_{CO}\theta_{O}. \tag{3.80}$$

These equations lead to the following explanation. At low temperatures, the surface of perovskites is covered by NO_{ads} (which dissociates with difficulty) and N_2O_{ads}. In such conditions, the reaction is zero-order with CO. At high temperatures, the dissociation of adsorbed NO occurs quickly. In these conditions the surface is mainly covered by O_{ads} but the reaction order to CO coverage changed from 0 to 1.

4.1.5. Alloy catalysts

In a previous section it was shown that supported Pt–Rh bimetallic catalysts are frequently used in the purification of automotive exhaust gases. The advantages of bimetallic catalysts are always connected to the increase in the activity and selectivity and in many cases also to the resistance to different poisons. Kim and d'Aniello [354,355] stressed the possibility that precious metals form alloy particles during the reactions that occur on three-way catalysts.

Nieuwenhuys et al. [356,357] investigated the interaction of NO with CO on silica-supported Pt_x–Rh_{1-x}

alloys with different compositions x=0; 0.25; 0.5; 0.75 and 1. At temperatures above 520 K the main reaction product was N_2 and only traces of N_2O were detected, no matter what the alloy composition. An Rh-rich alloy, $Pt_{0.25}Rh_{0.75}$, presented a noticeable activity caused by the beneficial presence of both Rh and Pt. The CO molecules tend to coordinate to Pt sites, thus explaining the low inhibition of CO on Rh sites, and the NO molecules coordinate primarily to Rh sites. The activity of this catalyst was superior to that of Pt or Pt-rich alloys, both under CO-rich and CO-lean conditions. In addition, IR analysis showed that the isocyanate band is lower than on pure Rh, indicating that in the case of the alloy, either only a few sites were available for the formation of these species or the reaction was faster. An Rh-rich alloy catalyst ($Pt_{10}Rh_{90}$) was also investigated by Ng et al. [358] who reported that the behaviour of a $Pt_{10}Rh_{90}$ (1 1 1) single crystal varied depending on the temperature. At low temperatures, i.e. <700 K, or low conversions, an important decrease in the selectivity to N_2 versus N_2O was obtained. Conversely, at high temperatures or high conversions, the selectivity to N_2 was total. Both selectivity and overall reaction rate were controlled by the NO adsorption/desorption equilibria. The surface of these catalysts corresponds to Pt diluted by Rh. To explain the catalytic behaviour, namely a superior activity compared with monometallic catalysts, these authors, in addition to Nieuwenhuys et al. [356,357], suggested that an averaged electronic effect resulting from interaction of the two metals also plays an important role.

Recently, it was mentioned that the use of amorphous alloy catalysts offered another possibility to carry out this reaction at high conversions with high selectivities. Hashimoto et al. [359,360] investigated the activity of $Ni_{70-x}Ta_{30}M_x$ and $Ni_{58}Nb_{40}M_2$ alloys containing a few at% (x=1, 2, 3) of noble metal (M= Rh, Pt, Ir, Ru, Pd). The activation of these catalysts was performed in a hydrogen fluoride solution. The activation treatment created very rough surfaces consisting of microcrystallites with a high surface concentration of platinum group elements. However, a prolonged time of exposure to hydrogen fluoride seems to have a negative effect. The following order of activity was found for both amorphous alloys: Rh> Pt>Ir≫Pd>Ru. The reaction occurs at relatively low temperatures (<475 K) on a few nm thick oxide films on the surface-activated amorphous alloy without an accompanying oxide growth. On non-activated surfaces, by contrast, the reactions at higher temperatures led to the formation and growth of a nickel oxide film.

High conversions were also reported by Inoue et al. [361,362] who showed that amorphous alloys like $Pt_{30}Zr_{30}$ permit high conversions (about 83% at 523 K) in conditions of high selectivity (N_2:N_2O=9:1).

4.1.5.1. Mechanism and kinetics. IR measurements performed by van Slooten and Nieuwenhuys [356] indicate that both Pt and Rh sites are present at the surface of the Pt–Rh alloy catalysts and that CO molecules have a tendency to adsorb on Pt atoms while NO molecules primarily adsorb on Rh atoms. The mechanism of the reaction of NO with CO they proposed [353] agrees with the mechanism proposed by Ng et al. [358] based on Auger electron spectroscopy and activity data on a Pt–Rh (1 1 1) monocrystal surface:

$$\mathrm{NO + M \rightarrow M{-}NO} \qquad (3.81)$$

$$\mathrm{M{-}NO + M \rightarrow M{-}N + M{-}O} \qquad (3.82)$$

$$\mathrm{CO + M \rightarrow M{-}CO} \qquad (3.83)$$

$$\mathrm{M{-}N + M{-}N \rightarrow N_2 + 2M} \qquad (3.84)$$

$$\mathrm{CO{-}M + M{-}O \rightarrow CO_2 + 2M} \qquad (3.85)$$

As intermediate steps, Ng et al. [358] suggested:

$$\mathrm{CO{-}M + M{-}O \rightarrow CO_2{-}M + M \rightarrow CO_2 + M} \qquad (3.86)$$

$$\mathrm{M{-}NO + M{-}N \rightarrow N_2 + M{-}O + M} \qquad (3.87)$$

$$\mathrm{M{-}NO + M{-}N \rightarrow N_2O + 2M} \qquad (3.88)$$

Step (3.88) could also follow another path:

$$\mathrm{M{-}NO + M{-}N \rightarrow M{-}N_2O + M \rightarrow N_2O + M} \qquad (3.89)$$

Ng et al. [358] found a difference in kinetic behaviour, depending on the temperature range. At temperatures below 700 K, the conversion of NO with CO on Pt–Rh alloy catalysts is remarkably insensitive to the reaction conditions: gas phase composition, reaction temperature and NO conversion. Under these conditions, the reaction is of a zero-order for both NO and CO pressure. Adsorbed NO strongly inhibits the NO dissociation reaction (step (3.82)), keeping the N surface coverage low. At temperatures above 700 K, the NO surface coverage decreases, accelerating the NO dissociation reaction and increasing the N+N reaction. Under these conditions the overall reaction becomes non-zero order with respect to both reactants.

4.1.6. *Monolithic catalysts*

Monoliths as structured catalysts have well-recognized applications [9] (and references herein). Monoliths have been successfully used as afterburners for engines to reduce the carbon monoxide, hydrocarbons and nitrogen oxides content in exhaust gases. However, the transfer from powder to monolithic catalysts presupposes some additional investigation. Many researches are still focusing on the investigation of mixtures of different oxides or of oxides and noble metal catalysts.

Stegenga et al. [174] investigated a Zr-stabilized Degussa monolith prepared by using washcoats corresponding to 10 wt% Cu–Cr loading on Al_2O_3 or 2.5 wt% La-stabilized Al_2O_3. These monoliths had a behaviour typical of three-way catalysts. In an overall oxidizing environment, the conversion of CO was high and the conversion of NO very low, whereas in a reducing environment, the conversion of NO was high and the conversion of CO fairly low. Around stoichiometric conditions, both NO and CO conversions reached a high level.

Monoliths with noble metal loading have also been investigated [9]. Unfortunately, the long-term stability of these catalysts is a very serious problem. Monoliths are extremely sensitive to temperature, poisons (lead, sulphur) and reactant concentrations and are moderately sensitive to changes in the space velocity. Prolonged exposure to the flow gases at high temperatures causes a loss of the active metal and a deterioration of the catalyst support. However, one should note that, compared with the packed beds, the mechanical integrity of a monolithic structure is superior and also the resistance against durst is higher. Some Japanese patents by Inoue et al. [361,362] and Muramatsu and Yoshida [363,364] also report an improved activity of honeycomb catalysts in the same reaction.

4.2. *Catalytic reduction of NO in the presence of hydrogen*

The reduction of NO in the presence of hydrogen is another line of intensive research. The interest for this reaction is associated with the removal of NO in automotive exhausts, where, as Shelef [155] pointed out, there are three hydrogen sources: molecular hydrogen, water vapour that is converted to H_2 in the water-gas shift reaction by the same catalysts that reduce NO, and the active hydrogen contained in hydrocarbons.

This reaction is included in the category of non-selective reduction, because it is generally accompanied by the formation of substantial quantities of NH_3. The formation of NH_3 is one of the obstacles to overcome in the practical application of catalysts for the removal of exhaust gases. The reduction of its content therefore represents a main goal. As in the case of the reduction of NO with CO, different types of catalysts have been investigated.

4.2.1. *Base oxide catalysts*

Shelef and Gandhi [365] first investigated the reduction of NO with hydrogen on copper–chromite catalysts. On these oxides, NH_3 is the main product of the reaction in a wide range of temperatures. The drop in the NH_3 formation at high temperatures varies greatly in the range 975–1025 K. The product distribution on these catalysts strongly depends on the inlet concentration. Generally speaking, the proportion of NO converted to NH_3 (selectivity to NH_3) decreases monotonically with the NO concentration, while the NH_3 yield reaches a maximum at intermediate inlet concentrations. Similar results have been obtained with other oxides.

4.2.1.1. Catalyst stability. Shelef and Gandhi [170,365] reported that water vapour present in large amounts in a stream containing NO influences the catalytic processes in several ways. First, in certain cases, the adsorption of water can alter the surface and inhibit the reduction of NO. Kobylinski and Taylor [172] showed that the contact of water with chromia catalysts can lead to the formation of a hydroxyl layer. Second, for base catalysts [155], the extent of reaction with hydrogen giving NH_3 formation is directly related to the catalyst activity in the shift reaction. On catalysts active in the shift reaction, more NH_3 is formed when the source of hydrogen is water than when it is molecular hydrogen.

Sulphur and lead may be major poisons and cause an important decrease in the NO reduction. The simultaneous action of Pb and sulphur has a detrimental effect on the catalyst performance.

4.2.2. Noble metal catalysts

Similarly to NO reduction in the presence of CO, noble metal catalysts are preferred because of high conversions at low temperatures and high selectivities to N_2. Therefore, it is not surprising that these catalysts have also been more investigated in the NO reduction with hydrogen than any other type of catalysts. Many studies concern the activity both in the presence of hydrogen and of carbon monoxide.

Research followed the same path as in the reduction of NO with CO concerning the effect of the nature and the loading of the metal, the nature of the support, the dispersion and the oxidation state inside the supported particles.

Studies by Shelef and Gandhi [202] indicated a decrease in the activity in the order Pd>Ru>Pt>Os while Taylor and Klimisch [366] indicated the following order: Pd>Pt>Rh>Ru (Fig. 10). It was noted that the activity of noble metal catalysts is significantly higher than that of base catalysts for the NO–H_2 reaction.

Both Shelef and Ghandi and Taylor and Klimisch found that the selectivity towards the formation of NH_3 was lower over Rh [199] and Ru [155,199] than over other metal catalysts. On Ru catalysts, at temperatures above 575 K, less than 10% of the NO is converted to NH_3 whereas, on Rh catalysts, this proportion could attain 20%. This behaviour was associated with the high capacity of Rh- and Ru-supported catalysts to decompose NH_3 into its elements. The absence of a low temperature NO–H_2 reaction over Ru was attributed to a very strong chemisorption of NO. However, on the whole, it is now clear that Rh catalysts exhibit higher activities and selectivities both in the reduction of NO with CO and in the reduction of NO with H_2 than other noble metal catalysts.

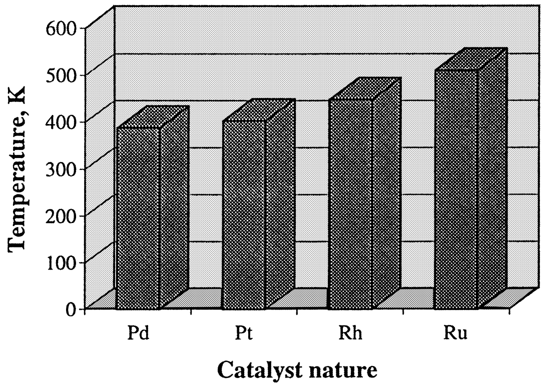

Fig. 10. Influence of the catalyst nature upon the temperature at which is removed 80% NO in a flow containing 0.5 wt% NO and 2 vol% H_2 (metal content: 0.5 wt%; space velocities: 24 000 GHSV).

Otto et al. [367,368] investigated the effect of rhodium and platinum loading. They showed that isolated sites cannot be expected to offer an optimum configuration for a transition complex required for the reduction of NO with hydrogen. An increase in the average size of the metal clusters or patches facilitates the formation of a favourable configuration of sites for the formation of the surface complex and for the reduction to proceed from N_2O to N_2. Therefore, the increase in the reaction rate with the metal loading up to the concentration of more than 2.7 μmol m^{-2} Rh does not require a change in the basic reaction mechanism, but can be explained by a rearrangement of the noble metal atoms into geometrical configurations better suited for the accommodation of the reactants.

The influence of the supported metal dispersion and the nature of the support on the activity and selectivity of the catalysts was also reported by Galvagno and Paravano [369]. Their results rested on the study of different gold-supported catalysts (Al_2O_3, SiO_2 and MgO). On Au/Al_2O_3 and Au/MgO catalysts a decrease in the selectivity to N_2 was observed, with an increased particle size, but this did not occur in the case of Au/SiO_2. However, no clear-cut influence of the nature of the support nature upon the activity was mentioned.

Savatsky and Bell [370] found that, in the case of Rh/SiO_2, the oxidation state of Rh is the most important factor controlling the reduction of NO with H_2. The oxidized catalyst is slightly more active than the prereduced catalyst, irrespective of the temperature, while on prereduced catalysts, up to 450 K, the amount of NH_3 formed is lower. It seems that the differences between the prereduced and pre-oxidized forms of the catalyst are due to the differences in the composition of the Rh particles under steady-state reactions. One possibility mentioned was the contribution of subsurface oxygen. The Rh dispersion was found to be unaffected by the type of catalyst pretreatment. A similar behaviour was previously observed by Taylor et al. [371] for ruthenium, platinum and palladium using alumina supports.

Pirug and Bonzel [372] carried out a low-pressure investigation of the reduction of NO with hydrogen on polycrystalline platinum and indicated a relation between the temperature at which the reaction started and the hydrogen-to-NO ratio. For a ratio of about 0.5, the reaction started at 440 K and selectivity to NH_3 was low; conversely, for a ratio of 5:1, the reaction started at the same temperature but large amounts of NH_3 and very little N_2O were produced. These results agree with those of Kobylinski and Taylor [172] who showed that the reaction started at 400 K for a ratio of 4:1.

Recently, Burch et al. [307] investigated a series of platinum catalysts prepared from different precursors. TAP experiments suggested some similarities between the reductions with H_2 and CO. The reaction takes place on the reduced Pt-sites resulting from the interaction of the reductant with the active metal surface. The experiments demonstrate that no direct reaction occurs between an incoming nitrogen monoxide molecule and an adsorbed carbon monoxide or H species.

The influence of different additives was also investigated in the same manner as for the reaction of NO with CO. Halasz et al. [233] investigated a series of $Pd–MoO_3$ catalysts supported on an Al_2O_3 surface and observed a very good selectivity to N_2+N_2O for a large range of parameters with a high loading of molybdenum. However, as was mentioned before (see Section 4.1.2.2) the presence of CO in addition to H_2, even in small amounts, still increases the activity and selectivity of these catalysts and the values obtained are superior to those obtained on a commercial 0.16 wt% Pd–0.03 wt% Rh honeycomb-shaped monolithic catalyst.

Tomishige et al. [378] modified an Rh/SiO_2 catalyst by selective reaction of $Sn(CH_3)_4$ with Rh metal particles at 423 K, followed by a reduction with hydrogen at 573 K. An in situ EXAFS observation of the NO–H_2 reaction established that the role of the Sn atoms in catalysis by $Rh–SnO_2/SiO_2$ is to conspicuously promote NO dissociation. This conclusion was based on the observation of the Sn–O bonding of 0.256 nm. The resulting oxygen atoms adsorbed on Sn atoms were easily removed by reduction of hydrogen at 373 K.

4.2.2.1. Catalyst stability. In the presence of hydrogen and at high temperatures, the dispersion of the most active supported Rh catalysts is not severely damaged, when compared with supported Pt treated in the same way. Under these conditions, Rh is only partially recovered in the form of extensively sintered particles [277].

The influence of other possible factors was discussed in Section 4.1.2.2.

4.2.2.2. Mechanism and kinetics. All the suggested mechanisms consider a dissociative interaction of NO with the metal surface. The numerous proposed equilibria could be associated with the characteristics of the supported polycrystalline noble metals.

The experiments carried out by Pirug and Bonzel [372,373] on polycrystalline platinum at low pressure indicated the following steps as possible:

$$NO + M \rightleftarrows NO{-}M \tag{3.90}$$

$$M{-}NO + M \rightarrow M{-}N + M{-}O \tag{3.91}$$

$$M{-}N + M{-}N \rightarrow N_2 + 2M \tag{3.92}$$

$$M{-}NO + M{-}N \rightarrow N_2O + 2M \tag{3.93}$$

$$M{-}N + NO \rightarrow N_2O + M \tag{3.94}$$

The interaction of the chemisorbed species with hydrogen can occur according to an Eley–Rideal type mechanism as was suggested for the formation of water or ammonia:

$$M{-}O + H_2 \rightarrow M + H_2O \tag{3.95}$$

$$M{-}N + 3/2\,H_2 \rightarrow M + NH_3 \tag{3.96}$$

or according to a Langmuir–Hinshelwood type mechanism as was suggested in the reaction leading to ammonia:

$$H_2 + 2M \rightarrow 2M{-}H \tag{3.97}$$

$$M{-}N + 3M{-}H \rightarrow 4M + NH_3 \tag{3.98}$$

Pirug and Bonzel [372,373] observed that, for a high H_2/NO pressure ratio, the competitive adsorption of H_2 and NO yields a comparatively larger amount of adsorbed hydrogen. The consequence is that the NO coverage is somewhat lower than for lower high H_2/NO pressure ratios and the onset of NO dissociation could shift to a lower temperature. This could explain the higher selectivity to NH_3 obtained in these conditions.

At moderate pressures (about 450 torr) and for a H_2/NO pressure ratio close to 1, Otto and Yao [368] obtained negligible quantities of ammonia. A kinetic investigation under these conditions revealed that the NO dissociation step was the rate-determining step. Actually, NO chemisorbs mainly non-dissociatively on the platinum surface. Recent TAP experiments of Burch et al. [307] are in the same sense.

For lower metal loading (0.2–2 μmol m^{-2}), the kinetics of the NO–H_2 reaction over Pt and Rh supported on alumina show certain similarities as resulting from the activation energy values (about 62 kJ mol^{-1}). Conversely, at high metal loading, i.e. higher than 5 μmol m^{-2}, the activation energies determined on Rh catalysts are about 20 kJ mol^{-1} lower than on Pt ones [367,368]. It is noteworthy that this corresponds to the ranges in which these catalysts exhibit better performances. It means that similarities found at low metal loading correspond to metal surfaces which are not able to activate NO molecules. During the increase of the loading, the metals reach a correct geometry and NO dissociation becomes possible.

The influence of the dispersion was also detected by Galvagno and Paravano [369] for supported gold catalysts. The change of the electronic properties of the Au surface occurs as a result of dispersion. This could determine various degrees of destabilization of the N–O bond in relation with chemisorption. The electron sites reached could totally dissociate NO. In such conditions very reactive atomic N species could interact to form N_2. Poor electron sites partially dissociated NO. These authors assumed that this is most probable as these species interact with hydrogen forming NH_3. Thus, it was suggested that an increased electron density on the metal sites leads to an increase in the selectivity to N_2. The role of the support was thus associated with the role of a promoter or poison.

To explain the water formation, Galvagno and Paravano [369] suggested two other possibilities, one based on an Eley–Rideal type of step:

$$\mathrm{NO{-}M} + 5/2\,\mathrm{H_2} \rightarrow \mathrm{H_2O} + \mathrm{NH_3} + \mathrm{M} \qquad (3.99)$$

and the other on a Langmuir–Hinshelwood type mechanism:

$$\mathrm{M{-}O} + 2\mathrm{M{-}H} \rightarrow \mathrm{H_2O} + 3\mathrm{M} \qquad (3.100)$$

both possibilities being different from those suggested by Pirug and Bonzel [372,373].

Bell et al. [370,374] investigated the mechanism of the NO reduction with H_2 based on infrared studies. The spectra were recorded under reaction conditions where the NO conversion was less than 50%. The surface was found to be saturated by adsorbed NO. The main species observed was Rh–$NO^{\nu-}$, even though small amounts of Rh–NO were also detected. Based on these data, they proposed the following step in addition to the previous ones:

$$\mathrm{M{-}NO} + \mathrm{M{-}H} \rightarrow \mathrm{M{-}N} + \mathrm{M{-}OH} \qquad (3.101)$$

$$\mathrm{M{-}NO} + \mathrm{M{-}N} \rightarrow \mathrm{N_2} + \mathrm{M{-}O} + \mathrm{M} \qquad (3.102)$$

$$\mathrm{M{-}O} + \mathrm{M{-}H} \rightarrow \mathrm{M{-}OH} + \mathrm{M} \qquad (3.103)$$

$$\mathrm{M{-}OH} + \mathrm{M{-}H} \rightarrow \mathrm{H_2O} + 2\mathrm{M} \qquad (3.104)$$

$$\mathrm{M{-}N} + \mathrm{M{-}H} \rightarrow \mathrm{M{-}NH} + \mathrm{M} \qquad (3.105)$$

$$\mathrm{M{-}NH} + \mathrm{M{-}H} \rightarrow \mathrm{M{-}NH_2} + \mathrm{M} \qquad (3.106)$$

$$\mathrm{M{-}NH_2} + \mathrm{M{-}H} \rightarrow \mathrm{NH_3} + 2\mathrm{M} \qquad (3.107)$$

According to this mechanism, Hecker and Bell [374] proposed an expression of the rate of the NO reduction by H_2 in the form

$$-r_{\mathrm{NO}} = \alpha \frac{k_{101} \cdot K_{97}^{0.5} \cdot p_{\mathrm{H_2}}^{0.5}}{K_{90} \cdot p_{\mathrm{NO}}}, \qquad (3.108)$$

where α is a coefficient that can vary between 1 and 3 as the selectivity to NH_3 varies from 1 to 0. Consequently, the production of N_2O, N_2 and NH_3 could, respectively, be described by the expressions:

$$r_{\mathrm{N_2O}} = \frac{k_{92} \cdot k_{101} \cdot K_{97}^{0.5} \cdot p_{\mathrm{H_2}}^{0.5}}{(k_{91} + k_{102})K_{90} \cdot p_{\mathrm{NO}}}, \qquad (3.109)$$

$$r_{\mathrm{N_2}} = \frac{k_{101} \cdot k_{102} \cdot K_{97}^{0.5} \cdot p_{\mathrm{H_2}}^{0.5}}{(k_{92} + k_{102})K_{92} \cdot p_{\mathrm{NO}}} \qquad (3.110)$$

and

$$r_{\mathrm{NH_3}} = \frac{k_{101} \cdot k_{102} \cdot K_{97} \cdot p_{\mathrm{H_2}}}{(k_{92} + k_{102})K_{92}^{2} \cdot p_{\mathrm{NO}}^{2}}. \qquad (3.111)$$

Even though the number of proposed equilibria exceeds 15 steps, as one can observe from Eq. (3.111), only few of them are rate-determining with respect to NO dissociation and the interaction between dissociated intermediates.

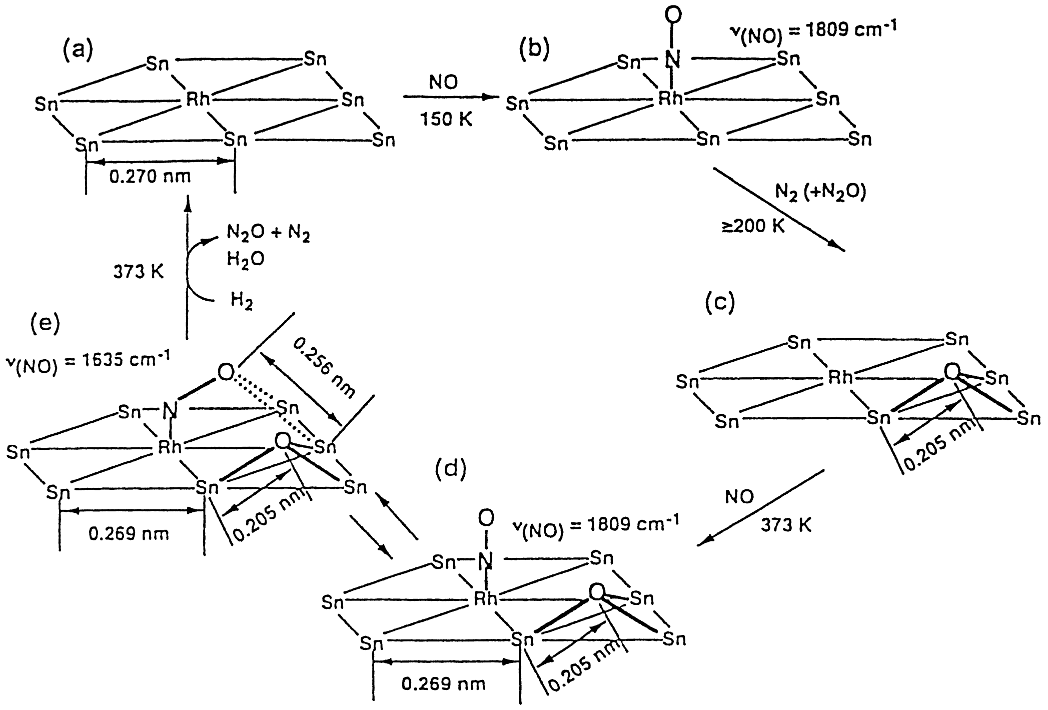

Scheme 5. Reaction of NO with H_2 over Rh–Sn/SiO_2 catalysts [645].

Recently, based on the in situ EXAFS observation of the molecular reaction intermediates and on FT-IR measurements, in the case of Rh–Sn/SiO_2 catalysts, Tomishige et al. [378] suggested the sequence given in Scheme 5.

Besides those observations, many experiments also reported oscillations. Nieuwenhuys et al. [375,376, 377], in the case of an Rh(1 0 0) oriented tip, presented some field emission microscope evidence of an oscillatory process. Pt(1 0 0) was the most investigated single crystal in this reaction [378,379]. Using Pt(1 0 0), Lombardo et al. [140,141] showed that the NO with hydrogen system is more complicated than the NO with CO system. The oscillatory behaviour was related to the 1 × 1→hex phase surface transformation of the noble metal. In the case of NO with CO, both reactants can induce the hex reconstruction whereas NO with hydrogen is unable to induce the reconstruction above 300 K. With only NO inducing the reconstruction, the NO coverage always has to remain above 0.5 in order to stabilize the noble metal surface in its 1 × 1 state, but when the coverage is high enough, oscillations are no longer possible. From LEED measurements, Slinko et al. [379] attributed the high activity of the hex phase to structural defects facilitating the dissociation of NO.

4.2.3. *Other supported metal catalysts*

Guglielminotti and Boccuzzi [380] showed that the deposition of iron on ZrO_2 generates an $Fe^{(2-x)+}$ state in strong interaction with the support which is very active in this reaction. It was suggested that a spillover of hydrogen species as hydroxyls on the support can favour this reactivity. However, the presence of oxygen in effluent gases causes a strong reduction in activity of this catalyst due to the inhibition of the NO dissociation.

4.2.4. *Alloys*

Two reasons triggered the investigation of alloy catalysts: one, to find some evidence related to the activity of bimetallic catalysts in the absence of the support; second, to find new materials active and stable in this reaction.

Obuchi et al. [381] investigated the catalytic properties of some Pd–Au and Pt–Cu alloys in the reaction of

NO with hydrogen, the real surface composition being monitored using Auger electron spectroscopy. They observed that the amount of NO adsorbed at ambient temperature decreased almost linearly with the increase in the gold or copper content. As a consequence, the reduction of NO was markedly suppressed. However, the drop in activity for the NO reduction was superior to that for the O_2 reduction, which suggests the necessity of large ensemble of Pd atoms for the NO dissociation.

The investigation by Heezen et al. [357], of SiO_2-supported Pt_x-Rh_{1-x} alloys using NO-to H_2 ratios between 1:1 and 1:3 indicated a behaviour different from that observed in the reaction of NO with CO. Pt is the most active catalyst under these conditions, while Rh-rich catalysts present high activities for the NO with CO reaction. However, the selectivity to N_2 on Rh catalysts, as was mentioned before for noble metal catalysts, is superior to that obtained on Pt, which produces relatively large amounts of N_2O and NH_3 at temperatures below 525 K.

New amorphous alloys obtained at very high cooling rates were also tested for the reduction of NO with hydrogen; the reaction led to N_2, N_2O and NH_3. Komiyama [382] reported that a $Ni_{80}P_{20}$ amorphous alloy showed an activity 10 times higher than the crystalline catalyst, but the steady state was reached after an initial decrease in the activity. A high activity (over 80% conversion) was also observed on Ni–Fe–Zr amorphous alloys. Although these alloys present a good activity, the presence of a relatively large amount of N_2O in the product mixture causes some problems. The presence of N_2O was attributed to a partial oxidation of the surface.

4.2.4.1. Mechanism and kinetics. Investigations performed on the alloy surfaces [357] led to mechanisms and kinetic laws involving the same steps as for supported noble metals.

4.2.5. Metal zeolites

Burch and Scire [383] examined the behaviour of some metal-exchanged ZSM-5 (Rh, Co, Cu, Pt) in the reduction of NO with hydrogen and found the following ranking of activity: Pt>Rh>Co>Cu>H-ZSM-5. This order agrees with that previously established by Kobylinski and Taylor [199] and Taylor and Klimisch [366] for supported noble metals. For all the investigated catalysts, the increase in the p_{H_2}/p_{NO} ratio corresponds to a decrease in the selectivity to (N_2+N_2O). However, Co-ZSM-5 seems to be less influenced by this parameter.

Very recently, Salama et al. [384] reported that the reduction of NO with H_2 takes place at relatively low temperatures (373–673 K) on Au/Na-Y zeolites obtained by mechanically mixing $AuCl_3$ with Na-Y. In situ FT-IR spectra indicated that the reaction occurs both on Au sites situated in the cages of zeolite and on Au sites implanted on the external zeolite surface.

These results show that although not reaching the selectivity obtained using organic reductants, the activity of these catalysts is fairly good in the presence of hydrogen but in oxygen-free conditions.

4.2.5.1. Reaction mechanism. TPD and FT-IR measurements made on Au/Na-Y zeolites [384] gave evidence suggesting the following mechanism. This, with the exception of the contribution due to the zeolite, is very close to that observed on supported noble metals:

$$H_2 + M \rightarrow 2H{-}M \tag{3.112}$$

$$NO + M \rightarrow NO{-}M \tag{3.113}$$

$$NO{-}M + H{-}M \rightarrow N{-}M + OH{-}M \tag{3.114}$$

$$N{-}M + NO{-}M \rightarrow N_2O + 2M \tag{3.115}$$

$$N{-}M + 3H{-}M \rightarrow NH_3{-}M \tag{3.116}$$

$$NH_3{-}M + H^+{-}Z \rightarrow NH_4^+{-}Z \tag{3.117}$$

$$H{-}M + HO{-}Z \rightarrow H_2O + Z \tag{3.118}$$

4.2.6. Perovskites

Grange et al. [385] investigated a large number of cobalt perovskites in the reduction of NO with H_2. In these experiments an excess of hydrogen (4% NO and 12% H_2) was used. At 623 K, the selectivity to N_2 was low because a large amount of N_2O was produced. The variation of selectivity to N_2 with the increase of the temperature indicates that an increase is achieved in a few cases but that this depends on the nature of the catalyst (Fig. 11).

However, the conversion of NO was total and N_2O was totally converted at above 823 K. The data presented in Fig. 11 suggest that it is very difficult to find a clear correlation between the chemical composition of the catalysts and selectivity.

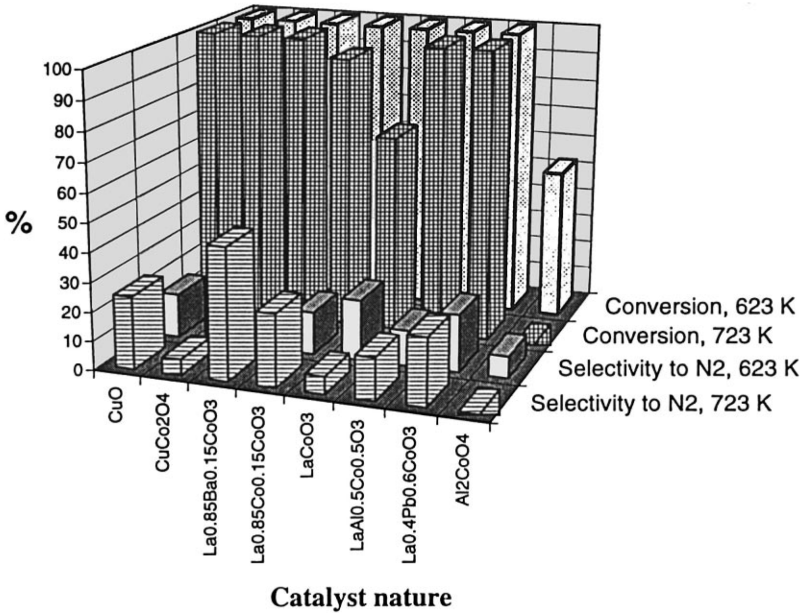

Fig. 11. NO reduction in the presence of H_2 on different perovskites (H_2-to-NO ratio=1.11, space velocities: 3240 h^{-1}; 19 g catalyst).

5. Selective catalytic reduction of NO in the presence of hydrocarbons

The SCR of NO by hydrocarbons is believed to be the most promising way to eliminate nitrogen oxide. The main advantage of the corresponding reaction is the use of a gas mixture very similar to that found in exhausts.

This catalytic process was first experimented on copper ion-exchanged zeolites by Iwamoto et al. [386,387] and Held et al. [388,389] independently. They showed that the catalytic activity of Cu-ZSM-5 could be greatly enhanced by small amounts of hydrocarbons in the presence of excess oxygen. Soon afterwards, Hamada et al. [390,391] found that H-zeolites and alumina were also active in the selective reduction of NO, but that the required temperatures were much higher. Examining ion-exchanged zeolites, Iwamoto et al. [392] reported that both MFI and mordenite structures were active. More recently, Hall et al. [393] conducted investigations in the same direction and found that an MFI structure was most favourable but that a ferrierite structure could also be considered. A positive effect of the ferrierite structure was also reported by Li and Armor [394], who showed that Co-ferrierite (Co-FER) doubles the nitric oxide conversion at temperatures above 775 K compared to Cu-ZSM-5. It is noteworthy that Co-FER is more selective than Co-ZSM-5 when methane is used. Unfortunately its activity strongly decreases in the presence of water. Later, other zeolite-like catalysts such as metallosilicates prepared by the Inui group [395] were also reported to be very active in this reaction.

These initial results opened new possibilities for the catalytic elimination of NO from exhaust gases, and nowadays the types of catalyst mentioned and the possible reductants are extremely varied. The enormous amount of interest of the scientific community for this topic is reflected both by the number of contributions in different journals [396] and by the number of patents. Very recently, Tabata et al. [397] published an excellent review study of the patent literature on catalysts used in the removal of NO_x, indicating that over 200 patents have already been published, most of them after 1990.

5.1. *Metal ion-exchanged zeolites*

Metal ion-exchanged zeolites are the most investigated class of catalysts for the reaction of NO with hydrocarbons. As suggested by the introduction to the present section, the research done on this topic considered the influence of different parameters: the structure of the zeolite, the nature of the metal, the influence of the conditions of preparation, the nature of the hydrocarbon, etc. No matter what parameter is considered, the temperature at which the conversion reaches higher values is lower than that needed for the decomposition of NO.

Influence of the zeolite structure and acidity. Concerning the influence of the zeolite structure, Iwamoto et al. [396,398,399] taking series of over-exchanged zeolites showed that at 523 K and in the presence of a NO (1000 ppm)+ C_2H_4 (250 ppm)+O_2 (2 vol%) mixture, the activity decreases in the following order: Cu-MFI-102>Cu-MFI-60>Cu-MOR-110=CuLTL48=Cu-FER-76>Cu-Y-76. Corma et al. [400] reported that exchanged beta zeolites exhibited activities similar to MFI-exchanged zeolites. Similar trends were also reported by Yokoyama and Misono [401] for cerium-exchanged zeolites in the presence of propene. A good conversion was also obtained for the SCR of NO under oxidizing atmosphere using a Cu-exchanged SAPO zeolite as a catalyst and propene as a reductant [402].

In this reaction the best zeolite structure also seems to depend on the nature of the hydrocarbon. Li et al. [403] showed that the MFI structure was more favourable to the reduction of NO in the presence of C_{2+} hydrocarbons, while the FER structure was more favourable to the SCR with CH_4.

Studies done on different zeolites indicated a different catalytic behaviour; in many cases their behaviour depended on the silicium-to-aluminium ratios. However, many of the results obtained in these studies suggest that the acid sites of the parent zeolites play an important role in the reaction. Early studies by Hamada et al. [390,404] reported a high activity of mixed oxides and solid superacid catalysts in the reduction of NO with hydrocarbons, and claimed that the amount of acid sites was the essential factor. More recently, several groups [405,406–410] pointed out that although some active ZSM-5 samples were used in the Na-form, the Brønsted acidic bridging hydoxyl groups were involved in the SCR of NO. Part of these are created during the reaction. Recent studies by Halasz et al. [409,410] indicate that bridging hydoxyl groups of the MFI structure probably constitute active sites for the oxidation of NO by O_2 to NO_2 above 200°C. Additional data supporting this hypothesis was given by Szanyi and Paffett [411] based on an in situ FT-IR investigation of the NO with O_2 reaction. They showed that the role of the acid sites is to nucleate the formation of N_xO_y species (which in fact are not very strongly bonded) and this behaviour occurs both on H-ZSM-5 and Na-ZSM-5 zeolites. Li and Armor [405] suggested that data obtained from Ga-MFI zeolites also indicated some synergetic effects between the gallium species, mainly precipitated on ZSM-5 surfaces and zeolitic H^+ (i.e. proton species belonging on Al framework). The role of Ga is to enhance the activation of CH_4, the NO reduction occurring on H^+ sites. As the authors suggested, the mechanism is similar to that suggested in the aromatization of propane or butane. The importance of the H^+ sites is also revealed by the fact that Ga–Na-ZSM-5 is inactive in the NO reduction.

Concerning the selectivity of the reaction, the results are sometimes contradictory. Yogo et al. [412] reported that the selectivity of the reduction of NO with CH_4 depends on the amount of acid sites of the H-form of zeolites. In spite of these conclusions, Satsuma et al. [408] showed that for a large family of M–H-mordenites (M=Ca, Sr, Ba, La, Ga) and H-ZSM-5, the acid properties of zeolites did not constitute the major factors determining the selectivity of the reduction of NO with C_3H_6. They also found that the activity depended on the amount of acidic sites in the zeolites, but not on the acid strength. This conclusion could also be supported by the results of Centi et al. [413] who studied the performances of a Cu-exchanged boralite and found that its catalytic activity was comparable to that of Cu-ZSM-5. They pointed out that B in the MFI structure leads to the formation of weaker Brønsted acid sites but that these in turn possess stronger Lewis acid sites.

Another explanation for the effect of the zeolite structure could be associated with the geometrical positions in which the exchanged metal is implanted. The zeolite structure could constrain the metallic species to a certain coordination and could also determine a certain electronic configuration because of its interaction with exchanged sites. Microporosity also plays an important role as Yokoyama and Misono [401] proposed for the MFI structure and Li and Armor [414] for FER.

Influence of the metal nature and its loading. Loaded cations can be regarded as the active species in the reduction of NO by hydrocarbons. Many investigations therefore focused on the role of the loaded metals, on their redox properties and on the reduction mechanisms associated with the exchanged ions. Cu-exchanged [396,397,398] as well as Ce-exchanged [401] zeolites are "selective" catalysts in the reduction of NO in the presence of C_{2+} hydrocarbons. Conversely, other metallic species like Co, Mn or Ni [415,416–419] or Ga or In [405,420,421] exhibit "selectivity" in the reduction with methane. The terms "selective" and "non-selective" catalytic reduction with respect to hydrocarbons was introduced at an early stage in the development of Cu-ZSM-5 lean NO_x catalysts by Iwamoto and Hamada [422]. They called "non-selective" the catalysts which in presence of oxygen are unable to reduce NO but can only oxidize the hydrocarbon. Generally CH_4 and C_2H_6 were considered as non-selective reductants, and all other hydrocarbons as selective ones. The presence of O_2 is essential to the reaction. Under oxidating conditions, Co-ZSM-5 zeolite is an active catalyst for reduction with methane, and the presence of nitrous oxide, which is another source of air pollution, was found to enhance the reduction of nitric oxide even in the absence of any oxygen. NO conversion was found to be proportional to the CH_4 level in the feed. Neither Co(II)-exchanged Y nor CoO supported on alumina is active for this reaction [416].

The way through which the metal is implanted does not seem to have a crucial importance. d'Itri and Sachtler [423] showed that impregnated Cu-ZSM-5 zeolites are also effective catalysts in the abatement of NO in the presence of C_{2+} hydrocarbons.

The differences between "selective" and "non-selective" exchanged-metal zeolites can be accounted for by the reaction mechanism. For catalysts exhibiting selectivity with C_{2+} hydrocarbons and non-selectivity with methane (mainly Cu- or Ce-exchanged zeolites), another role of the zeolite structure is, as Walker [424] pointed out, to provide the correct environment for exchanged metals and to ensure that the zeolites are not capable of over-oxidizing the partially oxidized species to CO_2 and H_2O. In such conditions, these zeolites act as bifunctional catalysts on which hydrocarbon species are activated by the zeolites while NO is activated by the exchanged metal. In addition, Li et al. [403] indicated several other arguments supporting the differences between the two groups of catalysts. They not only showed that copper sites in Cu-MFI have a low "selectivity" [425] but also that the instability of the gem-dinitrosyl species in the reaction conditions could be another factor. The aspect concerning the contribution of gem-dinitrosyl species is very important in the mechanism of NO reaction of these catalysts and therefore it should be discussed separately in the corresponding paragraphs.

For the second category, i.e. the zeolites selective with methane, both Li and Armor [405] and Kikuchi et al. [421] indicated the formation of NO_2 species as a determining step. However, there is also a difference between catalysts belonging to this category. It was shown that NO_x species are formed on metal sites for Co- or Ni-exchanged zeolites [403] but on zeolite acid sites in the case of Ga- or In-exchanged catalysts [404,425,426].

Iwamoto et al. [392] analysed the influence of a large number of metals in ZSM-5 and mordenites in the presence of propene, which is known as a very good reductant, and showed that among Na, Ca, Cr, Mn, Fe, Co, Ni, Cu, Zn and Ag, the most active catalysts were iron-exchanged ZSM-5 and iron-exchanged mordenite. The conversion to N_2 reaches the maximum for samples containing more than 50% exchanged iron. The activities of other cation-exchanged ZSM-5 zeolites like Ce [428,429], Pt [430] or Pd [429,431] were found to be lower than those of Cu-ZSM-5. However, Yokoyama and Misono [432] examining Ce, La, Pr, Nd, Ln, In, Pb, Cu, and Si in the presence of propene found that the best conversions were reached for a 60% cerium-exchanged ZSM-5. This level of exchange was obtained by treating the H-ZSM-5 with cerium acetate in an autoclave at 423 K. The relatively high conversion and selectivity obtained on Pb (100% exchange)-ZSM-5 at 673 K could be noted. All these experiments were carried out in the presence of oxygen. The addition of noble metals, such as Pt or Pd, was noticed by the same authors to cause a considerable decrease in the selectivity to N_2 and an increase in the activity for the oxidation of propene. The behaviour of vanadium and zinc-loaded mordenites in the presence of propane was also investigated [433,434]. However, the activity reached on these catalysts is not important.

A variety of zeolites (Y, mordenite, L) were also used to prepare iron-oxide clusters encaged in zeolites ($FeO_{1.5}$/zeolite) by oxidizing encapsulated $Fe(CO)_5$. The catalytic results showed that $FeO_{1.5}$/mordenite exhibited a high activity in the SCR of NO in the presence of propene at 620 K. The authors assumed [329] that the reaction involved a redox process between Fe^{2+} and Fe^{3+}. However, these authors did not measure the size and location of the cluster and it is not sure whether these clusters did not damage the zeolite lattice or were not, at least partially, on the surface of the zeolite crystallites.

Supported zeolites containing two different elements were also investigated in this reaction. A large number of compounds containing Cu or Co as their main components and almost all other metals included in the Mendeleev table were tested and also patented [397] (and references herein). Among these, only lanthanum [435] and cerium [436] added to copper seem to exhibit some effect. Alkaline metals exhibit a negative effect whereas Starkheev et al. [437] found the addition of earth-alkaline metals to be effective for Co-MFI zeolites in the SCR of NO with methane. However, up to now, no clear evidence has been given about the elements facilitating the second element, particularly what its contribution in the redox process, in the activation of the reactants or in the scavenging of the products is.

Concerning the effect of the degree of exchange for the copper ion, Iwamoto [396] indicated that the activity reaches a maximum for values of 80–100%, and that a small decrease occurs for higher values. A similar effect was found by Yokoyama and Misono [432] in the case of cerium, and by Hall et al. [393] for cobaltum. For ferrierite-exchanged zeolites, the differences between the TOF of catalysts containing Co^{2+} exchanged at the level of 42% and 54% were interpreted as a consequence of the preference of the cations for eight-ring channels sites first and for 10-ring channel sites later. Other studies carried out by Campo et al. [438] and Starkheev et al. [437] using Co-exchanged ZSM-5 reached similar conclusions. In addition, both groups showed that the optimal metal loading should be correlated with the Al content. Thus, for $Co/Al \leq 0.5$, the catalytic activity towards the SCR increased proportionally to the cobalt content, but decreased for $Co/Al > 0.5$.

Influence of the preparation procedures. The procedure through which the metal is implanted in the zeolite lattice is also an important factor. In the case of metal zeolites, the metal is not always totally directly bonded on the exchangeable positions. Therefore, we shall use the term ‘‘implanted’’ in order to define the deposition of isolated metal species on the zeolite, this meaning no special assumption of the positions in which this deposition occurred. Charjar et al. [439] investigated the activity of Cu-ZSM-5 zeolites prepared according to three different procedures: exchange, impregnation and precipitation. C_3H_8 was used as a reductant and the oxygen content was higher than 0.5 vol%. The activities, measured as turnover frequencies, indicated the following order: Cu-ZSM-5 (exchanged)>Cu-ZSM-5 (impregnated)>Cu-ZSM-5 (precipitated)$\gg$Cu/Al_2O_3. This supports the idea that ion exchange is the best technique to prepare these catalysts.

Influence of the nature of the reductant. Exhaust gases contain many kinds of hydrocarbons and many of these could represent a supplementary source of pollution. As mentioned above, it appears that a concomitant elimination of both pollutants by reduction of NO with unburned hydrocarbons could be a very attractive solution. Therefore, the interest for the investigation of the effect of different specific reductants is highly justified.

The positive effect of so-called ‘‘selectively reductive agents’’ – alkenes or alkynes – (ethene, propene, acetylene) has been proven [440]. Research done by Matsumoto et al. [441] indicates that, irrespective of the carbon number, olefins are much more effective than paraffins. The SCR of NO by hydrocarbons such as ethylene, propene, and propane occurs at temperatures as low as 473–673 K, the exact temperature depending on the metal and on the hydrocarbon. Ethylene seems to give an extremely high selectivity compared to the reaction with NH_3, even in an oxygen-rich atmosphere [442]. In addition to these data, Hall et al. [393] investigated a series of saturated hydrocarbons known to have a lesser reactivity and indicated the following order: i-C_4H_{10}>*n*-C_5H_{12} >2,2,4-tri-methylpentane>neo-C_5H_{12} >3,3-dimethylpentane>methane>C_3H_8 >3,3-diethylpentane (neononane). Taking into account the ‘‘Constant Index’’ which is generally used to describe the effect of chain-branching on cracking rates, they argued that

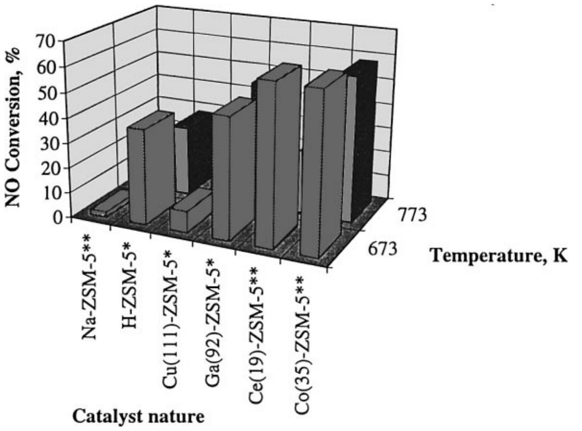

Fig. 12. NO conversion in the presence of the hydrocarbons ((*) C_2H_4; (**) C_3H_6) (NO:hydrocarbon:catalyst weight=6 g^{-1}; O_2 10 vol%).

the combustion of these molecules occurs outside the zeolite pore system. Tests made at different temperatures showed a strong molecular sieve effect in the SCR reaction with hydrocarbons exhibiting a high constant index, but not for their combustion. This effect was best represented in the case of neononane.

Since natural gas, which contains more than 90% methane, is widely used as a fuel source for many combustion processes and electric utilities, much of the recent research used it as a reductant [415,416–419,443]. Taking into account the new data, Iwamoto [396] himself considered that CH_4 must now be classified into the group of selective reductants on certain specific catalysts.

Figs. 12–14 present the NO conversion in the presence of hydrocarbons and methane on different metal zeolites.

Montreuil and Shelef [444] reported that in the presence of excess oxygen, the activity of soluble oxygenated organic compounds like alcohols (methanol, ethanol, propanol), aldehydes (acetaldehyde), ketone (acetone, methyl-ethyl-ketone), ethers (1,4-dioxane) is close to that of propene. Partially oxygenated reductants are more active when the system is rich in stoichiometry.

Influence of other factors. Concerning the influence of the oxygen content, recent studies by Radtke et al. [445] reported that the selective reduction of NO by ethene or propene in the presence of an oxygen excess over Cu-ZSM-5 produces substantial amounts of hydrogen cyanide at temperatures below 650 K. Above this temperature, selectivities for HCN as well as for N_2O present a significant decrease.

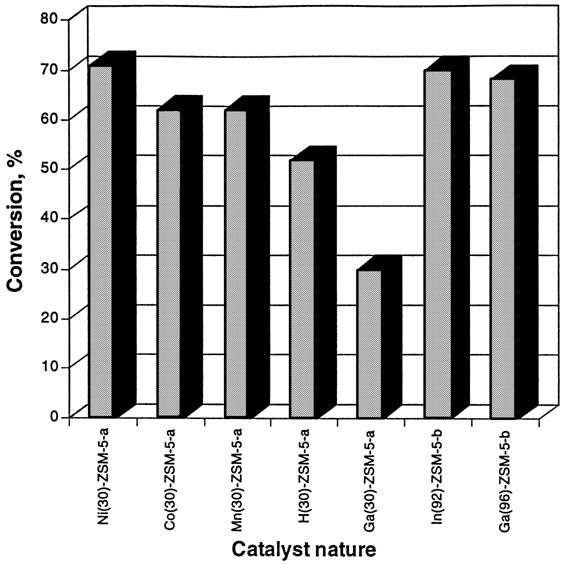

Fig. 13. NO conversion in the presence of methane on different ZSM-5 zeolites ((a) NO – 0.2%, CH_4 – 0.8%, O_2 – 10, space velocities – 5000 h^{-1}, 773 K; (b) NO –1000 ppm, CH_4 – 2000 ppm, O_2 – 10%, space velocities – 7000 h^{-1}, 773 K).

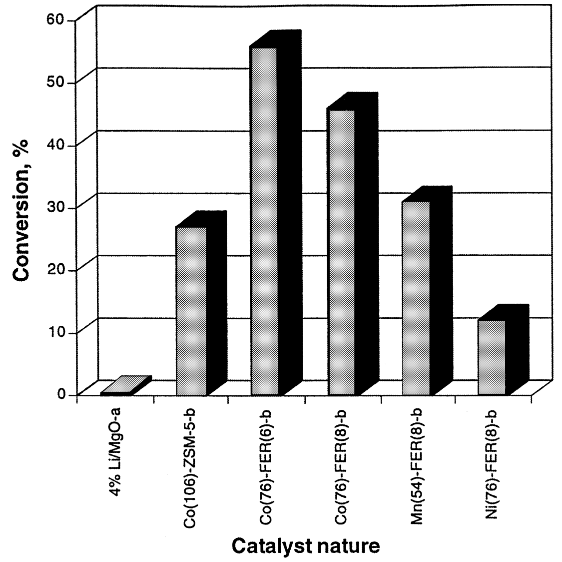

Fig. 14. Conversion of NO with methane on different catalysts ((a) NO – 0.082%, CH_4 – 0.082%, space velocities – 3000 h^{-1}, 773; (b) NO – 1610 ppm, CH_4 – 1015 ppm, O_2 – 2.5%, space velocities – 30 000 h^{-1}, 773 K).

D'Itri and Sachtler [423] specifically investigated the influence of the oxygen content and revealed that the maximum selectivity generally corresponds to an O_2/C_{2+} ratio sufficient for a total combustion of hydrocarbons. At higher O_2 concentrations, using copper implanted in ZSM-5 as active metal, the N_2 yield decreases but remains substantially higher than the one obtained in the presence of non-selective reductants such as CH_4 or CO.

Even though the SCR in the presence of hydrocarbons occurs with high conversions and selectivities, important quantities of untransformed hydrocarbons and nitrite–nitrate complexes or other compounds like NCO still remain in the effluent gases [429]. This is a very important problem to solve in future research. However, Sadykov et al. [446] consider that nitrite–nitrate complexes could be decomposed by modifying the redox as well as acid–base properties of the catalysts.

5.1.1. *Other molecular sieves used in the SCR of NO*

In order to investigate the contribution of the acidic properties of the MFI structures and to increase the stability of these catalysts in the presence of water vapour, Inui et al. [395,447–454] investigated the activity of MFI metallosilicates and of beta-metallosilicate catalysts in the SCR of NO in the presence of higher hydrocarbons (octane, cetane). These materials were obtained by incorporation of the metals in an MFI or beta type structure. Three classes of metallosilicates were synthesized and tested: (i) oxides of metals difficult to reduce and exhibiting strong acidities, i.e. Al and Ga; (ii) oxides of metals that are partially reducible, i.e. Fe, Co, Ni and Mn and (iii) oxides of metals that are easily reducible, i.e. Cu.

The investigation of the different influencing factors discussed in Section 5.1 showed results very similar to those obtained for metal-exchanged zeolites. The metal loading, the nature of the reductant and the oxygen content have the same influence as in metal-exchanged zeolites. Furthermore, the results obtained using H–Ga, H–Fe or H–Co silicates were not far from those obtained by impregnation of these species on zeolites exhibiting the same structure. The NO conversion reaches a maximum of 60% at about 673 K for H–Co-silicate and a little bit more at 773 K for H–Ga-silicate. Although CO_2 was the main product, CO, small amounts of aromatic and light paraffinic hydrocarbons are also formed on H–Fe-silicate, whereas there are important amounts of hydrocarbons on H–Ga- and H–Co-silicate. Similar results over H–Fe MFI silicates in the presence of propene as a reductant were reported by Kikuchi et al. [412]. The contribution of propene in the generation of carbonaceous deposits was again reported.

Concerning the influence of the acidity on activity, studies carried out by Inui et al. [451] on this category of zeolites reached conclusions similar to those reported by Satsuma et al. [408] using metal mordenites and ZSM-5 catalysts. Even though they have a strong acidity strength, Al-metallosilicates exhibit a very low activity in this reaction. Inui et al. [451] proved that the activity in the SCR using hydrocarbons should be correlated not only with the acidity but also with the activity for hydrocarbon combustion. This property could also be correlated with the redox properties of the metal. As a consequence, the best activities were obtained with metallosilicates exhibiting both average acidity and average activity in the oxidation of hydrocarbons. On bimetallic Fe–Ga-beta-type silicates, at low temperatures, in conditions of NO conversion similar to Ga-beta-type silicates, the quantity of unburned hydrocarbons is lower. Differences between the distribution of unburned hydrocarbons on beta-type silicates and MFI-type silicates are small [447,448,449].

Recently, Centi et al. [413] reported SCR data using another molecular sieve. They showed that copper-exchanged boralite also exhibits a high activity in the reduction of NO with propane in the presence of oxygen.

5.1.2. *Stability of metal-exchanged zeolites*

The Cu-ZSM-5 catalyst is the best one reported so far for the NO reduction by C_{2+} hydrocarbons under net oxidizing conditions. However, all zeolite-based catalysts are very sensitive to water and quickly deactivate. Cu-exchanged SAPO zeolites [402] also exhibit a low stability to water vapour. Even though the activity is about three times lower compared to Cu-ZSM-5, Pt-ZSM-5 gives a conversion in the range 473–523 K and is less affected by the presence of H_2O [455,456,457]. Ga-ZSM-5 exhibits a good activity in the SCR of NO, but is unfortunately also more sensitive to water vapour. Ni- and Mn-ZSM-5 catalysts [415,416–419] show a similar behaviour in the presence of water. A low stability in the presence of water was also reported for metal-exchanged ferrierites [394].

Investigations concerning catalyst deactivation due to the presence of water indicated a joint contribution of at least two effects: the modification of the geometry of the metallic active sites, namely of the coordination and of the position on the zeolite [458,459] and the dealuminization of the MFI structure with a modification of the Brønsted acidity. For the first effect, both Shelef [466] and Wichterlova et al. [459] suggested that the presence of water favours the sintering of copper. As for the second effect, a detailed investigation made by Sachtler et al. [460] indicated that the presence of water led to irreversible changes. In parallel with the modification of the Brønsted acidity, which determines changes in the chemisorption of reactant molecules, dealuminization leads to the formation of Al_2O_3. Simultaneously, part of the CuO clusters, primarily formed on the silicious portion of the zeolite, starts to be formed on the Al_2O_3, which means a loss of ion-exchange sites. As the deactivation becomes more severe, $CuAl_2O_4$ compounds start to be formed. Copper in this state is inactive toward the reduction of NO_x.

These structural modifications are accompanied by a modification in the interaction of the zeolite with hydrocarbons. Radtke et al. [461] reported that in these conditions the differences in the conversion using alkanes or alkenes become smaller.

The implanting of cobalt in the MFI structure was reported by Armor and Farris [462] to be less sensitive to water. Thus, Co-ZSM-5 in the presence of 2% water vapour over a period of 99 h at 1023 K keeps its activity, showing a very high hydrothermal stability. Previously, Li and Armor [405,419] reported on the stability of the same catalyst in an NO–methane–oxygen atmosphere. However, the presence of water was shown by the same authors [420,463,464] to decrease both the NO reduction and the CH_4 combustion activity for Co-FER structures. A high stability to steam was recently reported by Yogo et al. [426,465] for In-ZSM-5 zeolites. These catalysts were tested in mixtures in which the proportion of water vapour in the gases was as high as 10%. They found that water had little effect on the indium sites, but that the NO oxidation reaction was largely depressed by H_2O. Under these conditions H_2O is very likely to be preferentially adsorbed on acid aluminium sites. More important is that the poisoning of In-ZSM-5 zeolites by water is completely reversible and the initial activity can be restored if steam is removed from the reactant mixture.

Sulphur-containing compounds, such as hydrogen sulphide and sulphur dioxide [466], represent another strong contaminant for metal-exchanged zeolites. Although Cu-ZSM-5 catalyst has been reported to maintain a high activity in a model reactant containing sulphur dioxide [467] there is much more evidence indicating that in such conditions it quickly deactivates. The only zeolite which was shown to be less affected by the presence of SO_2 is 0.5 wt% Pt-ZSM-5 [457,458,459].

A possibility to improve the stability both to high humidity and to SO_2 was recently indicated by Sadykov et al. [446] who suggested that the honeycomb configuration obtained by including the active cation-exchanged ZSM-5 in a monolithic structure is consistent with the modification of the superficial properties of these catalysts, leading to the increase in the stability. However, this proposition raises some doubts because at the microscopic level the catalytic properties could not be changed in this way.

Considering metallosilicates, both beta- and MFI-type structures exhibit a high thermal resistance [453]. These data concord with a computer simulation evaluation made by the same authors [449]. An addition of SO_2 up to 200 ppm had no effect [451] and the conversion of hydrocarbons generally decreases monotonously with the increase of the water content up to 10%.

5.1.3. Mechanism and kinetics

The SCR of NO either with C_{2+} hydrocarbons or CH_4 is a very complex reaction. As was shown above, in the active catalysts both Cu and Co are under-exchanged. Very recently, Sachtler et al. [468] reported some findings indicating that a high dispersion of Cu was desirable for the reduction of NO with propene because the mononuclear complex Cu^{2+}–NO_2 seems to play a very active role. In a similar way, Li et al. [403] showed that in the case of Co (both on ZSM-5 and FER zeolites) the formation of adsorbed NO_2 on Co^{2+} sites is a necessary step.

Several reaction mechanisms have been proposed and can be classified into the following groups according to the influence of the reductant nature of the zeolite structure.

1. *Oxidation of NO to reactive NO_2 that reacts with hydrocarbons* [426,427,469–471]. This mechanism is typical of the SCR of NO with CH_4. The total reaction is thought to occur according to the following steps:

$$NO + O_2 \rightarrow NO_{2,ads} \quad \text{(on zeolites or newly created metal acid sites)} \tag{4.1}$$

$$NO_{2,ads} + CH_4 \text{ (as an example)} \rightarrow [X]\ (X = \text{reaction intermediate}) + nH_2O \tag{4.2}$$

$$[X] + NO \rightarrow N_2 + CO + mH_2O \tag{4.3}$$

$$[X] + NO_2 \rightarrow N_2 + CO_2 + mH_2O \tag{4.4}$$

$$CO + O_2 \text{ (or } NO_2) \rightarrow O_2\ (+NO) \tag{4.5}$$

This reaction mechanism was verified by a transient response study in the case of Ga- and In-ZSM-5 zeolites.

This behaviour agrees with the hypotheses summarized by Trifiro et al. [472] who indicated the following positions of oxygen as likely to interact with the zeolite lattice: (i) Brønsted acid sites associated with aluminium ions; (ii) Lewis acid sites or (iii) metal inserted in the zeolite framework. The oxygen activated on zeolite or newly created metal acid sites interacts with NO giving reactive NO_2 species. In the case of Ga- or In-ZSM-5, several experiments indicated the possibility of inserting these metals in the zeolite framework [421,473] after a few oxidation–reduction cycles. This process would generate new $[GaO]^+$ or $[InO]^+$ sites.

Additional arguments supporting implication of reactive NO_2 species were given by Li et al. [403,414], Sachtler et al. [468] and Blower and Smith [474]. A detailed FT-IR investigation of (NO/O_2) and NO_2 adsorption allowed Li et al. [403,414] and Sachtler et al. [468] to indicate that NO_x species could also be bonded on zeolite-Co^{2+} species and that the formation of adsorbed NO_2 on Cu^{2+} sites is in fact a determining step. The other group [474] gave additional arguments showing that the decomposition of nitromethane on a large family of metal-exchanged zeolites (Cu^{2+}, Zn^{2+}, Cd^{2+}, Mn^{2+}, Co^{2+}, Ni^{2+}, La^{3+}, UO_2^{2+}) produced N_2, CO and CO_2 among the major products.

However, the activation of methane on these zeolites, which represents a key step in this reaction, is still not very clear. Li et al. [403] and, later, Cowan et al. [475] suggested that the step presented hereafter was more likely than step (4.2):

$$NO_{2,ads} + CH_4 \rightarrow CH_3^{\bullet} + HNO_{2,ads} \tag{4.6}$$

this step occurring on Lewis zeolite-Co^{2+} sites. These radical species could then react following sequences (4.3) or (4.4) or with chemisorbed NO_2 to form nitromethane [475] which further reacts towards N_2 as suggested by Tanaka et al. [476].

2. *Oxidative conversion of hydrocarbons forming an intermediate by reaction with NO_x* (e.g. isocyanate radical, oxygen-containing compounds, etc.) This mechanism, typical for C_{2+} hydrocarbons, was first suggested by Ukisu et al. [440,477] for several oxides and by Obuchi et al. [478] for metal zeolites. Recently, Burch and Scire [383] favoured this mechanism in Cu-ZSM-5 zeolites.

Research done by Obuchi et al. [478] indicated that the radical forms present in the carbon deposits can reduce NO, perhaps as intermediate steps in the SCR. These radicals are different from the primary radicals generated by hydrocarbons and are produced from carbon deposits that do not contain much hydrogen, through a partial oxidation with oxygen. The role of the catalyst is to promote the formation of carbon deposits from the primary radical compounds by cracking or partial oxidation. Additional explanations for this mechanism were given by Ansell et al. [479] using TAP and TPD experiments. They stipulated that the key intermediates are coke (formed on the zeolite) and NO_2-type species (formed on the exchanged copper sites). They assumed that the role of oxygen is not relevant to the activation of the hydrocarbon but is crucial to the formation of Cu–NO_2 species. However, although many details concerning the transformation of coke deposits are very convincing, it is still unclear how these deposits can be generated. Several others supporting the formation of hydrocarbon radicals' arguments have also been given. The main one is that the reaction path depends on the nature of the hydrocarbon. If the reductant hydrocarbon is an alkane, the first step is its transformation into alkene on the acidic sites, as shown by Buckles and Hutchings [480]. In the second step, these alkenes can follow a complicated mechanism. A detailed investigation carried out by Hayes et al. [481] showed that the next step was the transformation of alkene into an allyl; it reacts thereafter with NO_x species to generate N_2 or with oxygen to generate CO_2.

Another mechanistic aspect of the reaction is connected to the formation of nitro-compounds. Yokoyama and Misono [482] reported that nitro-compounds should be considered as the first intermediates for the SCR in the reduction of NO with propene over Ce-ZSM-5 catalysts:

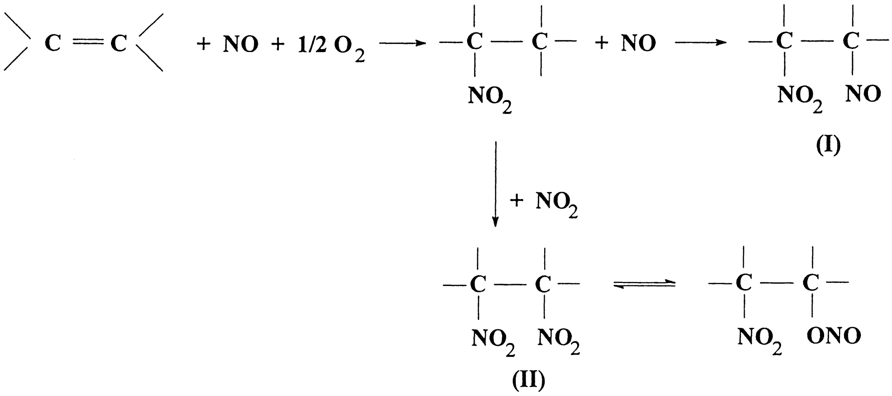

(4.7)

Later, Kharas [483] also indicated the formation of organonitrogen species. He suggested that intermediates in this reaction were formed via the insertion of NO to form *N*-nitroso-*N*-alkylhydroxylamate species. In addition to this suggestion, based on an FT-IR investigation, Hayes et al. [481,484] suggested that the reduction of nitrate species to N_2 occurs through the following steps:

$$R{-}NO_2 \rightarrow R{-}NO + R{-}NH{-}OH \tag{4.8}$$

$$R{-}NO + R{-}NH{-}OH \rightarrow R{-}CN + \text{other species} \tag{4.9}$$

$$R{-}CN + O_2/OH \rightarrow 2R{-}C(OH)CN \rightarrow N_2 + RCHO \tag{4.10}$$

$$R{-}NO + R{-}NH{-}OH \rightarrow R{-}N{=}N{-}R \tag{4.11}$$

$$R{-}N{=}N{-}R \rightarrow N_2 + 2R \tag{4.12}$$

Several other arguments supporting the existence of these intermediates were given by Sachtler et al. [485] on the basis of FT-IR measurements and of the study of the reaction of acetone-oxime, by Iwamoto and Takeda [486] who conducted a pulse study of the reactivity of ethene, and by Iwamoto et al. [487], Hall et al. [488,489] and Pognant et al. [490] who deduced them from other measurements (FT-IR, the study of the reaction in the presence of different hydrocarbons and comparative investigation of homogeneous and heterogeneous reactions of hydrocarbons with NO).

3. *Redox mechanism involving the successive oxidation and reduction of the catalyst surface by NO and the hydrocarbons.* Based on microscopic sequential reaction results, Inui et al. [451,453] proved that the role of the hydrocarbon was to reduce the surface of the catalysts. NO decomposed at the same time, this process occurring on the partially reduced surface parts of the catalysts, as long as the temperature was adequate and the rate of the NO decomposition faster or comparable to the rate of oxidation of the reduced surface:

$$C_xH_y + nO_{ad}[S] \xrightarrow{k_1} C_xH_y, ad(nO_{ad}[S]) \tag{4.13}$$

$$\begin{aligned} C_xH_y, ad(nO_{ad}[S]) + mO_{ad}[S] &\xrightarrow{k_2} xCO_2 + (y/2)H_2O \\ &+ (2x + y/2)[S] + [(n+m) - (2x + y/2)]O_{ad}[S] \end{aligned} \tag{4.14}$$

$$NO + [S] \underset{k_4}{\overset{k_3}{\rightleftarrows}} NO_{ad}[S] \tag{4.15}$$

$$2NO_{ad}[S] \xrightarrow{k_5} N_2 + O_2 + 2[S] \tag{4.16}$$

$$2NO_{ad}[S] \xrightarrow{k_6} N_2 + 2O_{ad}[S] \tag{4.17}$$

$$O_2 + 2[S] \xrightarrow{k_7} 2O_{ad}[S] \tag{4.18}$$

Kikuchi et al. had another outlook on the reaction mechanism of the SCR of NO on metallosilicates [393]. They suggested that the reaction occurs according to mechanism 2 with the contribution of carbonaceous deposits for H–Fe-silicates.

Another redox variant is that proposed by Burch and Millington [491]. According to them, the hydrocarbon reduces a copper site, giving a coordinatively unsaturated Cu^+ ion site. In the presence of nitrogen oxide, this site generates a dinitrosyl species, which by inversion converts into gaseous N_2O and O_{ad}. The nitrous oxide is then decomposed into nitrogen at another copper ion site, and the catalytic cycle is complete. The contribution of the organic molecule is to reduce the amount of oxygen.

Shelef [458] considers that, for Cu-catalysts, the determination of the oxidation state is crucial to understanding both the decomposition and the selective reduction mechanisms. The usual methods generally do not offer information on the reaction conditions and the extrapolation of the spectroscopic results can lead to inexact conclusions.

XANES studies performed by Liu and Robota [492] on the copper oxidation state during the SCR of nitric oxide by hydrocarbons revealed the presence of Cu(I) ions different to those formed through autoreduction by the desorption of oxygen as suggested for the direct decomposition of NO [493]. XANES spectra in the presence of propene are different from those observed in the methane mixture. According to these measurements, the cuprous ion in Cu-ZSM-5 is formed during a redox process:

$$\mathrm{O{-}Cu(II)} + \mathrm{C_3H_6O} \rightarrow \mathrm{Cu(I)C}_x\mathrm{H}_y + \mathrm{CO_2} + \mathrm{H_2O} \tag{4.19}$$

where C_xH_y could be more than one propene molecule, and then

$$\begin{aligned}&\mathrm{Cu(I)}\cdot \mathrm{C}_x\mathrm{H}_y + 2\mathrm{NO} + (x + y/4 - 1/2)\mathrm{O_2}\\ &\quad\rightarrow \mathrm{O{-}Cu(II)} + \mathrm{N_2} + x\mathrm{CO_2} + y/2\,\mathrm{H_2O}\end{aligned} \tag{4.20}$$

5.2. SCR of NO on supported metals

The activity of the supported platinum group metals was also investigated. One reason for that is the low stability of the much investigated Cu-ZSM-5 which casts doubts on its possible use in practice [492–496].

The experiments carried out by Burch et al. [307] using alumina-supported catalysts prepared from different precursors and with different Pt-loadings revealed an interdependence of the metal loading, the temperature of the maximum conversion of NO and the level of activity. Propene was used as a reductant. For a given platinum precursor, the temperature of the maximum NO_x conversion decreases while the corresponding activity increases as the metal loading increases. However, NO conversion on these catalysts is not completely selective to nitrogen. Significant quantities of N_2O are also produced. The selectivity to N_2O reaches up to 40% of the nitrogen monoxide converted. The temperature increase is accompanied by a decrease of the N_2O content in the reaction products.

In addition to these data, Hamada et al. [497] reported a cooperative effect between platinum and alumina. Evidence of this effect was drawn from the comparison between the activity of Pt/Al_2O_3 and the activity of Pt/SiO_2 in the reaction of NO with propane. The first catalyst, as was mentioned above, exhibits some activity in this reaction whereas the second catalyst is inactive. A physical mixture of Pt/SiO_2 with Al_2O_3 exhibited activities similar to those exhibited by Pt/Al_2O_3. This behaviour is consistent with data obtained with metal zeolites, indicating the necessity for some acidity in this reaction.

Another case of cooperation between catalyst components was reported by Iwasawa et al. [498] who indicated that bimetallic Pt/Sn catalysts prepared by modifying Pt/SiO_2 catalysts with $Sn(CH_3)_4$ exhibit an increase of the activity in the same reaction. Moreover, the selectivity to N_2 was total in this case. The authors attributed this behaviour to oxygen-deficient SnO_x species crowning platinum, as was proven from EXAFS measurements. The close proximity of two species allows for the best cooperation between them. Another cooperative effect in this reaction was identified by Yokoyama and Misono [401] using physical mixtures of Mn_2O_3 and Ce-ZSM-5 and Ueda et al. [499] using physical mixtures of Au/Al_2O_3 and Mn_2O_3.

The effect of different promoters introduced in catalysts via nitrate or acetate salts was also investigated by Burch and Watling [500]. From a very large number of elements (K, Cs, Mg, Ca, Ti, Co, Cu, Mo, La, Ce) only Ti and Mo seem to exhibit a positive effect compared to the parent Pt/Al_2O_3. All lead to a decrease in activity. Noble metal (Ag, Au, Pd, Rh) precursors were also tested but only Ag exhibited a slight positive effect. However, the various promoters used by these authors had no significant effect on the selectivity.

Other studies by Obuchi et al. [501] reported that for the same reductant there is a relationship between the activity and the nature of the platinum metal. At low temperatures (about 525 K), platinum catalysts present higher activities, while at 625 K their activity is inferior to that of γ-Al_2O_3-supported Rh or Ru. In all temperature ranges, the activity of Ir or Pd on the same support is inferior to Pt, Rh or Ru catalysts. Recent data obtained by Burch and Ottery [502] show that the nature of the reductant also has a great importance regarding selectivity. This is clearly shown with toluene, which induces a very high selectivity to N_2: no N_2O was formed.

With the exception of the system investigated by Iwasawa et al. [498], N_2O is formed on Pt (only 1/3 of the NO is converted into nitrogen). In contrast, more than 90% of the nitric oxide consumed is converted to nitrogen on Rh- or Ru-supported catalysts. Furthermore, Naito and Tanimoto [503] indicated that with a highly dispersed Rh on alumina, using propene as a reductant, the presence of oxygen leads to an important enhancement of the rate of NO reduction. A bimetallic 0.75 wt% Pd–0.25 wt% Rh gave the highest nitric oxide conversion, but the selectivity to nitrogen was only 45% at its maximum [503].

The nature of the support also plays an important role in unconventional noble metals. Ueda and Haruta [504] reported that NO to N_2 conversions of about 40% could be obtained on Au/Al_2O_3 catalysts in the presence of propene. Compared to catalysts on other supports the order of activity was: Al_2O_3 (675 K)> ZrO_2 (525 K)$\sim$$TiO_2$ (625 K)=MgO (625 K). This again stresses the role of acid–base sites in this reaction. The presence of O_2 is decisive in the removal of NO on these catalysts. The reduction of NO cannot proceed in the absence of oxygen.

5.2.1. *Catalyst stability*

Comparative experiments using honeycomb test samples (0.5% Pt, 0.5% Rh, 0.15% Ru, 0.2% Pt, 0.05% Rh, 0.2% Pt, 0.04% Au and 0.7% Cu-ZSM-5) in the presence of real diesel exhaust gas [501] showed that only platinum–rhodium and platinum catalysts were resistant to deactivation. The decrease in the activity of the ruthenium catalyst, which exhibits a substantial conversion with the model reactants, is attributed to a deactivation by sulphur dioxide.

5.2.2. *Mechanism and kinetics*

Burch et al. [307] performed a kinetic investigation of a C_3H_6–O_2–NO–Pt/Al_2O_3 system using a conventional microreactor and the temporal analysis of the product (TAP) technique. They suggested that the SCR of NO occurs following two simultaneous paths. The first one, very similar to that proposed by Obuchi et al. [478], considers the participation of reactive carbon species. Instead of polymeric deposits such as $C_xO_yH_z$ considered by this author and also investigated by Inui et al. [450], Burch et al. [307] take into account a molecular fragment formed by the reducing agent. Isolated carbon atoms are very active in bonding adsorbed nitrogen monoxide molecules, which can lead to the formation of carbon monoxide and adsorbed nitrogen N_{ad}. Isocyanate, NCO_{ad} or fulminate, and CNO_{ad} species are thought to be intermediates. However, TAP data of these authors indicated the crucial role of reduction of the platinum surface. Over a completely reduced Pt/Al_2O_3 surface, very little of the nitrogen monoxide desorbs as dinitrogen monoxide, because nitrogen monoxide dissociation leading to nitrogen as the main product takes place preferentially on these platinum sites. On oxidized surfaces, most of the nitrogen monoxide adsorbs and desorbs without dissociation. The combustion of each propene molecule generated several potentially active sites because each propene can remove nine oxygen atoms if its oxidation is complete. When the temperature is increased, both adsorption and dissociation of NO are easier and adsorbed nitrogen atoms become more mobile and recombinate to form N_2. The selectivity to N_2O then significantly decreases (Scheme 6). At low temperatures these dissociated species would interact with NO, whose desorption is difficult in such conditions leading to N_2O.

The mechanism proposed by Burch et al. [307] also explains why alkenes are more effective reductants than CO. One CO molecule can remove only one oxygen atom, thus liberating one site. This can allow NO adsorption but it is not sufficient for its dissociation.

Sasaki et al. [469] consider that the hydrocarbons (in this case propane) are partially transferred to

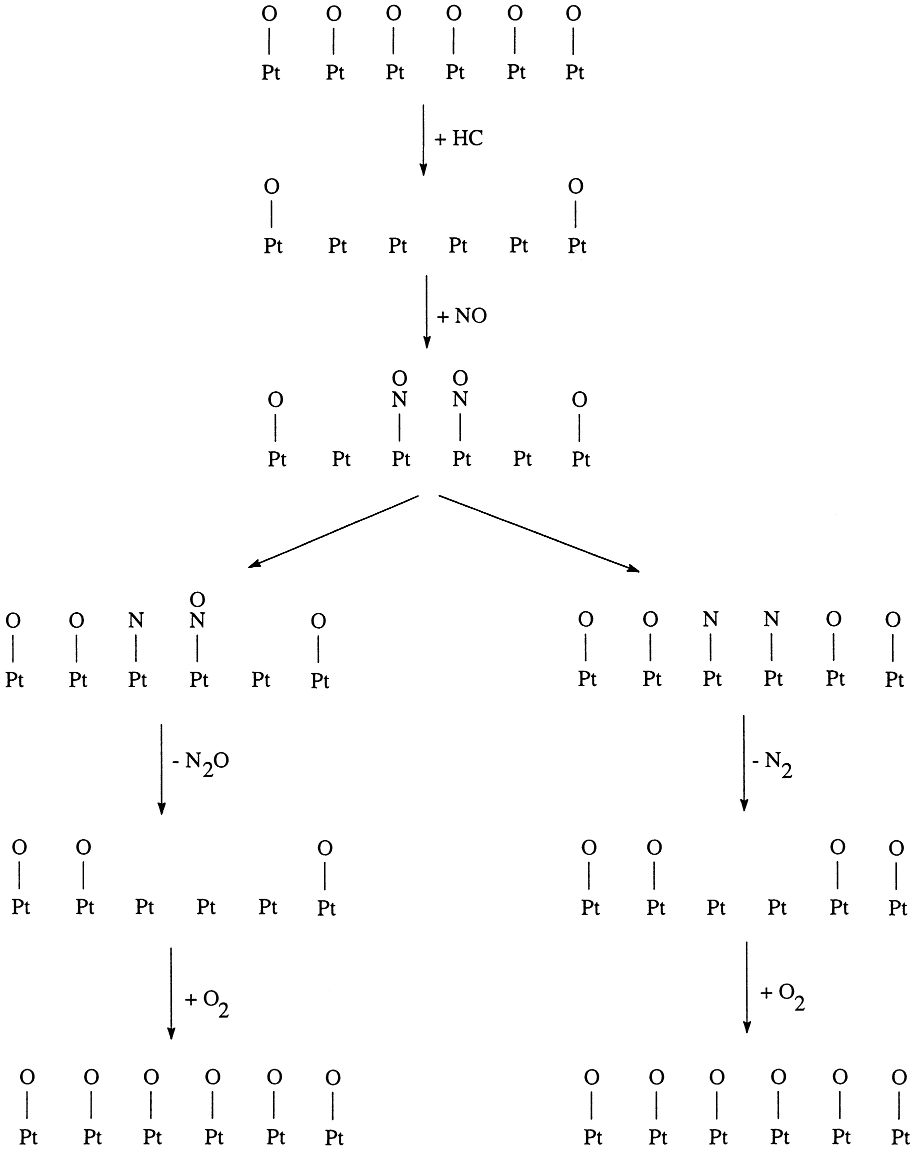

Scheme 6. SCR of NO with propene over a completely reduced Pt/Al_2O_3 surface [311].

oxidized species first. This is followed by the reaction of these species with NO (or NO_2) to form N_2 on the same catalysts:

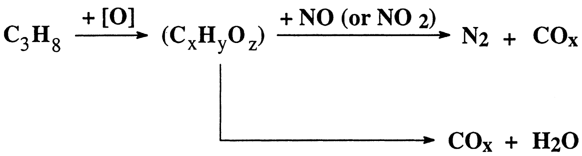

$$\begin{tikzcd} C_3H_8 \arrow[r, "+[O]"] & (C_xH_yO_z) \arrow[r, "+\mathrm{NO}\ (\mathrm{or\ NO_2})"] \arrow[dr] & N_2 + CO_x \\ & & CO_x + H_2O \end{tikzcd} \tag{4.21}$$

Naito and Tanimoto [503] performed an isotopic investigation of the reaction of NO with propene over an Rh/Al_2O_3 catalyst and suggested that the NO_2 and NO_3 species formed promote the dissociation of propene by quickly removing the hydrogen to leave irreversibly adsorbed propenyl species. N_2 and N_2O may be formed by the reaction of weakly adsorbed Rh–$NO^{\delta+}$ species with the propenyl species.

Like in the case of zeolites, these mechanisms try to stress either the dominant role of the activation of hydrocarbons or of the activation of NO. In fact it is very probable that both stages are equally important for a good catalyst.

5.3. *Catalytic reduction of NO in the presence of hydrocarbons over base metal oxides*

Iwamoto et al. [392] (and references herein) [505,506], Bethke et al. [507,508] (and references herein) and Tabata et al. [509] reached the following conclusions considering a large number of base oxides, supported oxides and promoted oxides.

1. The base oxides: SiO_2, TiO_2, V_2O_5, Cr_2O_3, MnO_2, Fe_2O_3, CoO, NiO, ZrO_2 have a very low or even have no activity in the presence of the most active reductants (C_2H_4 or C_3H_6); in contrast, Al_2O_3 and superacid SO_4^{2-}/TiO_2; SO_4^{2-}/ZrO_2 present some activity, the latter having a very high conversion to N_2 at 573 K. Al_2O_3 has mainly Lewis acid sites while SO_4^{2-}/TiO_2 has mainly Brønsted sites, but the catalytic data indicated that the activity of these oxides does not simply depend on the acidity only.
2. In deposited metal oxides (other than noble metals): Si, K, Ca, V, Cr, Mn, Fe, Co, Ni, Cu, Zn, or Ag on Al_2O_3; Cu on SiO_2; Cu or Co on Al_2O_3–SiO_2; Cu on TiO_2, the data indicated that only Cu, Co or Fe supported on Al_2O_3 exhibits an enhancement of the catalytic activity in the selective reduction of NO compared to the non-supported oxides. Bethke et al. [508] (and references herein) recently reviewed this category of catalysts and their analysis indicated that, using Al_2O_3 as support, a certain catalytic activity is achieved for those metals found to be active as metal-exchanged zeolites, i.e. Co, Ni and Cu. These data are additional evidence of the importance of the nature of the metal species being formed by interaction with the support. In addition, they found that the influence of the metal loading also exhibits trends similar to those determined for metal-exchanged zeolites.
3. Promoters have been found to improve the catalytic performance of these supported catalysts. Thus, the modification of copper-containing alumina-supported catalysts with cesium was found by Ukisu et al. [440,477,510] to have a beneficial effect. They evidenced that Cu/Al_2O_3 is less active than Cu–Cs/Al_2O_3 in the reduction of NO_x. This finding is rather surprising because all studies made using zeolites or other acidic materials stressed the importance of acidic sites in the activation of NO. Taking into account that in this case the reductant is a saturated hydrocarbon, the presence of strong basic sites like Cs, and of a strong oxidant like NO could lead to a behaviour similar to those occurring in the oxidative coupling of methane.

Tabata et al. [509] investigated another series of alumina-supported metal catalysts (Sn, W, Mo, Ga, Bi and Sb) using methanol as a reductant. They reported that the addition of Sn led to an important enhancement of the activity of alumina, especially in the low temperature range ($T<625$ K). They suggested that the effect of the Sn additive was directly related to the promotion of a reaction step leading to the formation of N_2 and CO_x. The increase of the metal content led to a decrease in the activity. These data agree with those reported by Iwasawa et al. [498] on bicomponent Pt/Sn and this behaviour could be explained by data from [508]. These authors showed that polar molecules such as alcohol could compete for surface sites with resulting water molecules and that the addition of lanthanum increases the accessibility of alcohol. It is probable that Sn plays the same role.

Catalysts based on ZrO_2 and including various metal species deserve a special interest. In the case of M–Zr–O (M=Cu, Ni, Mn, Fe and Co) obtained by co-precipitation, Bethke et al. [507] indicated that, in the presence of propene, Cu–Zr–O was the most active oxidic catalyst reported to date. A more important observation in this case is the high reactivity and selectivity of low-loading copper catalysts. Bethke et al. [507] suggested that the CuO forms clusters and that the size of the CuO cluster is limited. The reactive lattice oxygen in bulk CuO would reduce the selectivity of the catalysts for the reduction of NO in an oxidizing atmosphere. The consequence is that limiting the cluster size of CuO dispersed in inert matrices would reduce the non-selective reaction of hydrocarbons with the lattice oxygen.

The presence of neodymia promotes the activity of these catalysts. Cu–Ga_2O_3 has also been found to be an effective lean NO_x reduction catalyst. Bethke et al. [508] showed that Cu–Ga_2O_3 had a higher competitiveness factor and a higher NO conversion than Cu–

ZrO_2 at all oxygen concentrations investigated.The competitiveness factor was defined as $NO_{reacted}\times 100\%/(n\times HC_{reacted})$ where $NO_{reacted}$ is the NO reacted to form N_2 and n is the number of O atoms needed to combust the reacted hydrocarbon, $HC_{reacted}$, to O_2 and H_2O. This behaviour, as in zeolites containing gallium, depends on the necessary presence of a certain amount of Lewis acid sites on the support. This cooperative effect between the support, which could favour the adsorption of the reaction products, and the metallic species was also reported by Guglielminotti and Boccuzzi [380].

With this category of catalysts, as in the others, the nature of the reducing agent has a strong influence on the reaction, alkenes and alkynes being more active than alkanes [378,507]. In the latter case, *n*-heptane presents a good reactivity. The formation of the isocyanate species seems to depend on the chain length as well as on the type of hydrocarbon.

Very recently, Vannice et al. [511] proposed a new possibility, on the basis of investigations using CH_4 as a reductant. They supposed the activation of CH_4 was the same as on typical catalysts used in the methane oxidative coupling reaction and investigated basic Li/MgO catalysts with different lithium contents. Even though Li/MgO catalysts included very cheap components and exhibited a stable and long-term activity, the results are not relevant. The activities and selectivities were lower than those of some metal zeolites or rhodium-supported catalysts. Thus, no reaction occurred below 873 K and the selectivity to N_2O at about 950 K was still 20%. The addition of oxygen decreased the N_2 formation rates at higher NO concentrations (2%) but had little effect for approximately 1000 ppm of NO.

5.3.1. *Catalyst stability*

As was mentioned in the case of the reduction of NO with CO, all these oxide systems exhibit a low stability in the presence of water (see section on the reduction of NO with CO). However, Tabata et al. [509] reported that the addition of Sn to alumina could improve the catalyst durability in the presence of SO_2 and also of water.

5.3.2. *Mechanism and kinetics*

Ukisu et al. [394,440] suggested that the reduction of NO on the oxide surface occurs through the same isocyanate intermediate as in zeolites. The mechanism they proposed is similar to that proposed by Obuchi et al. [478] taking into account some kind of oxygenated intermediates. This conclusion seems to apply to all hydrocarbons.

In basic catalysts, Vannice et al. [511] indicated that the conversion data are consistent with the contribution of $[Li^+O^-]$ sites to activate the CH_4 molecule. No evidence of NO_2 as an intermediate was found on these catalysts and two competitive reactions were considered to account for the experimental data:

$$2NO + CH_4 + O_2 \rightarrow N_2 + CO_2 + 2H_2O \tag{4.22}$$

and

$$CH_4 + 2O_2 \rightarrow CO_2 + 2H_2O \tag{4.23}$$

6. NO decomposition

The decomposition of NO would represent the most attractive solution in emission control, because the reaction does not require that any reactant be added to NO exhaust gas and could potentially lead to the formation of only N_2 and O_2. Additional reductants such as hydrocarbons, CO, H_2 or ammonia can lead to the production of secondary pollutants like oxygenated hydrocarbons, CO, CO_2, N_2O or ammonia or, even, as was often reported in the past, cyanate and isocyanate compounds. This could be completely avoided in this case, except N_2O formation.

Up to now Cu-zeolites are the best catalysts. The arrangement of this section will therefore take into account the fact that the presentation must focus on the particularities of this group of catalysts which led to such behaviour. We shall successively examine supported metals and oxides, metal-exchanged zeolites, perovskites, amorphous alloys and membrane catalysts.

6.1. *Supported metals and oxides*

First experiments made by Sikada et al. [512] and Shelef et al. [513,514] on supported Pt–Ni and on supported Pt, respectively, indicated the very important influence of oxygen on the rate of decomposition. Winter [515] and then Boudart et al. [516] investigated a very large number of unsupported catalysts: MgO, ZnO, CaO, SrO, Ga_2O_3, SnO_2, TiO_2, Fe_2O_3, Co_3O_4, NiO, CuO, Rh_2O_3, IrO_2, CeO_2, HfO_2, Sc_2O_3, ZrO_2, ZrO_2–Sc_2O_3, ZrO_2–CaO, Y_2O_3, ThO_2, La_2O_3, Nd_2O_3, Sm_2O_3, Eu_2O_3, Dy_2O_3, Ho_2O_3, Er_2O_3, Tm_2O_3, Yb_2O_3, Lu_2O_3, alumina and alumina-supported platinum. A kinetic analysis indicated a strong oxygen inhibition in all cases. The turnover number calculated for the "most active" catalysts indicated the following order of activity: $Co_3O_4 > CuO > ZrO_2 \gg NiO > Fe_2O_3 > Al_2O_3$. At the same time the activation energies determined by Winter [515] indicated: $CuO > Rh_2O_3 > Sm_2O_3 > SrO$ as the "most active" oxides. Similar results were also reported by Shelef et al. [513] on cobalt oxides.

The decomposition of NO to N_2 and N_2O on a number of oxides: chromium oxides [167], iron oxides [169], nickel oxides [170], copper oxides [178] or manganous oxides [179] was also the object of more detailed studies of Shelef et al. aimed at determining surface interactions. The deposition of platinum on alumina surfaces increases the constant rate values by 10^4 times [516]. An optimistic argument for the removal of NO over Pt/Al_2O_3 was also expressed by Bauerle et al. [517]. However, Hightower and Leirsburg [518] showed that the catalytic decomposition of NO to O_2 and N_2 over noble metals or oxide catalysts is too slow to be considered on a practical scale. Re-questioning this problem, Yamashita and Vannice [519] reached the same conclusions in manganese oxides.

For noble metals, the theoretical calculations carried out by Broden et al. [520] revealed that the NO dissociation is more likely on Rh, Ir or Ru surfaces than on Pt. These data agree with those obtained for the reduction of NO in the presence of CO (see section on the reduction of NO in the presence of CO).

Recently, Hamada et al. [521] reported that the introduction of Ag by precipitation or co-precipitation in an Ag–Co_2O_3 catalyst generates a system which could be a candidate for the direct decomposition of NO. These studies indicated the necessity to ensure a very high Co/Ag ratio, the best results being obtained as a 20:1 ratio. However, the most prominent feature of the Ag-promoted cobalt oxide is that the inhibition of the reaction by oxygen is very much diminished.

6.2. *Metal zeolites*

A crucial turn in the investigations on NO decomposition occurred when Iwamoto et al. [522–527] first found that copper-exchanged zeolites, in particular Cu-ZSM-5 zeolites, were effective catalysts for NO decomposition. Since then, these catalysts have been the object of the most active investigations and much has been done to improve their properties as well as to characterize and understand the mechanism through which the reaction takes place.

The central question is why are copper-exchanged zeolites the best catalysts in this reaction? After seven years of research some aspects concerning the structure and function of these catalysts begin to clarify. Several factors seem to be more important: the nature of the zeolite, the nature of the metal, its loading, etc.

The positive contribution of the MFI structure. The first studies using Y zeolites indicated a constant activity as a function of time that was not observed for base oxides or supported noble metals. Iwamoto et al. [522] suggested that the main difference between the Cu–Na-Y zeolites and the CuO–SiO_2 catalysts in NO decomposition arises from the distinction of the thermal stabilities of oxygen adsorbates over these catalysts. On the CuO–SiO_2 surface, oxygen adsorbates can exist at high temperatures with a significant stability.

Comparing zeolites with other supports, Iwamoto et al. [523] also concluded that the amount of NO adsorbed on the Cu zeolites is much higher than on Cu/Al_2O_3 and Cu/SiO_2–Al_2O_3. Copper over-exchanged ZSM-5 catalysts have been shown to have an exceptionally high activity in NO decomposition [397]. The MFI structure as support for copper-exchanged zeolites revealed an important enhancement in the conversion and the selectivity [524–530]. Comparative studies using faujasite, Y, mordenite or ZSM-5 supports performed by Iwamoto et al. [524] indicated that the superiority of the ZSM-5 support is evident for the same level of copper exchange. Irrespective of the reaction conditions, the order is always the same: ZSM-5≫Y≅mordenite≫faujasite.

With respect to the role of the ZSM-5 support, Steinbach et al. [531] consider that ZSM-5 is only an effective support because it imposes a highly distorted and misfitted structure to the oxide lattice and gives it the appropriate porosity as well, both properties being deemed essential for an outstanding activity of the Cu-oxide. However, there is much evidence against this affirmation. The principal one is that copper is highly dispersed and is not able to construct its own lattice.

In fact, the situation is more complex and why ZSM-5 is the most effective support still remains an unsolved mystery. Is its very high reactivity related to the textural or acid properties? Other hypotheses such as the stabilization of a certain state or the possibility to ensure and maintain a high dispersion are also possible. An answer to this question could open new perspectives in the preparation of other active catalysts.

Centi and Perathoner [532] tried to find some answers to these questions and suggested that two significant differences make the MFI structure more adequate than other structures investigated. The first difference is that in all other cases parts of the copper are implanted in hidden positions where the shielding effects of the lattice oxygen prevent or limit the possibility of interaction with the reactant molecules. The second difference is related to the covalency of the bond between the metal and the zeolite lattice, this decreasing in the order MFI>mordenite>faujasite. Therefore, the local charge seen by molecules coordinating copper ions is considerably different from one zeolite to the other.

In a given family of zeolites this property could also be changed by modifying the silicon-to-aluminium ratio. Iwamoto et al. [524] reported that an SiO_2/Al_2O_3 ratio of 20–50 corresponded to the highest catalytic activity per Cu^{2+}. Conversely, Moretti [533], from a literature data investigation, evidenced that a decrease in the activity per copper atom occurred for an Si/Al ratio ranging between 11.7 and 27. Li and Hall [529], using zeolites with Si-to-Al ratios between 12 and 26, reached the same conclusions. Other NO decomposition experiments performed by Delmon et al. [534,535], using different over-exchanged Cu-ZSM-5 with Si-to-Al ratios between 15 and 60, reported that an increase of the Si-to-Al ratio up to 25 led to an increase in the conversion, and the activity started to decrease at ratios above 30.

Generally speaking, the modification of the silicon-to-aluminium ratio is interpreted in terms of the modification of the acidity. However, as Inui et al. [450] also indicated, acidic properties have no direct influence on NO decomposition. The modification of the acidity exerts an indirect control, by modifying the local charge, as Centi and Perathoner [532] suggested. The modification of the "acidity" would control the redox behaviour of the implanted metal and FT-IR and XPS measurements made by Delmon et al. [535] provided proofs of this effect.

In order to improve the favourable influence of the zeolite, one of the solutions proposed by Centi and Perathoner [532], was to substitute Al ions for other trivalent species like B, In, Ga or to substitute Si for other tetravalent species. However, the modification of the support only by the deposition of ZrO_2 obtained from alkoxide-derived sols had no effect, as Delmon et al. [535] indicated.

The detailed structural characteristics of the ZSM-5 zeolite seem to have an additional effect in permitting the performances mentioned in NO decomposition. This is a conclusion from experiments by Li and Hall [536] who showed that NO decomposition on catalysts pretreated in He started only after a certain time. During that time both an oxidation and a redistribution of copper occurred as shown by XPS data [537]. A micropore textural characterization of samples before and after the reaction indicated practically no difference. Moreover, the measurements indicated no difference between exchanged and non-exchanged samples. One must thus consider two other important properties exhibited by the zeolite texture. First, its very narrow channels avoid the formation of large metallic aggregates, which are inactive in this reaction, as was mentioned above in the case of metal oxides. Second, it is speculated that the linear channels could allow a migration of copper to the active positions using the zeolite oxygen as a vehicle during the treatment in oxidizing conditions, i.e. in the presence of nitrogen oxides or even oxygen. These suppositions agree with the results of measurements with labelled molecules using a microbalance performed by Valyon and Hall [538]. These authors observed that the oxygen released was different from the oxygen introduced. Another evidence was also reported by Hall et al. [539,540] from experiments in which they used $^{18}O_2$ and $^{15}N^{18}O$ isotopes. They indicated that the lattice oxygen was involved in this reaction and that oxygen atoms might be introduced at one place whereas O_2 may be formed and released from elsewhere on the solid. It was speculated that only a limited amount (<10%) of the lattice oxygen participated in this process. Iwamoto et al. [524] suggested that at high temperatures the oxygen produced can

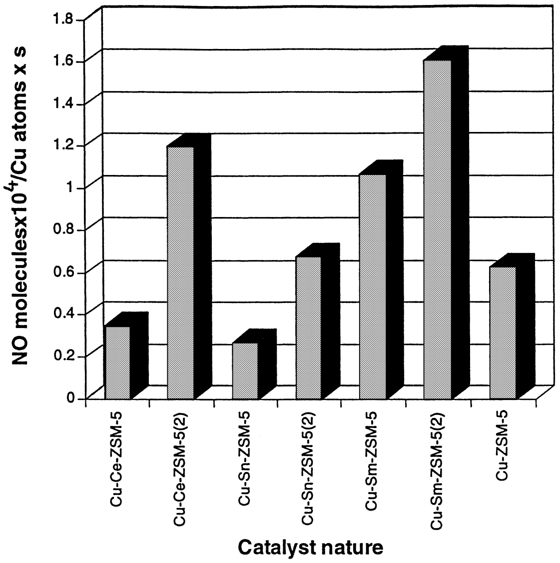

Fig. 15. Turnover frequency for NO decomposition over bicomponent zeolites (flow rate: 27 ml min^{-1}, catalyst weight: 0.5 g, temperature: 773 K).

desorb from the zeolite surface and that the regeneration of the active sites makes it possible to continue the catalytic decomposition cycle.

Influence of the metal nature and its loading. It is widely recognized that copper in ZSM-5 exhibits the best catalytic activity in NO decomposition. Other metal-exchanged zeolites present a low activity such as Co [403,414,541], Ce or Sm [535,542] or even no activity, such as Sn, Ag, Ni, Tl (Fig. 15) [542,543]. Shelef et al. [470] suggested that activity in NO decomposition could be correlated with the ability for these metals to oxidize NO to NO_2. Strong evidence supporting this was given by Chang and McCarty from isotope labelling results. However, the contribution of the nature of copper in this reaction is more complex and more details will be given in Sections 6.1 and 6.2.

Another certainty in this reaction is that copper should be in an over-exchanged state. The higher activities always occur in the 723–773 K temperature range. The decomposition rate as a function of the ion-exchange level reveals an S shape with an increasing slope up to 80% exchange. After that, the activity of the Cu-ZSM-5 zeolites still increases with the level of the copper exchange up to a plateau that generally corresponds to a 200% exchange [411,536,538]. Very surprisingly, in the case of high siliceous ZSM5-5 zeolites (Si-to-Al ca. 80), Pirone et al. [544] found that the NO decomposition activity increased with the copper content up to about 640% Cu over-exchange. However, in such case some small CuO crystallites could be formed.

The literature does not give any unequivocal explanation as to why Cu-ZSM-5 should be over-exchanged [134,396,545,546]. One of the certainties is that copper must be implanted very close to the aluminium lattice. Recent studies by Parrillo et al. [547,548] based on isopropylamine-TPD-TGA investigations show that the total exchange of the cationic species bonded to framework Al^{3+} sites is possible only for high copper loading. Isopropylamine decomposes on Brønsted acid sites at temperatures as low as 575–650 K. After Cu exchange, isopropylamine is still decomposed at these temperatures until the loading of copper exceeds 180 μmol Cu sites/g. This indicates that for low copper loading an important part of these sites remains unchanged while copper could be exchanged into external Si–OH sites for under-copper-exchanged zeolites. Other previous studies show that this is possible in conditions of typical copper exchange [549–551]. Copper-exchanged sites are able to decompose isopropylamine only at temperatures higher than 650 K.

The exchange of Si–OH sites could lead to some Cu^{2+} aggregates but the relatively narrow pores of ZSM-5 and the absence of cages would limit the number of atoms clustering around the exchange point to a very small value. Over-exchanged catalysts could be obtained after one step or after three or more exchange procedures [552]. One of the possibilities to increase the level of copper exchange is to modify the pH. Iwamoto et al. [553] indicated that a pH between 7 and 8 is optimal for an over-exchange. This behaviour was explained considering that the exchange between Na^+ and $Cu_2(OH)^{3+}$, $Cu(OH)^+$, $Cu_2(OH)_2^{2+}$ or $Cu_3(OH)_2^{4+}$ formed at a specific pH [553] (and references herein) probably took place in zeolites.

In order to increase the exchange level of copper Iwamoto et al. [553] also investigated the effect of the addition of different bases on the ion-exchange level and on the catalytic activities of the corresponding resulting zeolites. Using copper nitrate as a precursor, the experimental data indicated that there was no correlation between the ion-exchange level and the catalytic activity in the presence of basic additives. The exchange levels varied in the order NH_4OH>-$Ba(OH)_2$>$Ca(OH)_2$>NaOH>KOH>pyridine>$Mg(OH)_2$ >ethylendiamine>none, while the catalytic activity varied in the order NH_4OH>$Mg(OH)_2$>none>$Ba(OH)_2$ >pyridine>$Ca(OH)_2$>ethylenediamine>KOH=NaOH. The low effect of ethylenediamine was attributed to the high dimensions of the resulting copper complex. However, the beneficial effect of ammonia both on the exchange level and on the catalytic activity of the resulting zeolites is noteworthy.

However, the increase of the exchange level over 300% causes a strong decrease in the activity [134,537] due both to the blocking of the pores and the segregation of copper in inactive crystallites.

Recently, Eranen et al. [554] suggested another possibility to increase the catalytic activity of Cu-ZSM-5 zeolites. They introduced copper-impregnated silica fibres during Na-ZSM-5 syntheses and the resulting zeolite was then exchanged following the Iwamoto procedure. An important enhancement of the activity was reported, even in the presence of 5% oxygen in the feed.

The nature of the salt precursor could also influence the activity of Cu-ZSM-5 because different dispersions were measured in the corresponding catalysts. Experiments carried out by Delmon et al. [542] starting from acetate or nitrate show comparable activities while the catalysts obtained from chlorides exhibit a substantially lower activity. This behaviour could be correlated with the recently reported data [555] about the high dispersion of $CuCl_2$ in ZSM-5 zeolites or with a negative long-term effect of the chlorine remaining in the catalysts. CO-FT-IR measurements as well as XPS could give very useful information in this sense.

Influence of promoters added to Cu-zeolite catalysts. Another possibility to improve the catalytic performances of Cu-ZSM-5 is the use of promoters. A first attempt to improve the catalyst was made by Iwamoto et al. [556] starting with Cu-Y zeolites. They tested a series of possible promoters: Ni, Co, Zn, Ag, Cu, Fe, Mn, Ca, and found that only Ni and Co exhibited a positive influence. Later, Kagawa et al. [557] tested a very large number of cations. Zeolites were prepared by successive or simultaneous ion exchange. All cations except yttrium and silver gave catalysts less active than pure over-exchanged Cu-zeolites. It is also noteworthy that, at 823 K, the bicomponent zeolites containing Ba, Sr, Co, Ni or Pt in addition to Cu show roughly the same activity as Cu(133)-ZSM-5 (ZSM-5 exchanged with a quantity of copper 133% that corresponding to the exchange capacity) but with a copper content more than 50% lower [557]. The introduction of a basic cation like Li, Na, K, or Cs was found to have a negative effect [557]. Zhang and Flytzani-Stephanopoulos [558,559] reported a positive effect of cerium. Their results agreed with those obtained by Kagawa in the case of Mg, Ni, Sr and Pd catalysts. The authors suggested that the effect of cerium was to hinder the sintering of the catalytically active components rather than to degrade the zeolite support [560]. A positive effect of cerium was also observed by Delmon et al. [543]. Eranen et al. [554] prepared bicomponent catalysts using two techniques: the exchange of zeolites including metals (Co, Ni, Ga) during synthesis, or the impregnation of copper-exchanged zeolites with the second metal (Co, Ni, Ag). In all cases the conversion to N_2 was found to be inferior to that obtained over pure copper-exchanged zeolites. Soon after that, Budi et al. [435] and Kucherov et al. [561] reported a noticeable influence of lanthanum on Cu-ZSM-5. They interpreted this behaviour in terms of a treatment-induced modification of the bond between the isolated Cu^{2+} cations and the framework oxygens of ZSM-5, linked in turn to the Al^{3+} ions. Delmon et al. [562] also found an important increase in the TOF values after introducing a low amount of samarium (Fig. 15). High loading of the promoter was found to have a negative effect. However, to this day there is no explanation as to the mechanism through which transitional co-cations such as Ce, Sm or Y promote the copper activity. Other experiments carried out by Delmon et al. [543,563,564] using Ag-, Sn-, Zr- or Ni–Cu-ZSM-5 zeolites indicated only a slight effect. Zeolites containing only the other metal M-ZSM-5 (M=Ce, Sn, Sm or Tl) exhibited a very low activity (Fig. 16).

Iwamoto et al. [556] prepared exchanged catalysts using two different procedures: first copper and then the second metal, or first the second metal and then copper. The exchange levels of copper and of the other metal ions in the two-component system were each about 30%. The authors concluded that the order of ion exchange has little influence on the activity. Con-

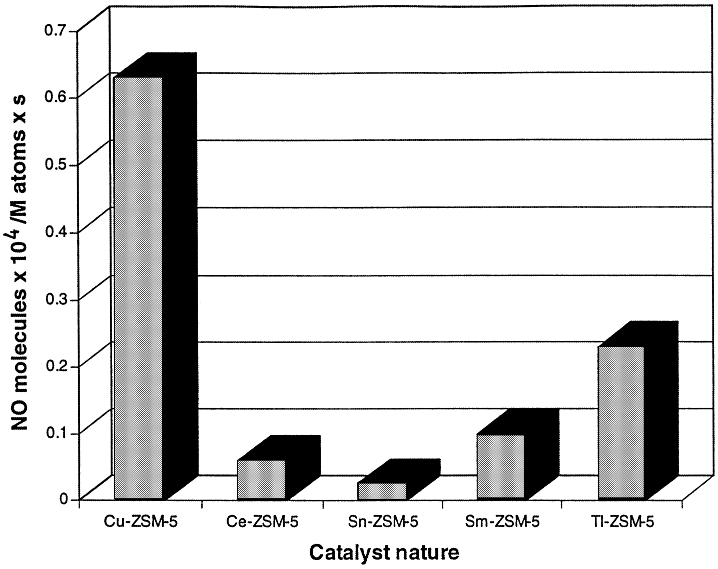

Fig. 16. Turnover frequency for NO decomposition over metal zeolites (flow rate: 27 ml min^{-1}, catalyst weight: 0.5 g, temperature: 773 K).

versely, Delmon et al. [562–564] showed that the exchange mode is very important, the best activities being obtained on co-exchanged samples.

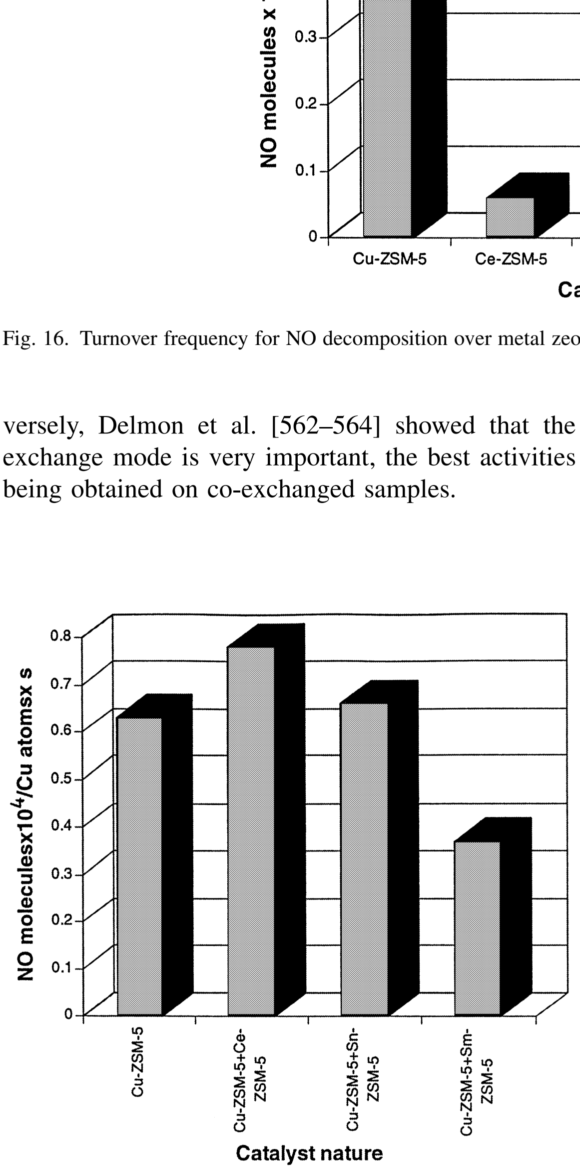

Fig. 17. Turnover frequency for NO decomposition over physical mixtures (1:1) of metal zeolites (flow rate=27 ml min^{-1}, catalyst weight: 0.5 g, temperature: 773 K).

The physical mixture [563,564] of an over-exchanged Cu-ZSM-5 with monoexchanged Ce-, Sm-, Sn-, or Tl-ZSM-5 (Fig. 17) was also investigated. Delmon et al. [563,564] found no effect, except a very small influence in the case of Ce-ZSM-5. The physical mixture of an over-exchanged zeolite with a large number of metal-oxides [564]: CeO_2, SnO_2, ZrO_2, Nb_2O_5–Co_3O_4, MoO_3/Al_2O_3 (Fig. 18) was also investigated. In all cases a negative effect upon the total NO conversion and a decrease in the selectivity to N_2 in favour of N_2O were evidenced. It was assumed that in that case, the oxides contribute to a further oxidation of the superficial copper.

Influence of other factors. Increase of the pressure has a beneficial effect upon the conversion. Iwamoto et al. [556] reported an approximately 50% increase of the conversion when the NO pressure was incremented from 0.18% to 2.05%, which indicates a reaction order of about 1.2–2.5. The contact time also has a positive effect, whereas the presence of oxygen or water vapour strongly diminishes the catalytic activity.

6.2.1. State of the copper in Cu-ZSM-5 zeolites

One of the most investigated problems concerns the nature of the active copper. Even though a number of suggestions have been made, the situation is still unclear. The complexity of the problem stems from

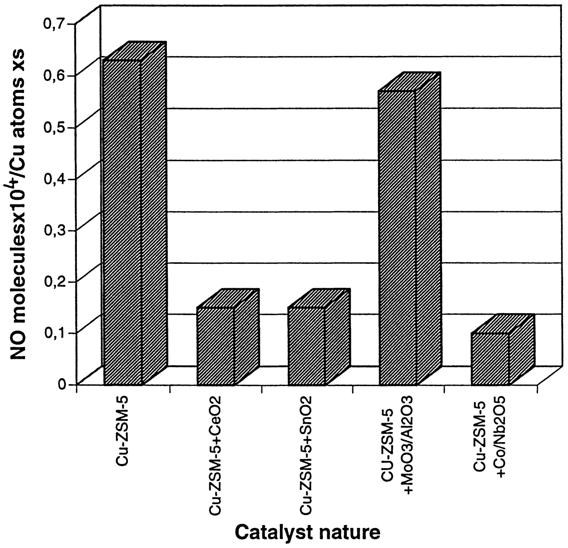

Fig. 18. Turnover frequency for NO decomposition over physical mixtures of Cu-ZSM-5 with metal oxides (flow rate: 27 ml min^{-1}, catalyst weight: 0.5 g, temperature: 773 K).

the fact that the implanted copper is in different locations and chemical states in the zeolite lattice. Investigation is very difficult, because even in over-exchanged zeolites the copper loading is below 2.5 wt% for a total surface area of catalysts exceeding 400 $m^2\,g^{-1}$.

Some of the research groups active in this area consider that active copper is a $[Cu–O–Cu]^{2+}$ dimeric species whereas others consider that the active species is monoatomic copper in the vicinity of an Al atom of the zeolite framework.

Iwamoto [396] first suggested that NO decomposition requires the presence of two copper ions in close vicinity. Based on previous works by Naccache et al. and Jacobs et al. [396] (and references herein), Iwamoto and co-workers consider that these species are formed during the ion-exchange procedure, when water molecules coordinated near the Cu^{2+} ions are easily ionized and dissociated because of strong electric fields near this ion, this generating $Cu(OH)^+$ and Brønsted acid sites. By dehydration at elevated temperatures, a dimerization or polymerization could occur to form $Cu^{2+}–O^{2-}–Cu^{2+}$ species. However, other Cu^+ species could also be generated during the ionic exchange.

Yashima et al. [133] also consider the concentration of copper ions to be a critical factor governing the specific activity. They also indicate that part of the copper is not active in the over-exchanged zeolites and suggest that it is necessary to ensure the creation of a certain proportion of active species in the form of two adjacent Cu^{2+} to obtain active catalysts. An excess of Cu^{2+} ions may form aggregates, such as small particles of CuO that are less active than the Cu^{2+} present as a counter ion, or may block the pores of ZSM-5.

Most suggestions indicating the existence of diatomic $[Cu–O–Cu]^{2+}$ clusters are based on evidence concerning the O bridging species, also known as "extralattice oxygen" (ELO). These species do not belong on the zeolite lattice and are formed during the dehydration of exchanged $Cu(OH)^+$:

$$2Cu(OH)^+ \rightarrow [Cu-O-Cu]^{2+} + H_2O \qquad (5.1)$$

Much of the evidence about the existence of this dimeric species was given by Sachtler's group [565–567]. They indicated that copper bridged through ELO oxygen represents an important part of the total copper. The reductive adsorption of nitrogen monoxide on Cu^{2+} results in the formation of $Cu^+–NO^+$ while the dissociative thermal desorption at 550 K not only restores the Cu^{2+} ions but also appears to regenerate the $[Cu–O–Cu]^{2+}$ complex. Other evidence was given by Valyon and Hall [546,568] who identified FT-IR bands corresponding to species formed by the association of NO with ELO. The existence of this species was also previously suggested for Fe-Y zeolites by Boudart et al. [569,570], from both IR and Mossbauer studies, and more recently by Shpiro et al. [571,572], based on EXAFS, XPS and FT-IR.

Another point of view is that adopted by Wichterlova's group [573–576], who suggest that monomeric atomic species in the vicinity of framework Al are the active sites. They thought that only copper belonging to these sites can exhibit catalytic activity.

In order to clarify this problem many physical methods were used but none could exhaustively describe all Cu. Each illustrates only part of the characteristics and most of the studies try to correlate this information.

ESR technique. Among these techniques, ESR was used extensively because it is very sensitive and provides information on both the environment and the coordination of cupric ions, especially in very dilute systems. Cu^+ is a diamagnetic species and in consequence cannot be visualized by ESR.

Giamello et al. [577] and Kucherov et al. [578] showed that freshly prepared Cu-ZSM-5 samples exhibited an axial, broad and scarcely resolved EPR spectrum typical of hydrated Cu^{2+} ions in a zeolitic framework. A treatment under vacuum at increasing temperatures changed the spectrum profile due to the progressive appearance of various distinct Cu^{2+} species and decreased the signal intensity. However, this behaviour of the Cu^{2+} ions in zeolites is not specific for ZSM-5, as was previously reported by Jacobs et al. [579,580], but the comparison with SiO_2 [581] or the Y zeolite [582] brings out some differences.

Dehydrated Cu-ZSM-5 exhibits symmetrical signals with hyperfine splitting originating from the copper nuclear spin 3/2 [576,583]. An increase in copper content leads to a loss of resolution of the perpendicular component. The value of the parallel component of the axially symmetrical signals of dehydrated Cu^{2+} indicates the presence of two kinds of coordination (both square pyramidal) for a low copper content while an increase in the Cu concentration leads to the appearance of a new coordination (planar) [575,584–587].

The evacuation of Cu-ZSM-5 upon heating in a vacuum causes a drop in the signal intensity and the disappearance of the signals with $g_{\|}=173$ G, $A_{\|}=173$ G and $g_{\perp}=2.07$ [588] at temperatures above 1073 K. Kucherov et al. [589] showed that only 20% of this drop could be attributed to the reduction of the cupric ion. In their opinion, the change in the population of unpaired electrons according to Curie's law or a decrease in the spectrometer sensitivity due to the decrease in the cavity quality factor at high temperatures are the most likely explanations of the effect observed. Furthermore, in the presence of a He flow, the same authors showed that no measurable reduction of the cupric cations occurred. However, the exposure of Cu-ZSM-5 to a high temperature-reducing environment causes a fast reduction of copper [590].

Another point of view is that presented by Sachtler's group [566] who considers that the diminution of the signal could be due to the formation of a dimeric "silent" $[Cu–O–Cu]^{2+}$ species. Although copper in this complex would be in the oxidation state Cu(II), it would not give ESR signals, this reflecting a diamagnetic ground state resulting from antiferromagnetic coupling.

The ESR spectra of Cu^{2+} are not altered in the presence of NO at 773 K. At low temperatures (i.e. 293 K), however, the formation of adsorption complexes between the isolated cupric ions and NO causes measurable changes in the coordination of Cu^{2+}. The complete restoring of the spectra is achieved by treating the samples at 423 K [587,589,591]. It has also been shown that the oxidation of cuprous ions in Cu-ZSM-5 in the presence of NO occurs very rapidly [592]. In the reaction conditions, square planar isolated cupric ions are most reactive and it is therefore plausible that the same sites are the active sites. These are also most susceptible to deactivation [589,593]. The appearance of a second isolated Cu^{2+} species accompanied by some dealumination of the ZSM-5 support was also thought to be a cause of deactivation [566,591].

The treatment of Cu-ZSM-5 at high temperatures (i.e. >873 K) causes a modification in the Cu^{2+} coordination. This modification is due to a bond modification between the isolated Cu^{2+} ions and the framework oxygen. The new state corresponds to a square pyramidal coordination and the transformation is irreversible [594,595]. Based on in situ measurements, Tanabe et al. [590] expressed a point of view similar to that of Sachtler and Sarkany [566], indicating that the corresponding deactivation is due to a migration of copper ions to sites where gas molecules, such as nitric oxide, cannot reach them.

From the same kind of ESR measurements, Larsen et al. [596] proposed an autoreduction mechanism which would lead to the simultaneous formation of copper in two different oxidation states:

$$[Cu^{2+}OH^-]^+ \rightarrow Cu^+ + OH \tag{5.2}$$

$$[Cu^{2+}OH^-]^+ + OH \rightarrow Cu^{2+}O^- + H_2O \tag{5.3}$$

$$2[Cu^{2+}OH^-]^+ \rightarrow Cu^+ + Cu^{2+}O^- + H_2O \tag{5.4}$$

This would create a Cu(II) superoxide complex in an oxidizing atmosphere.

The existence of two Cu^+ and Cu^{2+} ions in close proximity could act as a "buffer" system favouring a redox process. The existence of a redox reaction involving copper in Cu/Na-ZSM-5 was also suggested by Sarkany et al. [565] on the basis of FT-IR measurements. This redox process could occur on a system composed of copper implanted in a position close to the aluminium framework and another one implanted on the silica part. The implantation of copper species on the silica part has already been proven. Wooley et al. [597] reported that Na can be exchanged into a pure silicalite and that this exchange is due to the presence of "nested silanols" at vacancy defects. McCabe and Wong [216] and Sachtler et al. [565] also agree with such a process.

XANES and EXAFS. The combination of XANES and EXAFS also enables the study of the electronic and geometric structural changes in Cu-ZSM-5 [598]. However, this information is mediated over all Cu(I) and Cu(II) species and cannot distinguish between different isolated atoms. Hamada et al. [599] first investigated the structure of Cu-ZSM-5 and reported that no differences could be detected between fresh, pretreated and tested catalysts. Other studies carried out by Liu and Robota [492,493,600–603] disagreed with this opinion and showed that a variety of dynamic changes take place both in electronic and geometric structures of Cu during in situ experiments. Fresh Cu-exchanged zeolites indicate the presence of randomly distributed fully coordinated Cu(II) ions, the coordination being possibly due to O atoms from water in the zeolite. After calcination in air, they observed a modification in the coordination, the copper being then implanted on the zeolite through the framework O atoms. This behaviour is a consequence of the loss of water and is in perfect agreement with ESR data reported. However, experiments made by Liu and Robota [492,493] on the activation of the same catalysts in He indicate an autoreduction of Cu(II) to Cu(I), as opposed to those reported by Kucherov et al. [589]. The coordination of the Cu(I) species determined by EXAFS [600–603] corresponds to two oxygen atoms with a Cu–O distance of 1.94 Å. In situ measurements made by the same authors [600–603] also indicate a very high reactivity of Cu(I) species, which also corresponds to the ESR determinations [589,593]. Although Cu(I) is formed at elevated temperatures even in the presence of oxidizing species like NO in the gas stream, at room temperature it reacts rapidly and the chemical balance shifts towards Cu(II). In catalytic conditions (723–773 K), in Cu-ZSM-5 zeolites, a small part of copper is maintained as cuprous ions. Substantial differences were observed between over- and under-exchanged zeolites in the decomposition of NO. Both over- and under-exchanged zeolites indicate the simultaneous presence of Cu(I) and Cu(II) but samples containing more copper exhibit higher Cu(I) concentrations, and therefore a higher activity. Because a higher activity is associated with a higher O_2 desorption capacity, Kharas et al. [598] suggest that in catalytic conditions cuprous ions may be regenerated by a redox process implying dicopper species:

$$2Cu^{2+}O^{2-} \rightarrow 2Cu^{+} + O \qquad (5.5)$$

Photoluminescence technique. Additional information about the location of the copper in ZSM-5 was given by Wichterlova et al. [572–575] and Anpo et al. [598] based on photoluminescence measurements Cu^{+}. This technique cannot visualize Cu^{2+} and only indirect information was obtained after the controlled reduction of the catalysts with CO. Therefore, other complementary data like ESR or even IR are necessary to ensure more confidence. Wichterlova et al. [572–575] showed that copper ions are located in two sites with different coordinations. One was thought to be located in the vicinity of framework Al pairing arrangements, whereas the other one in the vicinity of single framework Al atoms. Copper ions located in the first sites are mainly coordinated in square pyramidal environments whereas those located adjacent to single Al atoms are in square planar environments. Only copper ions located in the vicinity of a single Al framework are suspected to exhibit redox behaviour. The highest population of these species is achieved in silica-rich zeolites and for a high Cu content. The distribution of copper between these sites was found not to be affected by the redox treatments in various atmospheres.

XPS technique. XPS is also a very efficient tool in the investigation of the superficial copper state. 2p 3 component of Cu in copper-zeolites clearly show (like in mixed oxides) a resolved shoulder indicating the presence of a higher binding energy component. The main peak is located at binding energies close to 933 eV. Comparison with data on Cu_2O leads to assign this peak to Cu(I). The shoulder is generally located at binding energies between 934 and 935 eV and is assigned to Cu(II). This shoulder exhibits a satellite located at 941–944 eV. The ratio of the area corresponding to the peak located at 933 eV and the sum of those located at 934–935 and 941–944 eV give information about the superficial Cu(I)-to-Cu(II) species ratio. Narayana et al. [604] investigated hydrated and

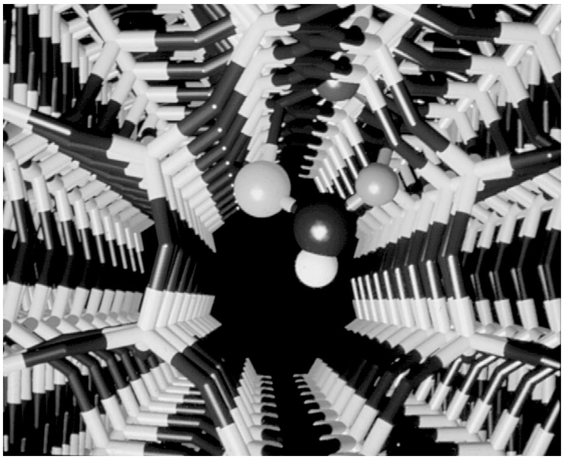

Fig. 19. Representation of the [$2Cu^{II}$, $2Cu^{I}$, 3OH] cluster model of Catlow. Framework oxygen are represented by the black sticks and silicon by the white sticks, respectively [616].

dehydrated Cu–Na-Y zeolites. Using correlation with ESR measurements they considered that the shoulder should actually contain two signals attributed to the splitting of Cu_{2p3} lines into two components. These would correspond to octahedrally and tetrahedrally coordinated Cu(II). A decreased value of the ratio corresponding to these species would indicate the appearance of Cu(II) ions in a distorted octahedral symmetry. A thermal treatment of the catalysts in helium, before the reaction, causes a very strong reduction of divalent copper. The introduction of a second metal in a low loading, like samarium or cerium, brings about a stronger reduction of copper, and the divalent copper is practically completely reduced. The spectra of a Cu–Sm-ZSM-5 catalyst before and after the reaction are presented in Fig. 19. More interesting are the results obtained in the presence of cerium, that also exhibit two peaks assigned to the states Ce(III) and Ce(IV). In that case, an oxidation of the cerium was observed simultaneously with a reduction of the copper.

XPS could also bring evidence about the migration of the copper inside the ZSM-5 zeolite. Reach-silicon zeolites exhibit a very clear signal of the 2p component of Si. Therefore, the ratio of the relative surface area of copper to that of silicon gives information about the superficial population of copper in different steps of catalyst preparation and activation. Variation of this ratio led to assume that, during a helium treatment at high temperatures (773 K), a redispersion takes place inside the channels of the ZSM-5 zeolite concomitantly with the copper reduction. This process is more accentuated during the reaction maybe because of the presence of different oxidants (NO, O_2). Tanabe et al. [590] showed that during the superficial copper redistribution, a migration of Cu^{2+} in the five-membered ring of the zeolite is possible. In this position Cu^{2+} cannot interact with gas molecules. This implies a complete deactivation of copper ions. The presence of a second metal influences this process. The same behaviour was not evidenced in other copper-impregnated catalysts. The results reported by Haack and Shelef [605] for a under-exchanged (40%)-Cu-ZSM-5 zeolite and by Shpiro et al. [486] for over-exchanged zeolites agree with the above conclusions. Shpiro et al. also confirm that copper exists as isolated ions or small clusters and adopts either an oxidation state (I) or an oxidation state (II) in over-exchanged zeolites.

Molecular dynamics and computer-aided design. Another attempt to explain the structure and dynamics of copper-exchanged zeolites is based on the computer-aided design of active catalysts. A first attempt was made by Fripiat et al. [606,607] who indicated that T12 and T2 sites are preferred sites for the substitution of Cu. More recently, Miyamoto et al. [608–611] investigated the same problem using a combination of quantum chemistry, molecular dynamics and computer graphics. Some conclusions could be drawn from their calculations. Cu^{+} always migrates towards the neighbourhood of the T12 sites where it is located in the adjacent position of an Al atom. Simulation of Cu^{2+} and CuO, as possible species resulting from the dehydration of exchanged species, indicated that both species also prefer a location close to Al sites (Fig. 19). Cu^{2+} is not stable inside the channels of ZSM-5 lattice. The Cu^{+} state is more stable in oxidizing reaction conditions. The reversible formation of oxidized and reduced copper species seems to be easy, according to these calculations. This would explain the possibility to decompose NO_x, the process corresponding to a redox mechanism. These calculations also suggest that the redox cycle involves two copper atoms in close proximity, a conclusion which is not very surprising. All these data are consistent with the experimental results obtained by Iwamoto et al. [612].

Catlow et al. [613–616] reevaluated this problem. In order to accommodate a 150% exchange, the model system constructed by them considered the replacing, in a 96 silicon T-sites per unit cell, eight of the 96 silicon atoms with aluminium and 150% copper loading was achieved by introducing four Cu^+ and four Cu^{2+} ions at random extra-framework sites within the host zeolite. The charge imbalance arising from the over-exchange was restored by introducing four OH^- species. Analysis of the resulting copper clusters from the 20 fully relaxed systems revealed that 41% of the copper species were paired with the most common cluster being a hydroxyl bridged Cu(I)–Cu(II) copper pair (Fig. 19). About 4% of the extra-framework copper structures consist of $Cu_3(OH)_n$ clusters. A very interesting conclusion of these calculations is that in mordenite like structure, tetraatomic clusters like $Cu_4(OH)_n$ are stable in a population of 15% while in ZSM-5 these structures are not stable.

Other calculations made by Yokomichi et al. [617] indicated that the reaction occurs on Cu^+ sites. All these sites would be covered by one molecule of NO in a first step and the second molecule would be adsorbed on these species in a second step. The reaction would occur by reaction of two NO molecules adsorbed on a same site.

Short summary. At the present time, there is much evidence suggesting that active sites are two copper atoms in close proximity. These copper atoms should be in a square planar coordination and at least one of them should be in close proximity to an isolated framework Al zeolite atom. The reaction implies a redox behaviour and therefore the formation of Cu(I) is a very important step. These species are very reactive but in conditions of catalytic reaction (723–773 K) they could be formed by decomposition of ELO ($2Cu^{2+}O^{2-}$) even in an oxidizing gas stream (NO, O_2). In such conditions, a certain population of Cu(I) species is maintained. The location of copper is not immediately achieved during the exchange preparation process but during the activation and during the beginning of the reaction. Migration of copper seems to be favoured by the texture of the ZSM-5 channels, but during this process part of the copper could enter in the five-membered ring of the zeolite and that implies a complete deactivation of these species. The presence of promoters like Ce or Sm could "catalyse" the exchange of copper in the active positions even for loadings below 200%.

6.2.2. *Mechanism and kinetics*

Supported metals and oxides. Another area where the situation is still unclear is the mechanism through which the decomposition of NO takes place.

In oxides and platinum supported on an alumina surface, Boudart et al. [516] postulated two elementary steps that coincide with those previously proposed by Winter [515]:

$$\mathrm{M} + \mathrm{NO} \xrightarrow{k_1} \mathrm{M{-}NO} \rightarrow \mathrm{M{-}O} + \mathrm{M{-}N} \tag{5.6}$$

$$2\mathrm{M{-}O} + 2\mathrm{M{-}N} \xrightarrow[k_3]{k_2} 4\mathrm{M} + \mathrm{N_2} + \mathrm{O_2} \tag{5.7}$$

The experimental data obtained on these catalysts accounted for a rate expression of the type

$$r = Nk(\mathrm{NO})/(1 + \alpha K(\mathrm{O_2})), \tag{5.8}$$

where k is the reaction rate; K the adsorption equilibrium constant; α the conversion factor; N is the turnover number.

For the expression of the turnover number, N, Winter [515] suggested the relation

$$N = \frac{k_7 k_6 A f(V)}{k_8}, \tag{5.9}$$

where A is the area of the catalyst; $f(V)$ is a function of the volume and temperature of the reaction.

Because of the low activity of oxides and supported platinum catalysts, few further kinetic or mechanistic studies were made. However, very recently, Yamashita and Vannice [519] reexamined the problem of NO decomposition on manganese oxides, indicating that the reaction occurred according to a Langmuir–Hinshelwood model and was of a second order relative to NO:

$$2\mathrm{NO} + \mathrm{M} \rightarrow 2\mathrm{NO{-}M} \tag{5.10}$$

$$2\mathrm{NO{-}M} \rightarrow \mathrm{N_2} + 2\mathrm{O{-}M}\ (\rightarrow \mathrm{N_2O} + \mathrm{O{-}M}) \tag{5.11}$$

$$2\mathrm{O{-}M} \rightarrow \mathrm{O_2} + 2\mathrm{M} \tag{5.12}$$

Correspondingly, the expression of the reaction rate has the form

$$r_{\mathrm{NO}} = \frac{kK_{\mathrm{NO}}^2 p_{\mathrm{NO}}^2}{(1 + K_{\mathrm{NO}} p_{\mathrm{NO}} + K_{\mathrm{O_2}}^{1/2} p_{\mathrm{O_2}}^{1/2})^2}. \tag{5.13}$$

Metal-exchanged zeolites. In the case of Cu-ZSM-5, most parts of the studies were dedicated to understanding the reaction mechanism. Iwamoto et al. [522] first suggested that the decomposition activity of Cu–Na-Y was probably correlated with the location of the Cu(II) ions in specific positions in the zeolite framework. Generally the transition metal cations have a tendency to occupy the inferior TS1 and TS2 sites.

Data generally indicate the existence of two paths for the decomposition of NO:

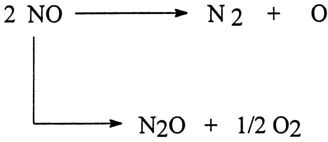

(5.14)

Considering the effect of the pretreatment temperature upon the activity, Iwamoto et al. [556] suggested that the active centres in NO decomposition were Cu(I) ions. The valence state of the copper ion can be readily changed by increasing temperature ($Cu^{2+} \rightarrow Cu^+$) or as a consequence of a reaction with NO ($Cu^+ \rightarrow Cu^{2+}$). There is now a general agreement about this fact. The only difference, as we mentioned in the previous paragraph, is whether the active copper belongs to dimeric or only to monoatomic species.

Most of the arguments in favour of one mechanism or the other are based on FT-IR measurements in the presence of NO as a probe molecule. There appears to be a very good agreement concerning the assignment of the bands [618–621] (Table 5). At room temperature the dominant bands are those due to $NO^{\delta+}$ species formed on Cu^{2+} sites and of gem-dinitrosyl and $NO^{\delta-}$ species formed on Cu^+ sites. At room temperature, other bands due to N_2O, NO_2 and nitrate species are also observed.

Based on the observation that the bands attributed to the NO^- species decreased while those attributed to the NO^+ species increased even at room temperature, Iwamoto et al. [524] suggested that NO^- species are intermediates in the NO decomposition. They showed that the decrease of the NO^- absorption bands as a function of time corresponds to a second-order rate equation. As a consequence, they suggested that the reaction cycle could be

$$2Cu^{2+} \overset{\text{elevated temperatures}}{\rightarrow} 2Cu^+ \underset{-N_2,O_2}{\overset{2NO}{\rightleftharpoons}} 2Cu^{2+}{-}NO^-(\text{single, twin}) \qquad (5.15)$$

This behaviour is described by a surface reaction mechanism represented in Scheme 7. The heart of this mechanism as well as of all others is the formation of gem-dinitrosyl species. The splitting of the N–O bond occurs in a subsequent step.

Another point of view is that of Giamello et al. [577,581] who suggested that dinitrosyl occurs via Cu^+NO, which is a paramagnetic species. This mechanism supposes isolated copper species which firstly interact with NO generating mononitrosyl and, in the second step, react with a second NO molecule to form gem-dinitrosyl species. In this model NO decomposition occurs according to a consecutive reaction in which N_2O is the active intermediate (Scheme 7). The copper ions would be involved in a redox-cycle including these reactions. Centi et al. [622,623] and Marquez-Alvarez et al. [624] also agree with such a model. However, Shelef [545] suggests a reaction mechanism indicating that the whole reaction occurs at Cu^{2+} sites with unsaturated coordination bonds and that there is no redox cycle during the reaction. Disagreeing with this point of view, Hall et al. [536,546,625,626] presented evidence supporting the redox mechanism but also indicated conditions under which the Shelef mechanism could be correct. For temperatures lower than 573 K or conversion of NO to N_2 lower than 40% where N_2 was released but not O_2, NO can act as its own reducing agent. In such conditions NO_2 is always present under steady-state reaction conditions [546].

According to the redox mechanism proposed by Hall et al. [536,546] gem-dinitrosyls decompose forming N_2O and leaving an O atom. The formation of N_2O is generally observed in the first stage of NO decomposition. The stoichiometry of the reaction is maintained because the released oxygen regenerates ELO species. Valyon and Hall [546] suggested that IR spectra bands located at around 1634 cm^{-1} are due to the presence of ELO species. In a further step, ELO species interact with NO generating NO_2 and then ELO is reformed by

$$2M{-}NO_2 + NO \rightarrow 2M{-}O + N_2 + O_2 \qquad (5.16)$$

New evidence also obtained from FT-IR measurements supports the role of oxidized nitrogen adspecies. First evidence about the contribution of $(NO_2^-)(NO)$ species in the NO decomposition was presented by Valyon and Hall [546] as we indicated

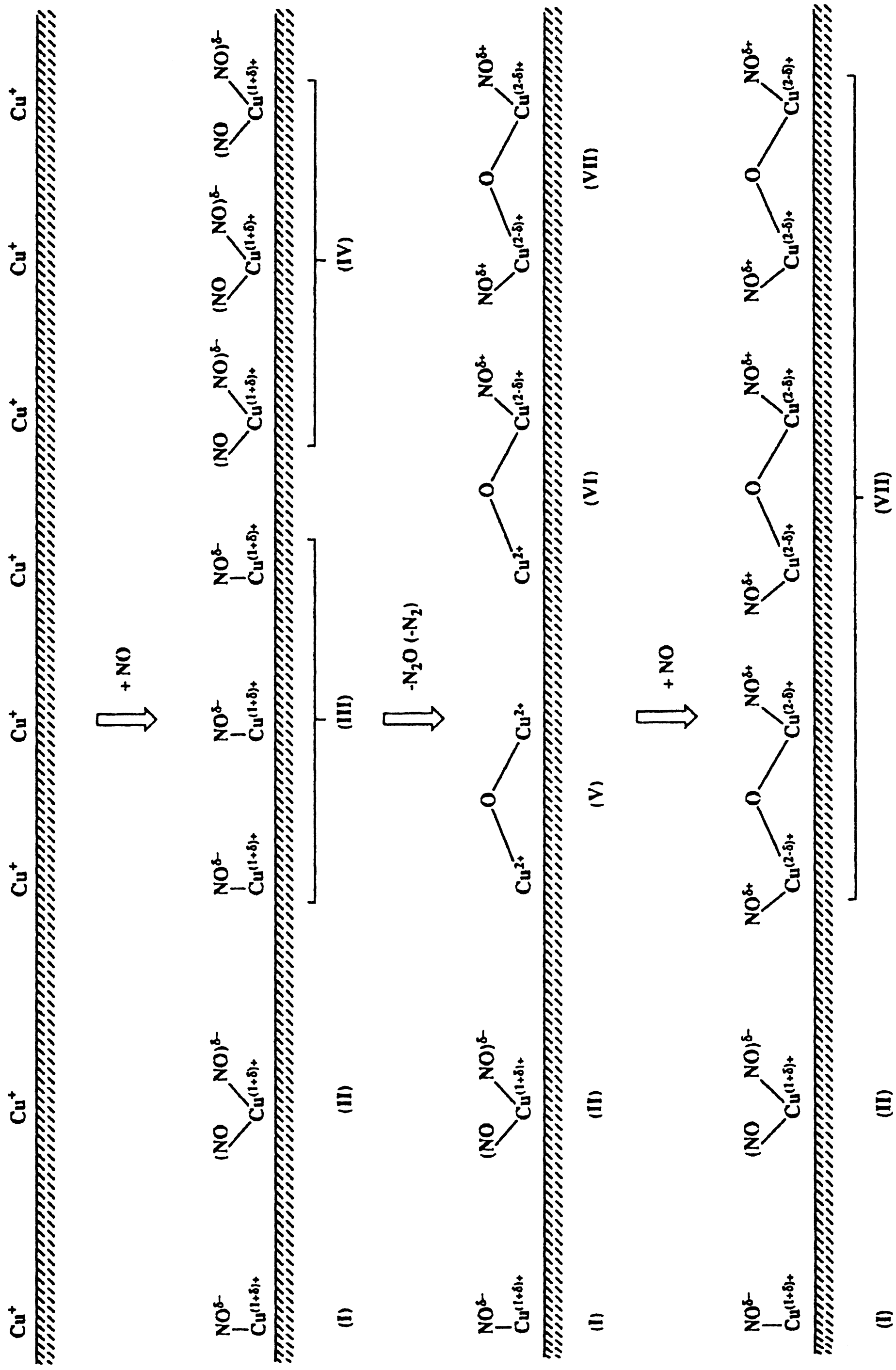

Scheme 7. Surface reaction mechanism in NO decomposition over Cu-ZSM-5 according to M. Iwamoto et al. [618].

above. A recent study by Bell et al. [627] investigating Cu-ZSM-5 during the exposure to NO and NO_2 at reaction temperatures came to question its importance. They proposed two ways for the formation of N_2O, one involving the decomposition of the predominant gem-dinitrosyl species, another the decomposition of $(NO_2^-(NO))$ species. According to these the NO decomposition occurs along the following steps:

$$Cu^+ + NO \rightleftharpoons Cu^+(NO) \quad (5.17)$$

$$Cu^+(NO) + NO \rightleftharpoons Cu^+(NO)_2 \quad (5.18)$$

$$Cu^+(NO)_2 \rightleftharpoons Cu^{2+}O^- + N_2O \quad (5.19)$$

$$Cu^{2+}O^- + NO \rightleftharpoons Cu^{2+}O^-(N{=}O) \quad (5.20)$$

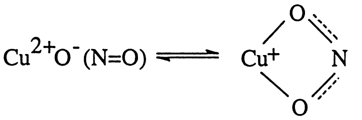

(5.21)

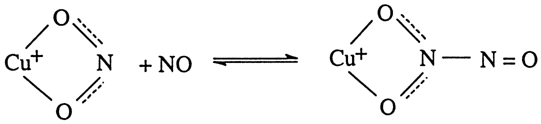

(5.22)

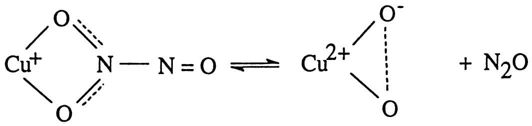

(5.23)

$$Cu^+ + N_2O \rightleftharpoons Cu^{2+}O^- + N_2 \quad (5.24)$$

$$Cu^{2+}O^- \rightleftharpoons Cu^+ + O \quad (5.25)$$

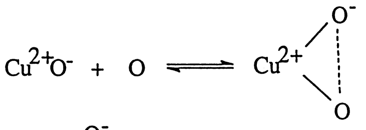

(5.26)

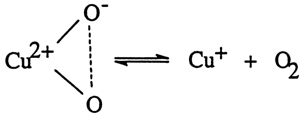

(5.27)

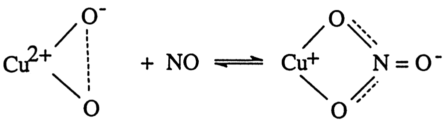

(5.28)

According to this mechanism, the formation of O_2 occurs via two processes: O atoms first desorb from $Cu^{2+}O^-$ and then react with an additional $Cu^{2+}O^-$ to produce superoxide $Cu^{2+}O_2^-$ species. This suggestion replaces the ELO previously discussed.

Recent studies by Chang and McCarthy [541] and Cheung et al. [630] disagree with Bell et al. [627] and with previous data and consider that in fact $(NO_2^-(NO))$ species are determinant in the decomposition of NO. Centi and Perathoner [623] also agree with this point of view.

The importance of the oxidized nitrogen adspecies was stressed by Delmon et al. [628] in promoted Cu-ZSM-5 zeolites. In situ FT-IR measurements indicated a positive influence of Ce and Sm species upon the intensity of these bands, this increase corresponding to an increase of the activity. In addition, Delmon et al. [628] suggested that the two copper atoms involved in the redox decomposition of NO are not equivalent, one being Cu(II) and the other Cu(I). The recent discovery of an oscillatory behaviour reported by Ciambelli et al. [629] gives other arguments in favour of the contribution of these species.

The kinetic studies of Hall et al. [536,546] yielded the following rate equation for NO decomposition on Cu-ZSM-5 zeolites:

$$r = kp_{NO}/(1 + Kp_{O_2}\,1/2). \quad (5.29)$$

The presence of equilibrium constant K at denominator assumes that the formation of NO_3:

$$M{-}NO_2 + O \rightleftarrows M{-}NO_3 \quad (5.30)$$

is an annihilating step. K is the equilibrium constant of this step.

Summarizing, there are few mechanistic propositions at the present time. Most consider that NO decomposition occurs by a redox mechanism involving two copper atoms in close proximity. Iwamoto et al. [524] and Hall et al. [536,546,625,626] consider that this reaction involves two copper atoms in a close proximity which are equivalent and bridged by ELO whereas Delmon et al. [628] suggest that these are not equivalent, one being as Cu(II) and another as Cu(I). The importance of the oxidized nitrogen adspecies in this reaction was stressed by several groups [536,541,546,625,626,628,630]. Bell et al. [627] also agree with the proposals considering the necessity of two copper atoms in a close proximity and the contribution of the oxidized species but, in addition, they consider that ELO is not determinant in this reaction but superoxide $Cu^{2+}O_2^-$ species is. Another point of view is that of Giamello et al. [577,581] who suggested that dinitrosyl occurs via Cu^+NO by a consecutive reaction. They consider N_2O as the active intermediate. Contrarily to these suggestions, Shelef [545] considers a reaction mechanism in which NO decomposition occurs at Cu^{2+} sites with unsaturated coordination bonds without any redox cycle. This mechanism could be possible in conditions of low conversion when NO could act as its own reductant.

6.3. Perovskites

Perovskites are another promising category of catalysts in the NO decomposition. The use of these materials depends on the ability of Cu^{2+} ions to be reduced to Cu^+, which in turn could be promptly reoxidized to Cu^{2+}. The insertion of copper in a relatively stable crystalline oxide phase in which other cations are present could favour this redox process. This would depend on the specific electric charge and the radii of both host and guest ions. The work with perovskites actually also involves many other structures without copper.

Kagawa et al. [631] reported data obtained on a large number of oxides: $La_{1-x}\,Sr_xMO_3$ (M=Co, Mn, Fe), $La_{1-x}\,Sr_x\,Co_{1-y}Fe_yO_3$, $La_{1-x}Sr_x\,Co_{1-y}Cr_yO_3$, $La_{1-x}Sr_xCo_{1-y}Ni_yO_3$, $La_{1-x}Sr_xCo_{1-y}Cu_yO_3$, $La_{1-x}\,Sr_xCo_{1-y}Mn_yO_3$ and on $YBa_2Cu_3O_y$, Misono et al. [632] on $La_{2x}A_xCu_{1-y}B_yO_4$ (A=Sr, B=Al, Zr), Forni et al. [633] on $Sr_xCu_yO_{z+d}$ and Ca_2CuO_{3+d}. More recently Zhao et al. [634] studied systems similar to those investigated by Kagawa et al. [631]. Still other systems were investigated by Shin et al. [635] and Shimada et al. [636].

Unfortunately, these catalysts only exhibit some activity in the conversion of NO at temperatures higher than 900 K and the activity values are lower than those obtained on Cu-ZSM-5. The selectivities are also low.

Palladium deposited over $MgAl_2O_4$, MgO or $Mg_2Si_3O_8$ structures and Cu-molybdates [637] seems to exhibit the same properties as perovskites.

6.3.1. Mechanism

An XPS/FT-IR study of the interaction between NO and $YBa_2Cu_3O_7$ performed by Lin et al. [638] indicated that the nitrate ion was the predominant nitrogen-containing species at temperatures below 540 K and decayed at elevated temperatures (>820 K). The nitrite ion is observed in relatively low concentrations at lower temperatures but becomes the predominant nitrogen-containing species at high temperatures. Based on these measurements the authors suggested the following mechanism:

$$2OBaCuO + NO \rightarrow OBaNCuO + OBaOCuO \tag{5.31}$$

$$OBaNCuO + NO \rightarrow OBaNCuONO \tag{5.32}$$

$$OBaNCuONO \rightarrow ONOBaNCuO \tag{5.33}$$

$$ONOBaNCuO \rightarrow NOOBaNCuO \tag{5.34}$$

$$NOOBaNCuO \rightarrow ONOPBaNCu \tag{5.35}$$

This reaction scheme corresponds to a combination of Langmuir–Hinshelwood and Eley–Rideal mechanisms at high temperatures:

$$M{-}N + M{-}N \rightarrow N_2 + 2M \tag{5.36}$$

$$M{-}N + NO_g \rightarrow N_2O + M \tag{5.37}$$

$$O{-}M + NO_g \rightarrow NO_{2,g} \tag{5.38}$$

6.4. Amorphous alloy

Komiyama et al. [639] showed that $Ni_{80-x}Fe_xP_{20}$ amorphous alloy ribbons have a high initial activity in NO decomposition but that an important decrease takes place during the establishment of a steady state. They argued that an oxidative dissociation occurs on these catalysts, in which the oxidation of the amorphous surface is the rate-limiting step. During NO decomposition on $Ni_{60}Fe_{20}P_{20}$ a sudden decrease of activity was evidenced at 636 K, which is the glass transition of alloy. However, many details are still missing about the possible formation of different oxide phases, at least on the surface, or on the recrystallization process which could occur in such conditions. These data indicate an important deactivation of these catalysts when the transition from the amorphous to the crystalline state occurs.

6.5. Membrane catalysts

Significant non-Faradayic effects on the decomposition of NO were reported by Huggins et al. [640] using a stabilized zirconia (Sc_2O_3 (8%)–ZrO_2) membrane reactor with porous Pt electrodes. They assumed that the solid electrolyte plays a major role in the decomposition of NO due to the presence of some active sites (F-centres or oxygen vacancies) whose number increases significantly when the oxygen was pumped away from the membrane surface. Later, the same authors [641] eliminated the porous Pt electrode and reported that the membrane surface was effectively capable of promoting the decomposition of NO. At the same time, the reaction rate was increased twofold.

A confirmation of these assumptions was given by Mason et al. [642,643] who showed that if the membranes are previously reduced, a high number of F-centres are concomitantly produced and the reaction rate increases.

Cicero and Jan [644] obtained similar results using an yttrium-stabilized zirconia. They reported conversions of about 91% in the 923–1323 K temperature range.

7. General remarks and future work

In spite of the tremendous work done in this field, the best solution for the removal of NO has still not been found. SCR using ammonia as reductant is an effective process and is already industrialized. However, this process involves the use of an expensive, and furthermore polluting product, as reductant. In time, these catalysts are also deactivated by sulphur or heavy metal compounds. For the reduction of NO both with CO or H_2, the best catalysts are those containing Rh. However, these catalysts are also sensitive to different poisons. On the other hand, Rh is the most expensive noble metal and identification of some substitutes for it could offer very promising catalysts. For the reduction of NO with hydrocarbons as well as for NO decomposition, the best catalysts are metal zeolites, namely Cu, Co, Ce or even Pt. However, these catalysts exhibit catalytic activity only in a very limited range of temperature, and in addition are extremely sensible to water and different poisons, sulphur again being the principal one.

The active components are now more or less known. Substitution of some of these, like rhodium of platinum, with non-expensive bi or multicomponent systems could be a possible solution. However, the most important work should be directed in designing a new support. This new material should present a high stability against water or sulphur compounds, should exhibit oxygen storage properties and should achieve an extremely high dispersion of the active components, similar to those determined in the metal zeolites.

8. Further reading

F. Nozaki, F. Matsukawa, Y. Mano, Bull. Chem. Soc. Jpn. 48 (1975) 2764
H. Permana, K.Y.S. Ng, Ch.H.F. Peden, S.J. Schmieg, D.K. Lambert, D.N. Belton, J. Phys. Chem. 99 (1996) 16340
M.L. Unland, J. Phys. Chem. 77 (1973) 1952
M.L. Unland, Science 179 (1973) 567
K. Sawabe, Y. Matsumoto, Surf. Sci. 303 (1994) L385
C.H.F. Peden, D.N. Belton, S.J. Schmieg, J. Catal. 155 (1995) 204
D.N. Belton, C.L. DiMaggio, S. Schmieg, K.Y.S. Ng, J. Catal. 157 (1995) 559
K. Tomishige, K. Asakura, Y. Iwasawa, Chem. Lett. (1994) 235

References

[1] J.N. Armor, Appl. Catal. B 1 (1992) 221.
[2] G.L. Manney, L. Froidevaux, J.W. Waters, R.W. Zurek, W.G. Read, L.S. Elson, J.B. Kumer, J.L. Mergenthaler, A.E. Roche, A. O'Nelll, R.S. Harwood, I. MacKenzie, R. Swinbank, Nature 370 (1994) 429; J. Kramlik, W.P. Linak, Prog. Energy Combustion Sci. 20 (1994) 149.
[3] A.C. Stern, H.C. Wohlers, R.W. Boubel, W.P. Lowry, Fundamental of Air Pollution, Academic Press, New York, 1973, 9.93.
[4] D. Maric, J.P. Burrows, J. Photochem. Photobiol. A 66 (1992) 291.
[5] D.R. Stull, E.F. Westrum Jr., G.L. Sinke, The Chemical Thermodynamics of Organic Compounds, Wiley, New York, 1969.
[6] H. Bosch, F. Janssen, Catal. Today 2 (1988) 369.
[7] F. Janssen, R. Meijer, Catal. Today 16 (1993) 157.
[8] R.I. Pusateri, J.R. Katzer, W.H. Monaque, AIChE J. 20 (1974) 219.
[9] A. Cybulski, J.A. Moulijn, Catal. Rev.-Sci. Eng. 36 (1994) 179.
[10] T. Naito, Y. Suzuki, T. Namekowa, S. Yamada, R. Jinbo, K. Maeda, T. Mitsuyoshi, T. Tate, A. Kato, S. Tominga, Jpn. Patent 03 127 630, 1991.
[11] J.B. Lefers, P. Lodder, Eur. Patent 427 344, 1991.
[12] K. Hedden, N. Schoen, Eur. Patent 496 096, 1992.
[13] K. Konishi, Y. Kato, T. Matsuda, Jpn. Patent 04 166 235, 1992.
[14] M. Kennedy, J. Rietmann, T. Fransen, J.G. van Ommen, J.R.H. Ross, Abstracts of EUROPACAT-1 Conference, Montpellier, 1993.

[15] M. Markvart, V. Pour, Int. Chem. Eng. 15 (1975) 546.
[16] G.L. Bauerle, S.C. Wu, K. Nobe, Ind. Eng. Chem. Prod. Res. Dev. 17 (1978) 117.
[17] T. Shikada, K. Fujimoto, T. Kunugi, H. Tominaga, S. Kaneko, Y. Kubo, Ind. Eng. Chem. Prod. Res. Dev. 20 (1981) 91.
[18] T. Shikada, K. Fujimoto, T. Kunugi, H. Tominaga, J. Chem. Tech. Biotechnol. A 33 (1983) 446.
[19] I.M. Pearson, H. Ryu, W.C. Wong, K. Nobe, Ind. Eng. Chem. Prod. Res. Dev. 22 (1983) 381.
[20] Y. Murakami, M. Inomata, K. Mori, T. Ui, K. Suzuki, A. Miyamoto, T. Hattori, in: G. Poncelet, P. Grange, P.A. Jacobs (Eds.), Preparation of Catalysts III, Studies in Surface Science and Catalysis, vol. 16, Elsevier, Amsterdam, p. 531.
[21] M.D. Amiridis, I.E. Wachs, G. Deo, J.-M. Jehng, D.S. Kim, J. Catal. 161 (1996) 247.
[22] G.C. Bond, K. Bruckman, J. Chem. Soc., Faraday Discuss. 72 (1982) 235.
[23] I.E. Wachs, R.Y. Saleh, S.S. Chan, C.C. Cherisch, Appl. Catal. 15 (1985) 339.
[24] C. Cristiani, P. Forzatti, G. Busca, J. Catal. 116 (1989) 586.
[25] G. Busca, Mater. Chem. Phys. 19 (1988) 157.
[26] G.T. Went, S.T. Oyama, A.T. Bell, J. Phys. Chem. 94 (1990) 4240.
[27] T. Machej, J. Haber, A.M. Turek, I.E. Wachs, Appl. Catal. 70 (1991) 115.
[28] G.T. Went, L.-J. Leu, A.T. Bell, J. Catal. 134 (1992) 479.
[29] R.B. Bjorklund, L.A.H. Andersson, C.U. Engemar, L. Sjueqvist, A. Lund, J. Phys. Chem. 96 (1992) 26.
[30] H. Eckert, I.E. Wachs, J. Phys. Chem. 93 (1989) 6796.
[31] K. Nishiwaki, N. Kakuta, A. Uena, H. Nakabayashi, J. Catal. 118 (1989) 498.
[32] R.A. Rajadhyakasha, G. Hausinger, H. Zeilinger, A. Ramsteter, H. Schmelz, H. Knozinger, Appl. Catal. 51 (1989) 61.
[33] F.I. Boer, L.L. Hegedus, T.R. Gouker, H.P. Zak, Chem. Technol. 312 (1990) 312.
[34] P. Wanthoz, M. Ruwet, T. Machej, P. Grange, Appl. Catal. 69 (1991) 149.
[35] H. Matralis, S. Fiasse, R. Castillo, Ph. Bastians, M. Ruwet, P. Grange, B. Delmon, Catal. Today 17 (1993) 141.
[36] E.T.C. Vogl, A. Boot, A.J. van Dillen, J.W. Geus, F.J.J.G. Janssen, F.M.G. van der Kerkhof, J. Catal. 114 (1988) 313.
[37] M. Schneider, M. Maciejewski, S. Tschudin, A. Wokaun, A. Baiker, J. Catal. 149 (1994) 326.
[38] U. Scharf, M. Schneider, A. Baiker, A. Wokaun, J. Catal. 149 (1994) 344.
[39] M. Schneider, A. Baiker, J. Mater. Chem. 2 (1992) 587.
[40] P. Ciambelli, G. Bagnasco, L. Lisi, M. Turco, G. Chiarello, M. Musci, M. Notaro, D. Robba, P. Ghetti, Appl. Catal. B 1 (1992) 61.
[41] Y. Watanabe, M. Imanori, M. Takeuchi, S. Matsuda, S. Uno, T. Mori, F. Nakajima, Jpn. Patent 75 128 680, 1975.
[42] A. Baiker, P. Dollenmeier, M. Glinski, A. Reller, Appl. Catal. 35 (1987) 351.
[43] A. Baiker, P. Dollenmeier, M. Glinski, US Patent, 4 789 533, 1988.
[44] G.C. Bond, S.F. Tahir, Appl. Catal. 71 (1991) 1.
[45] B.E. Handy, M. Maciejewski, A. Baiker, J. Catal. 134 (1992) 75.
[46] L. Lietti, P. Forzatti, G. Ramis, G. Busca, F. Bregani, Appl. Catal. B 3 (1993) 13.
[47] L. Lietti, P. Forzatti, J. Catal. 147 (1994) 241.
[48] G. Claerbout, M. Ruwet, H. Matralis, P. Grange, Appl. Catal. 76 (1991) L9.
[49] O.B. Lapina, V.M. Mastikhin, L.G. Simonova, Yu.O. Bulgakova, J. Mol. Catal. 69 (1991) 61.
[50] O.B. Lapina, V.M. Mastikhin, A.A. Shubin, V.N. Krasilnikov, K.I. Zamaraev, Prog. NMR Spectrsc. 24 (1992) 457.
[51] O.B. Lapina, V.M. Mastikhin, A.V. Nosov, T. Beutel, H. Knozinger, Catal. Lett. 13 (1992) 203.
[52] O.B. Lapina, A.V. Nosov, V.M. Mastikhin, K.A. Dubkov, V.V. Mokrinski, J. Mol. Catal. 87 (1994) 57.
[53] S. Morikawa, K. Takahashi, J. Mogi, S. Kurita, Bull. Chem. Soc. Jpn. 55 (1982) 2254.
[54] G. Ramis, G. Busca, P. Forzatti, Appl. Catal. B 1 (1991) 29.
[55] J.P. Chen, R.T. Yang, Appl. Catal. A 80 (1992) 135.
[56] T.A. Semenova, T.N. Lillikina, T.A. Mednikova, Teor. Eksp. Khim. 27 (1991) 595.
[57] N. Yoshida, H. Yamazaki, Jpn. Patent 0 440 241, 1992.
[58] K. Kawamura, M. Ioka, Jpn. Patent 0 474 533, 1992.
[59] S. Szakacs, G.J. Altena, T. Fransen, J.G. van Ommen, J.R.H. Ross, Catal. Today 16 (1993) 237.
[60] N. Yoshida, I. Hamada, Jpn. Patent 03 114 545, 1991.
[61] T. Naito, T. Namekawa, Y. Suzuki, K. Maeda, R. Jinbo, Y. Tate, A. Kato, S. Tonigana, Jpn. Patent 03 169 345, 1991.
[62] M. Kobayashi, F. Kinoshita, N. Masaki, Jpn. Patent 03 270 733, 1991.
[63] T. Tachi, A. Kato, H. Yamashita, Nippon Kagaku Kaishi 8 (1992) 812.
[64] K. Tanabe, Catal. Today 8 (1990) 1.
[65] K.A. Vikulov, A. Andreini, E.K. Poels, A. Bliek, Catal. Lett. 25 (1994) 49.
[66] I.E. Wachs, G. Deo, B.M. Weckhuysen, A. Andreini, M.A. Vuurman, M. de Boer, M.D. Amiridis, J. Catal. 161 (1996) 211.
[67] P. Forzatti, L. Lietti, Heterogeneous Chem. Rev. 3 (1996) 33.
[68] S. Kasaoka, E. Sasaoka, H. Iwasaki, Bull. Chem. Soc. Jpn. 62 (1989) 1226.
[69] G.M. Lopez, J.C. Conesa, P. Esteban, H. Dexpert, D. Bazin, Proceedings of the Italian Physical Society Conference, 1990, p. 551.
[70] I.E. Wachs, G. Deo, A. Andreini, M.A. Vuurman, M. de Boer, J. Catal. 160 (1996) 322.
[71] H. Niyama, K. Murata, A. Ebitani, E. Echigoya, J. Catal. 48 (1977) 194.
[72] H. Niyama, K. Murata, E. Echigoya, J. Catal. 48 (1977) 201.
[73] H.E. Curry-Hyde, A. Baiker, Ind. Eng. Chem. Res. 29 (1990) 1985.
[74] H.E. Curry-Hyde, H. Musch, A. Baiker, Appl. Catal. 65 (1990) 211.
[75] H.E. Curry-Hyde, H. Musch, M. Schrame-Marth, A. Wokaun, A. Baiker, J. Catal. 133 (1992) 397.

[76] M. Schrame-Marth, A. Wokaun, H.E. Curry-Hyde, A. Baiker, J. Catal. 133 (1992) 415.

[77] M. Schrame-Marth, A. Wokaun, H.E. Curry-Hyde, A. Baiker, J. Catal. 133 (1992) 431.

[78] M. Schrame-Marth, A. Wokaun, A. Baiker, J. Catal. 138 (1992) 306.

[79] J. Engweiler, J. Nickl, A. Baiker, K. Kohler, C.W. Schlapfer, A. von Zelewsky, J. Catal. 145 (1994) 141.

[80] K. Kohler, C.W. Schlapfer, A. von Zelewsky, J. Nickl, J. Engweiler, A. Baiker, J. Catal. 143 (1993) 201.

[81] U. Scharf, H. Schneider, A. Baiker, A. Wokaun, J. Catal. 145 (1994) 464.

[82] H. Schneider, U. Scharf, A. Wokaun, A. Baiker, J. Catal. 147 (1994) 145.

[83] B.L. Duffy, H.E. Curry-Hyde, N.W. Cant, P.F. Nelson, J. Catal. 149 (1994) 11.

[84] H. Matralis, S. Theret, Ph. Bastians, M. Ruwet, P. Grange, Proc. 13 Iberoamericano de Catalysis, 1992, vol. II, p. 637.

[85] H. Matralis, S. Theret, Ph. Bastians, M. Ruwet, P. Grange, Appl. Catal., to be published.

[86] H. Niiyana, T. Ookawa, E. Echigoya, Nippon Kagaku Kaishi (1975) 1871.

[87] T. Grzybek, Fuel 69 (1990) 604.

[88] T. Grzybek, H. Papp, Appl. Catal. B 1 (1992) 271.

[89] F. Nozaki, K. Yamazaki, T. Inomata, Chem. Lett. (1977) 521.

[90] L. Singoredjo, M. Slagt, J. van Wees, F. Kaptejn, J.A. Moulijn, Catal. Today 7 (1990) 157.

[91] J.H.A. Kiel, A.C.S. Edelaar, W. Prins, W.P.M. van Swaaij, Appl. Catal. B 1 (1992) 41.

[92] P. Ciambelli, M.F. Fortuna, D. Sannino, A. Baldacci, Abstract of TOCAT-2 Conference, Japan, 1994, p. 317.

[93] L. Singoredjo, R. Korver, F. Kapteijn, J.A. Moulijn, Appl. Catal. B 1 (1992) 297.

[94] S.-C. Wu, C. Chu, Atmos. Environ. 6 (1972) 309.

[95] C.U.I. Odenbrand, P.L.T. Gabrielsson, J.G.M. Brandin, L.A.H. Andersson, Appl. Catal. 78 (1991) 109.

[96] N.-Y. Topsoe, T. Slabiak, B.S. Clausen, T.Z. Srnak, J.A. Dumesic, J. Catal. 134 (1992) 742.

[97] H.G. Lintz, A. Turek, Appl. Catal. A 85 (1992) 13.

[98] G. Ramis, G. Busca, V. Lorenzelli, F. Bregani, Abstracts of EUROPACAT-1 Conference, Montpellier, 1993.

[99] G. Ramis, G. Busca, F. Bregani, Catal. Lett. 23 (1994) 353.

[100] E. Hums, G.W. Spitznagel, Proceedings of the Symposium on NO_x Reduction, San Diego, 1994, vol. 39, American Chemical Society, Washington, DC, 1994, p. 130.

[101] E. Hums, Chem. Ztg. 115 (1991) 33.

[102] E. Hums, Ind. Eng. Chem. 31 (1992) 1030.

[103] F. Lange, H. Schmelz, H. Knozinger, J. Electron. Spectrosc. Rel. Phenom. 57 (1991) 307.

[104] F. Lange, H. Schmelz, H. Knozinger, Appl. Catal. B 8 (1996) 245.

[105] N. Inomata, A. Miyamoto, Y. Murakami, J. Catal. 62 (1980) 140.

[106] R.A. Rajadhyaksha, G. Hausinger, H. Zeilinger, A. Ramstetter, H. Schmelz, H. Knozinger, Appl. Catal. 51 (1989) 61.

[107] R.A. Rajadhyaksha, H. Knozinger, Appl. Catal. 51 (1989) 81.

[108] N.-Y. Topsoe, J. Catal. 128 (1991) 499.

[109] N.-Y. Topsoe, H. Topsoe, Catal. Today 9 (1991) 77.

[110] M.M. Kantcheva, K.I. Hadjiivanov, D.G. Klissurski, J. Catal. 134 (1992) 299.

[111] J.A. Odriozola, H. Heinemann, G.A. Somorjai, J.F. Garcia de la Banda, P. Pereira, J. Catal. 119 (1989) 71.

[112] J.A. Odriozola, H. Heinemann, G.A. Somorjai, J.F. Garcia de la Banda, M.L. Granados, J.C. Conesa, J. Phys. Chem. 95 (1991) 240.

[113] B.L. Duffi, H.E. Curry-Hyde, N.W. Cant, P.F. Nelson, J. Phys. Chem. 98 (1994) 7153.

[114] U.S. Ozkan, Y. Cai, M.W. Kumthekar, J. Catal. 149 (1994) 390.

[115] U. Baltensperger, M. Ammann, U.K. Bochert, B. Eichler, H.W. Gaggeler, D.T. Jost, J.A. Kovacs, A. Turler, U.W. Scherer, A. Baiker, J. Phys. Chem. 97 (1993) 12325.

[116] U.S. Ozkan, Y. Cai, M.W. Kumthekar, L. Zhang, J. Catal. 142 (1993) 182.

[117] H. Schneider, S. Tschudin, M. Schneider, A. Wokaun, A. Baiker, J. Catal. 147 (1994) 5.

[118] M. Takagi, T. Kawai, M. Soma, T. Onishi, K. Tamaru, J. Phys. Chem. 80 (1976) 430.

[119] M. Takagi, T. Kawai, M. Soma, T. Onishi, K. Tamaru, J. Catal. 50 (1977) 441.

[120] M. Takagi-Kawai, T. Kawai, M. Soma, T. Onishi, K. Tamaru, J. Catal. 57 (1979) 528.

[121] T.Z. Srnak, J.A. Dumesic, B.S. Clausen, E. Tornquist, N.-Y. Topsoe, J. Catal. 135 (1992) 246.

[122] N.-Y. Topsoe, Science 265 (1994) 1217.

[123] N.-Y. Topsoe, H. Topsoe, J.A. Dumesic, J. Catal. 151 (1995) 226.

[124] N.-Y. Topsoe, H. Topsoe, J.A. Dumesic, J. Catal. 151 (1995) 241.

[125] J.A. Dumesic, N.-Y. Topsoe, H. Topsoe, Y. Chen, T. Slabiak, J. Catal. 163 (1996) 409.

[126] V. Tufano, M. Turco, Appl. Catal. B 2 (1993) 9.

[127] M. Turco, L. Lisi, R. Pirone, P. Ciambelli, Appl. Catal. B 3 (1994) 133.

[128] W.L. Prins, Z.L. Nuninga, Catal. Today 16 (1993) 187.

[129] J.A. Dumesic, N.-Y. Topsoe, T. Slabiak, P. Morsing, B.S. Clausen, E. Tornqvist, H. Topsoe, in: L. Guczi et al. (Eds.), New Frontiers in Catalysis, Studies in Surface Science and Catalysis, vol. 75, part B, Elsevier, Amsterdam, p. 1325.

[130] T. Seiyama, T. Arakawa, T. Matsuda, Y. Takita, N. Yamazoe, J. Catal. 48 (1977) 1.

[131] J.G.M. Brandin, L.A.H. Anderson, C.U.I. Odenbrand, Catal. Today 4 (1989) 187.

[132] E.Y. Choi, I.-S. Nam, Y.G. Kim, J.S. Chung, J.S. Lee, M. Nomura, J. Mol. Catal. 69 (1991) 247.

[133] T. Komatsu, M. Nunokawa, I.S. Moon, T. Takahara, S. Namba, T. Yashima, J. Catal. 148 (1994) 427.

[134] M. Iwamoto, H. Yahiro, K. Tanda, N. Mizuno, Y. Mine, S. Kagawa, J. Phys. Chem. 95 (1991) 3727.

[135] W. Wang, S.-J. Hwang, Appl. Catal. B 5 (1995) 187.

[136] J.P. Chen, M.P. Hauslanday, R.T. Yang, J. Catal. 151 (1995) 135.

[137] L.S. Cheng, R.T. Yang, N. Chen, J. Catal. 164 (1996) 70.
[138] M. Mizumoto, N. Yamazoe, T. Seiyama, J. Catal. 55 (1978) 119.
[139] M. Markvart, P. Pour, J. Catal. 7 (1967) 279.
[140] S.J. Lombardo, T. Fink, R. Imbihl, J. Chem. Phys. 98 (1993) 5526.
[141] S.J. Lombardo, F. Esch, R. Imbihl, G. Ertl, Surf. Sci. 271 (1992) L367.
[142] M.F.H. van Tol, J. Siera, P.D. Cobden, B.E. Nieuwenhuys, Surf. Sci. 274 (1992) 63.
[143] C.G. Takoudis, L.D. Schmidt, J. Chem. Phys. 87 (1993) 964.
[144] T. Katona, L. Guczi, G.A. Somorjai, J. Catal. 132 (1991) 440.
[145] J.M. Martin-Martinez, L. Singoredjo, M. Mittelmeijer-Hazeleger, F. Kapteijn, J.A. Moulijn, Catal. Today 7 (1990) 157.
[146] M. Wakihara, Y. Chiban, Eur. Patent 470 728, 1992.
[147] E.V. Sanapin, V.L. Ivasenko, A.A. Davydov, L.P. Buyantueva, S.P. Ivasenko, SU Patent 1 658 508, 1991.
[148] G.V. Grekova, A.V. Velicho, V.L. Ivasenko, SU Patent 1 643 063, 1991.
[149] V.E. Maizlish, A.V. Veliskho, SU Patent 1 719 036, 1992.
[150] J.F. Roth, R.C. Doerr, Ind. Eng. Chem. 53 (1961) 293.
[151] R.A. Baker, R.C. Doerr, J. Air Pollut. Control Assoc. 14 (1964) 409.
[152] R.A. Baker, R.C. Doerr, Ind. Eng. Chem. Process Des. Dev. 4 (1965) 188.
[153] R.L. Klimisch, G.J. Barnes, Environ. Sci. Technol. 6 (1972) 543.
[154] J.W. London, A.T. Bell, J. Catal. 31 (1973) 32.
[155] M. Shelef, Catal. Rev.-Sci. Eng. 11 (1975) 1.
[156] A.T. Bell, in: A.T. Bell, M.L. Hair (Eds.), Vibrational Spectroscopies for Adsorbed Species, ACS Symposium Series, vol. 137, American Chemical Society, Washington, DC, 1980, p. 13.
[157] M.C. Kung, H.H. Kung, Catal. Rev.-Sci. Eng. 27 (1985) 425.
[158] A. Zecchina, E. Garrone, E. Guglielminotti, in: Catalysis, vol. 6, Royal Society of Chemistry, London, 1983, p. 90.
[159] J.L.G. Fierro, J.F.G. de la Banda, Catal. Rev.-Sci. Eng. 28 (1986) 265.
[160] V.A. Matyshak, O.V. Krylov, Catal. Today 25 (1995) 1.
[161] J.H. Lunsford, Adv. Catal. 22 (1972) 265.
[162] C. Naccache, M. Che, Y. Ben Taarit, Chem. Phys. Lett. 13 (1972) 109.
[163] C.P. Cheng, G.L. Schrader, J. Catal. 60 (1979) 276.
[164] K.I. Zamaraev, V.M. Mastikhin, Colloids Surf. 12 (1984) 401.
[165] M. Shelef, K. Otto, J. Catal. 10 (1968) 408.
[166] M. Shelef, K. Otto, H.S. Gandhi, J. Catal. 12 (1968) 361.
[167] K. Otto, M. Shelef, J. Catal. 14 (1969) 226.
[168] M. Shelef, J. Catal. 15 (1969) 289.
[169] K. Otto, M. Shelef, J. Catal. 18 (1970) 104.
[170] H.S. Gandhi, M. Shelef, J. Catal. 24 (1972) 241.
[171] M. Shelef, J.T. Kummer, Chem. Eng. Prog., Symp. Ser. 67 (1972) 115.
[172] T.P. Kobylinski, B.W. Taylor, J. Catal. 31 (1973) 450.
[173] S. Stegenga, N. Dekker, J. Bijsterbosch, F. Kapteijn, J. Moulijn, G. Belot, R. Roche, in: A. Crucq (Ed.), Catalysis and Automotive Pollution Control II, Studies in Surface Science and Catalysis, vol. 71, Elsevier, Amsterdam, 1991, p. 353.
[174] S. Stegenga, R. van Soest, F. Kapteijn, J.A. Moulijn, Appl. Catal. B 2 (1993) 257.
[175] F. Kapteijn, S. Stegenga, N. Dekker, J. Bijsterbosch, J.A. Moulijn, Catal. Today 16 (1993) 273.
[176] J.T. Yates, T.E. Madey, J. Chem. Phys. 45 (1966) 1613.
[177] E.L. Force, R.J. Ayen, Chem. Eng. Prog., Symp. Ser. 68 (1973) 126.
[178] H.S. Gandhi, M. Shelef, J. Catal. 28 (1973) 1.
[179] H.C. Yao, M. Shelef, J. Catal. 31 (1973) 377.
[180] H.C. Yao, M. Shelef, J. Phys. Chem. 78 (1974) 2490.
[181] J.W. London, A.T. Bell, J. Catal. 31 (1973) 96.
[182] J.L.G. Fierro, in: J.L.G. Fierro (Ed.), Spectroscopic Characterization of Heterogeneous Catalysts, B, Studies in Surface Science and Catalysis, vol. 57, Elsevier, Amsterdam, 1990, p. 67.
[183] Y. Fu, Y. Tian, P. Lin, J. Catal. 132 (1991) 85.
[184] R. Hierl, H.P. Urbach, H. Knozinger, J. Chem. Soc., Faraday Trans. 88 (1992) 355.
[185] R.T. Rewick, H. Wise, J. Catal. 40 (1975) 301.
[186] A.R. Balkenende, O.L.J. Gijzeman, J.W. Geus, Appl. Surf. Sci. 37 (1989) 189.
[187] A.R. Balkenende, H. den Daas, M. Huisman, O.L.J. Gijzeman, J.W. Geus, Appl. Surf. Sci. 47 (1991) 341.
[188] A.R. Balkenende, R. Hoogendam, T. de Beer, O.L.J. Gijzeman, J.W. Geus, Appl. Surf. Sci. 55 (1992) 1.
[189] A.R. Balkenende, C.J.G. van der Gift, E.A. Meulenkamp, J.W. Geus, Appl. Surf. Sci. 68 (1993) 161.
[190] A.T.S. Wee, J. Lin, A.C.H. Huan, F.C. Loh, K.L. Tan, Surf. Sci. 304 (1994) 145.
[191] F. Boccuzzi, E. Guglielminotti, G. Martra, G. Cerrato, J. Catal. 146 (1994) 449.
[192] F. Boccuzzi, M. Baricco, E. Guglielminotti, Appl. Surf. Sci. 70 71 (1993) 147.
[193] G. Busca, J. Mol. Catal. 43 (1987) 225.
[194] E. Guglielminotti, J. Phys. Chem. 98 (1994) 4884.
[195] E. Guglielminotti, J. Phys. Chem. 98 (1994) 9033.
[196] A. Kudo, M. Steinberg, A.J. Bard, A. Campion, M.A. Fox, T.E. Mollouh, S.E. Webber, J.M. White, J. Catal. 125 (1990) 565.
[197] V. Higgs, J. Pritchard, Appl. Catal. 25 (1986) 149.
[198] M. Shelef, G.W. Graham, Catal. Rev.-Sci. Eng. 36 (1994) 431.
[199] T.P. Kobylinski, B.W. Taylor, J. Catal. 33 (1974) 376.
[200] G.L. Bauerle, G.R. Service, K. Nobe, Ind. Eng. Chem. Prod. Res. Dev. 11 (1972) 54.
[201] M. Shelef, H.S. Gandhi, Platinum Metals Rev. 18 (1974) 2.
[202] M. Shelef, H.S. Gandhi, Ind. Eng. Chem. Prod. Res. Dev. 11 (1972) 393.
[203] K. Otto, M. Shelef, Z. Phys. Chem. Neue Folge 85 (1973) 308.
[204] R.L. Klimish, K.C. Taylor, Environ. Sci. Technol. 7 (1993) 127.

[205] W.C. Bernhardt, in: R.L. Klimish, J.G. Larson (Eds.), The Catalytic Chemistry of Nitrogen Oxides, Plenum Press, New York, 1975, p. 86.
[206] W.A. Mannion, K. Aykan, J.G. Cohn, C.E. Thomson, J.J. Money, in: J.E. McEvov (Ed.), Catalysts for the Control of Automotive Pollutants, Advance Chemical Series, vol. 143, American Chemical Society, Washington, DC, 1975, p. 1.
[207] C.A. Clausen III, M.L. Good, J. Catal. 46 (1977) 58.
[208] K.C. Taylor, in: R.L. Klimish, J.E. Larson (Eds.), The Catalytic Chemistry of Nitrogen Oxides, Plenum Press, New York, 1975, p. 58.
[209] J.C. Schlatter, K.C. Taylor, J. Catal. 49 (1977) 42.
[210] J.T. Kumer, J. Phys. Chem. 90 (1986) 4747.
[211] K.C. Taylor, J.C. Schlatter, J. Catal. 63 (1980) 53.
[212] S.L. Tauster, L.L. Murell, J. Catal. 41 (1976) 192.
[213] W.C. Hecker, A.T. Bell, J. Catal. 84 (1983) 200.
[214] W.C. Hecker, A.T. Bell, J. Catal. 85 (1974) 389.
[215] B.K. Cho, B.H. Shanks, J.C. Bailey, J. Catal. 115 (1989) 486.
[216] R.W. McCabe, C. Wong, J. Catal. 121 (1990) 422.
[217] W.C. Hecker, A.T. Bell, J. Catal. 84 (1983) 220.
[218] T.R. Ward, P. Alemany, R. Hoffman, J. Phys. Chem. 97 (1983) 7691.
[219] G. Srinivas, S.C. Chuang, S. Debnath, J. Catal. 148 (1994) 748.
[220] G. Srinivas, S.C. Chuang, Preprints of Symposium on NO_x Reduction, San Diego, 1994, vol. 39, American Chemical Society, Washington, DC, 1994, p. 167.
[221] W.C. Hecker, R.B. Breneman, in: A. Crucq, A. Frennet (Eds.), Catalysis and Automotive Pollution Control, Studies in Surface Science and Catalysis, vol. 30, Elsevier, Amsterdam, 1986, p. 257.
[222] S.H. Oh, C.C. Eickel, J. Catal. 128 (1990) 526.
[223] J. Kaspar, C. de Leitenburg, P. Fornasiero, A. Trovarelli, M. Graziani, J. Catal. 146 (1994) 136.
[224] D.K. Paul, T.H. Ballinger, J.T. Yates Jr., , J. Phys. Chem. 94 (1990) 4617.
[225] D.K. Paul, J.T. Yates Jr., , J. Phys. Chim. 95 (1991) 1699.
[226] X. Xu, D.W. Goodman, Catal. Lett. 24 (1994) 31.
[227] M. Valden, J. Aaltonen, E. Kausisto, M. Perra, C.J. Barnes, Surf. Sci. 307 308 309 (1994) 193.
[228] R. Sigg, E. Wicke, Z. Phys. Chem., Neue Folge 103 (1976) 181.
[229] A. El Hamadaoui, G. Bergeret, J. Massardier, M. Primet, A. Renouprez, J. Catal. 148 (1994) 47.
[230] I. Halasz, A. Brenner, M. Shelef, K.Y.S. Ng, Appl. Catal. A 82 (1992) 51.
[231] I. Halasz, A. Brenner, M. Shelef, Catal. Lett. 16 (1992) 311.
[232] I. Halasz, A. Brenner, M. Shelef, Catal. Lett. 22 (1993) 147.
[233] I. Halasz, A. Brenner, M. Shelef, Appl. Catal. B 2 (1993) 131.
[234] T.E. Hoost, G.W. Graham, M. Shelef, O. Alexeev, B.C. Gates, Catal. Lett. 38 (1996) 57.
[235] J.R. Regalbuto, E.E. Wolf, J. Catal. 109 (1988) 12.
[236] Y.J. Megler, A. van Aalst, B.E. Nieuwenhuys, Preprints of Symposium on NO_x Reduction, San Diego, 1994, vol. 39, American Chemical Society, Washington, DC, 1994, p. 161.
[237] Y.J. Megler, A. van Aalst, J. van Delft, B.E. Nieuwenhuys, J. Catal. 161 (1996) 310.
[238] C.T. Campbell, J.M. White, Appl. Surf. Sci. 1 (1978) 347.
[239] T.W. Root, L.D. Schmidt, G.B. Fisher, Surf. Sci. 134 (1983) 30.
[240] T.W. Root, L.D. Schmidt, G.B. Fisher, Surf. Sci. 150 (1985) 173.
[241] D.G. Castner, G.A. Somorjai, Surf. Sci. 83 (1979) 60.
[242] D.N. Belton, S.J. Schmieg, J. Catal. 144 (1993) 9.
[243] H. Permana, K.Y.S. Ng, Ch.H.F. Peden, S.J. Schmieg, D.K. Lambert, D.N. Belton, J. Catal. 164 (1996) 194.
[244] L.A. DeLouise, N. Winograd, Surf. Sci. 159 (1985) 199.
[245] G.W. Graham, A.D. Logan, M. Shelef, J. Phys. Chem. 97 (1993) 5445.
[246] Q. Gao, R.D. Ramsier, H. Neergaard Waltenburg, J.T. Yates Jr., J. Am. Chem. Soc. 116 (1994) 3901.
[247] T.R. Ward, R. Hoffman, M. Shelef, Surf. Sci. 289 (1993) 85.
[248] J.T. Kumer, J.T. Yao, Y.F. Yu, Y. McKee, SAE Paper 760 143, Detroit, MI, 1976.
[249] H.S. Gandhi, A.G. Piken, H.K. Steprem, M. Shelef, R.G. Delosh, M.E. Heyde, SAE Paper 770 196, Detroit, MI, 1977.
[250] J.C. Summers, S.A. Ausen, J. Catal. 58 (1979) 131.
[251] S.G. Hindin, US Patent 3 870 455, 1973.
[252] F.J. Sergey, J.M. Masellei, M.V. Ernest, US Patent 3 903 020, 1974.
[253] O. Masakazu, K. Yoshizo, Jpn. Patent 7 617 195, 1976.
[254] R.G. Silver, J.L. Summers, W.B. Williamson, in: A. Crucq (Ed.), Catalysis and Automotive Pollution Control II, Studies in Surface Science and Catalysis, vol. 71, Elsevier, Amsterdam, 1991, p. 167.
[255] C. Leclercq, C. Dathy, G. Mabilon, L. Leclercq, in: A. Crucq (Ed.), Catalysis and Automotive Pollution Control II, Studies in Surface Science and Catalysis, vol. 71, Elsevier, Amsterdam, 1991, p. 181.
[256] H.C. Yao, Y.F. Fu Yao, J. Catal. 254 (1984) 254.
[257] J.M. Schwartz, L.D. Schmidt, J. Catal. 148 (1994) 22.
[258] S.H. Oh, J. Catal. 124 (1990) 477.
[259] G.R. Rao, J. Kaspar, S. Mariani, R. di Monte, M. Graziani, Catal. Lett. 24 (1994) 107.
[260] A.F. Diwell, R.R. Rajaram, H.A. Shaw, T.J. Truex, in: A. Crucq (Ed.), Catalysis and Automotive Pollution Control II, Studies in Surface Science and Catalysis, vol. 71, Elsevier, Amsterdam, 1991, p. 139.
[261] B. Harrison, A.F. Diwell, C. Hallett, Platinum Metals Rev. 32 (1988) 73.
[262] P. Loof, B. Kasemo, L. Bjornkvist, S. Anderson, A. Frestad, in: A. Crucq (Ed.), Catalysis and Automotive Pollution Control II, Studies in Surface Science and Catalysis, vol. 71, Elsevier, Amsterdam, 1991, p. 253.
[263] G.S. Zafiris, R.J. Gorte, J. Catal. 139 (1993) 561.
[264] G.S. Zafiris, R.J. Gorte, J. Catal. 143 (1993) 86.
[265] B.K. Cho, B.H. Shanks, J.E. Bailey, J. Catal. 115 (1989) 486.
[266] B.K. Cho, J. Catal. 148 (1994) 697.
[267] S. Oh, J. Catal. 124 (1981) 477.
[268] H. Schaper, E.B.M. Doesburg, L.L. van Reijen, Appl. Catal. 7 (1983) 211.

[269] H. Schaper, D.J. Amesz, E.B.M. Doesburg, L.L. van Reijen, Appl. Catal. 9 (1984) 124.

[270] M. Bettmann, R.E. Chase, K. Otto, W.H. Weber, J. Catal. 117 (1989) 447.

[271] M. Shelef, L.P. Haack, R.E. Soltis, J.E. de Vries, E.M. Logothetis, J. Catal. 137 (1992) 114.

[272] J.E. Kubsh, J.S. Rieck, N.D. Spencer, in: A. Crucq (Ed.), Catalysis and Automotive Pollution Control II, Studies in Surface Science and Catalysis, vol. 71, Elsevier, Amsterdam, 1991, p. 125.

[273] A. Kudo, M. Steinberg, A.J. Bard, A. Campion, M.A. Fox, T.E. Mallouk, S.C. Webber, J.M. White, J. Catal. 125 (1990) 565.

[274] D.A. Lorimer, A.T. Bell, J. Catal. 59 (1979) 223.

[275] H. Niiyama, M. Tanaka, H. Iide, E. Echigaya, Bull. Chem. Soc. Jpn. 49 (1976) 207.

[276] W.C. Hecker, A.T. Bell, J. Catal. 85 (1984) 389.

[277] D.D. Beck, C.J. Carr, J. Catal. 144 (1993) 296.

[278] K.R. Krause, P.S. Schabes-Retchkiman, L.D. Schmidt, J. Catal. 134 (1992) 204.

[279] K.R. Krause, L.D. Schmidt, Catal. Lett. 14 (1992) 141.

[280] J.M. Schwartz, L.D. Schmidt, J. Catal. 138 (1992) 283.

[281] K.R. Krause, L.D. Schmidt, J. Catal. 140 (1993) 424.

[282] Y.J. Mergler, B.E. Nieuwenhuys, J. Catal. 161 (1996) 292.

[283] S. Lee, H. Permana, K.Y.S. Ng, Carbon 32 (1994) 145.

[284] K.C. Taylor, Catal. Rev.-Sci. Eng. 35 (1993) 457.

[285] M.L. Unland, J. Catal. 31 (1973) 459.

[286] F. Solymosi, J. Sarkany, Appl. Surf. Sci. 3 (1979) 68.

[287] K.L. Kostov, H. Rausher, D. Menzel, Surf. Sci. 287 288 (1993) 283.

[288] R. Dictor, J. Catal. 109 (1988) 89.

[289] R.A. Dalla Betta, M. Shelef, J. Mol. Catal. 1 (1976) 431.

[290] F. Solymosi, T. Bansagi, J. Phys. Chem. 83 (1979) 552.

[291] D.D. Eley, G.M. Kiwanuko, C.H. Rochester, J. Chem. Soc., Faraday Trans. 1 69 (1973) 2062.

[292] B.A. Morrow, I.A. Cody, J. Chem. Soc., Faraday Trans. 1 71 (1975) 1021.

[293] A. Giullet, M. Coudurier, J.B. Donnet, Bull. Soc. Chim. Fr. 7 8 (1975) 1563.

[294] M.F. Brown, R.D. Gonzales, J. Catal. 44 (1976) 477.

[295] B.A. Morrow, L.E. Moran, J. Phys. Chem. 81 (1977) 2667.

[296] A.A. Davydov, A.T. Bell, J. Catal. 49 (1977) 345.

[297] G.M. Alikina, A.A. Davydov, I.S. Sazonova, Kinet. Katal. 27 (1986) 875.

[298] E. Guglielminotti, F. Boccuzi, J. Catal. 141 (1993) 486.

[299] R. Krishnamurthy, S.S.C. Chuang, M.W. Bakalos, J. Catal. 157 (1995) 512.

[300] R. Krishnamurthy, S.S.C. Chuang, J. Phys. Chem. 99 (1995) 16727.

[301] S.S.C. Chuang, R. Krishnamurthy, C.-B. Tan, Colloids and Surfaces A: Physicochemical and Engineering Aspects, vol. 105, 1995, p. 35.

[302] D.N. Belton, C.L. Di Maggio, K.Y.S. Ng, J. Catal. 144 (1993) 273.

[303] D.W. Goodman, C.H.F. Peden, G.B. Fisher, S.H. Oh, Catal. Lett. 22 (1993) 271.

[304] S.B. Schwartz, L.D. Schmidt, G.B. Fisher, J. Phys. Chem. 90 (1986) 6194.

[305] C.H.F. Peden, D.W. Goodman, D.S. Blair, P.J. Berlowitz, G.B. Fisher, S.H. Oh, J. Phys. Chem. 92 (1988) 1562.

[306] M. Bowker, Q. Guo, Y. Li, R.W. Joyner, Catal. Lett. 18 (1993) 119.

[307] R. Burch, P.J. Millington, A.P. Walker, Appl. Catal. B 4 (1994) 65.

[308] R.M. Lambert, C.M. Comrie, Surf. Sci. 46 (1974) 61.

[309] H. Miki, T. Nagase, K. Sato, H. Watanabe, S. Sugai, K. Kawasaki, T. Kioka, Surf. Sci. 287 288 (1993) 448.

[310] S. Sugai, K. Shimizu, H. Watanabe, H. Miki, K. Kawasaki, Surf. Sci. 287 288 (1993) 455.

[311] T.E. Fischer, S.R. Kelemen, J. Catal. 53 (1978) 24.

[312] M.W. Lesley, L.D. Schmidt, Surf. Sci. 155 (1985) 215.

[313] S.B. Schwartz, L.D. Schmidt, Surf. Sci. 206 (1988) 169.

[314] Th. Fink, J.P. Dath, M.R. Basset, R. Imbihl, G. Ertl, Surf. Sci. 245 (1991) 96.

[315] Th. Fink, J.P. Dath, R. Imbihl, G. Ertl, Surf. Sci. 251 252 (1991) 985.

[316] J.P. Dath, Th. Fink, R. Imbihl, G. Ertl, J. Chem. Phys. 96 (1992) 1582.

[317] M.M. Slin'ko, N.I. Jaeger, Oscillating Heterogeneous Catalytic Systems, Studies in Surface Science and Catalysis, vol. 86, Elsevier, Amsterdam, 1994, p. 138.

[318] A.A. Tolia, Ch.T. Williams, Ch.G. Takoudis, M.J. Weaver, J. Phys. Chem. 99 (1995) 4599.

[319] Ch.T. Williams, A.A. Tolia, H.Y.H. Chan, Ch.G. Takoudis, M.J. Weaver, J. Catal. 163 (1996) 63.

[320] K. Yaldram, N. Ahmed, M.A. Khan, Surf. Sci. 274 (1992) L515.

[321] K. Yaldram, K.M. Khan, N. Ahmed, M.A. Khan, J. Catal. 147 (1994) 96.

[322] M.S. Tzou, K. Asakura, Y. Yamazaki, H. Kuroda, Catal. Lett. 11 (1991) 33.

[323] Y. Kato, K. Konishi, T. Matsuda, Jpn. Patent 0 459 054, 1992.

[324] S. Qiu, R. Ohnishi, M. Ichikawa, J. Phys. Chem. 98 (1994) 2719.

[325] S. Qiu, R. Ohnishi, M. Ichikawa, J. Chem. Soc., Chem. Commun. (1992) 1425.

[326] M. Ichikawa, T.M. Salama, S. Qiu, R. Ohnishi, Abstracts of TOCAT-2, Japan, 1994, p. 319.

[327] T.M. Salama, R. Ohnishi, M. Ichikawa, in: H. Chon, S.-K. Ihm, Y.S. Uh (Eds.), Progress in Zeolite and Microporous Materials, Studies in Surface Science and Catalysis, vol. 105, Elsevier, Amsterdam, 1997, p. 1541.

[328] K.-H. Lee, B.-H. Ha, in: H. Chon, S.-K. Ihm, Y.S. Uh (Eds.), Progress in Zeolite and Microporous Materials, Studies in Surface Science and Catalysis, vol. 105, Elsevier, Amsterdam, 1997, p. 1571.

[329] E.L. Salinas, P. Salas, I. Schifter, M. Moran, S. Castillo, E. Mogica, in: H. Chon, S.-K. Ihm, Y.S. Uh (Eds.), Progress in Zeolite and Microporous Materials, Studies in Surface Science and Catalysis, vol. 105, Elsevier, Amsterdam, 1997, p. 1565.

[330] Y. Okamoto, Y. Ohto, H. Kikuta, H. Gotoh, T. Imanoka, Abstracts of TOCAT-2, Tokyo, Japan, 1994, p. 315.
[331] C.M. Fu, V.N. Korchak, W.K. Hall, Ind. Eng. Chem. Prod. Res. Dev. 19 (1980) 299.
[332] Sh.I. Sidamonidze, N.Sh. Tskakaya, B.G. Chankvatadze, SU Patent 1 175 395, 1992.
[333] B. Viswanathan, Catal. Rev.-Sci. Eng. 34 (1992) 337.
[334] L.G. Tejuca, J.L.G. Fierro, J.M.D. Tascon, Adv. Catal. 35 (1989) 237.
[335] R.A. Dalla Betta, H.S. Gandhi, J.T. Kummer, M. Shelef, US Patent 3 819 536, 1974.
[336] H.S. Gandhi, J.T. Kummer, M. Shelef, US Patent 3 853 069, 1974.
[337] R.J.H. Voorhoeve, J.P. Remeika, P.E. Freeland, B.T. Matthias, Science 177 (1972) 353.
[338] R.J.H. Voorhoeve, J.P. Remeika, D.W. Johnson Jr., , Science 180 (1973) 62.
[339] P.K. Gallagher, D.W. Johnson Jr., J.P. Remeika, F. Schrey, L.E. Trimble, E.M. Vogel, R.J.H. Voorhoeve, Mater. Sci. Bull. 10 (1975) 529.
[340] R.J.H. Voorhoeve, J.P. Remeika, L.E. Trimble, H.S. Cooper, F.J. Disalvo, P.K. Gallagher, J. Solid State Chem. 14 (1975) 395.
[341] R.J.H. Voorhoeve, D.W. Johnson Jr., J.P. Remeika, P.K. Gallagher, Science 195 (1977) 827.
[342] Y.-F.Y. Yao, J. Catal. 36 (1975) 266.
[343] N. Mizuno, M. Yamato, M. Tanaka, M. Misono, Chim. Mater. 1 (1989) 232.
[344] J.M.D. Tascon, L. Gonzales-Tejuca, C.H. Rochester, J. Catal. 95 (1985) 558.
[345] L. Simonot, F. Garin, G. Maire, Appl. Catal. B 11 (1997) 181.
[346] A.K. Ladavos, Ph.J. Pomonis, Appl. Catal. B 1 (1992) 101.
[347] N. Mizuno, H. Toyama, M. Tanaka, M. Yamato, M. Misono, Bull. Chem. Soc. Jpn. 64 (1991) 1383.
[348] D. Jovanovic, V. Dondur, A. Terlecki-Baricevic, B. Grbic, in: A. Crucq (Ed.), Catalysis and Automotive Pollution Control II, Studies in Surface Science and Catalysis, vol. 71, Elsevier, Amsterdam, 1991, p. 371.
[349] N. Mizuno, M. Yamata, M. Misono, J. Chem. Soc., Chem. Commun. (1988) 887.
[350] I. Halasz, A. Brenner, M. Shelef, K.Y.S. Ng, Catal. Lett. 11 (1991) 327.
[351] J. Lin, A.T.S. Wee, K.L. Tan, K.G. Neoh, W.K. Teo, Inorg. Chem. 32 (1993) 5522.
[352] N. Mizuno, M. Yamata, M. Tanaka, M. Misono, J. Catal. 132 (1991) 360.
[353] A.K. Ladavos, Ph.J. Pomonis, Appl. Catal. B 2 (1993) 27.
[354] S. Kim, M.J. d'Aniello, Appl. Catal. 56 (1989) 23.
[355] S. Kim, M.J. d'Aniello, Appl. Catal. 56 (1989) 45.
[356] R.F. van Slooten, B.E. Nieuwenhuys, J. Catal. 122 (1990) 429.
[357] L. Heezen, V.N. Kilian, R.F. van Slooten, R.M. Wolf, B.E. Nieuwenhuys, in: A. Crucq (Ed.), Catalysis and Automotive Pollution Control II, Studies in Surface Science and Catalysis, vol. 71, Elsevier, Amsterdam, 1991, p. 381.
[358] K.Y.S. Ng, D.N. Belton, S.J. Schmieg, G.B. Fisher, J. Catal. 146 (1994) 394.
[359] K. Teruuchi, H. Habasaki, A. Kawashima, K. Asami, K. Hashimoto, Appl. Catal. 76 (1991) 79.
[360] K. Hashimoto, K. Teruuchi, H. Habasaki, A. Kawashima, K. Asami, Jpn. Patent 03 126 846, 1991.
[361] H. Inoue, T. Masumoto, H. Komiyama, Jpn. Patent 58 159 847, 1983.
[362] H. Inoue, T. Masumoto, H. Komiyama, Jpn. Patent 83 159 847, 1983.
[363] A. Muramatsu, K. Yoshida, Jpn. Patent 0 404 236, 1992.
[364] A. Muramatsu, K. Yoshida, Jpn. Patent 0 404 237, 1992.
[365] M. Shelef, H.S. Gandhi, Ind. Eng. Chem. Prod. Res. Dev. 13 (1974) 80.
[366] K.C. Taylor, R.L. Klimisch, J. Catal. 30 (1973) 478.
[367] H.C. Yao, Y.-F.Y. Yao, K. Otto, J. Catal. 56 (1979) 21.
[368] K. Otto, H.C. Yao, J. Catal. 66 (1980) 229.
[369] S. Galvagno, G. Paravano, J. Catal. 55 (1978) 178.
[370] B.J. Savatsky, A.T. Bell, ACS Symp. Ser. 178 (1982) 105.
[371] K.C. Taylor, R.M. Sinkevitch, R.L. Klimisch, J. Catal. 35 (1974) 34.
[372] G. Pirug, H.P. Bonzel, J. Catal. 50 (1977) 64.
[373] H.P. Bonzel, G. Pirug, Surf. Sci. 62 (1977) 45.
[374] W.C. Hecker, A.T. Bell, J. Catal. 92 (1985) 247.
[375] M.F.H. van Tol, A. Gielbert, B.E. Nieuwenhuys, Catal. Lett. 16 (1992) 297.
[376] M.F.H. van Tol, A. Gielbert, B.E. Nieuwenhuys, Appl. Surf. Sci. 67 (1993) 179.
[377] M.F.H. van Tol, A. Gielbert, B.E. Nieuwenhuys, Chem. Phys. Lett. 205 (1993) 207.
[378] J. Siera, P. Cobden, K. Tanaka, B.E. Nieuwenhuys, Catal. Lett. 10 (1991) 335.
[379] M.M. Slinko, T. Fink, T. Loher, H.H. Madden, S.J. Lombardo, R. Imbihl, G. Ertl, Surf. Sci. 66 (1992) 257.
[380] E. Guglielminotti, F. Boccuzzi, Appl. Catal. B 8 (1996) 371.
[381] A. Obuchi, M. Nakamura, A. Ogato, K. Mizuno, A. Ohi, H. Ohuchi, J. Chem. Soc., Chem. Commun. (1992) 1150.
[382] H. Komiyama, Petrotech (Tokyo) 5 (1982) 922.
[383] R. Burch, S. Scire, Catal. Lett. 27 (1994) 177.
[384] T.M. Salama, R. Ohnishi, T. Shido, M. Ichikawa, J. Catal. 162 (1996) 169.
[385] M. Ruwet, P. Grange, B. Delmon, Unpublished results.
[386] M. Iwamoto, Proceedings of Meeting of Catalytic Technology for Removal of Nitrogen Monoxide, Tokyo, Japan, 1990, p. 17.
[387] M. Iwamoto, H. Yahiro, Y. Yu-u, S. Shundo, N. Mizuno, Shokubai 32 (1990) 430.
[388] W. Held, A. Koenig, T. Richter, L. Puppe, SAE Paper 900 496.
[389] W. Held, A. Koenig, Ger. Offen, DE 3 642 018, 1987.
[390] H. Hamada, Y. Kintaichi, M. Sasaki, T. Ito, M. Tabata, Appl. Catal. 64 (1990) L1.
[391] Y. Kintaichi, H. Hamada, M. Tabata, M. Sasaki, T. Ito, Catal. Lett. 6 (1990) 239.
[392] S. Sato, H. Hirabayashi, H. Yahiro, N. Mizuno, M. Iwamoto, Catal. Lett. 12 (1992) 193.
[393] F. Witzel, G.A. Sill, W.K. Hall, J. Catal. 149 (1994) 229.
[394] Y. Li, J.N. Armor, Appl. Catal. B 3 (1993) L1.

[395] T. Inui, in: H. Chon, S.-K. Ihm, Y.S. Uh (Eds.), Progress in Zeolite and Microporous Materials, Studies in Surface Science and Catalysis, vol. 105, Elsevier, Amsterdam, 1997, p. 1441.

[396] M. Iwamoto, in: J. Weitkamp, H.G. Karge, H. Pfeifer, W. Holderich (Eds.), Zeolites and Related Microporous Materials: State of the Art 1994, Studies in Surface Science and Catalysis, vol. 84, Elsevier, Amsterdam, 1994, p. 1395.

[397] T. Tabata, M. Kokitsu, O. Okada, Catal. Today 22 (1994) 147.

[398] S. Sato, Y. Yu-u, H. Yahiro, N. Mizuno, M. Iwamoto, Appl. Catal. 70 (1991) L1.

[399] M. Iwamoto, H. Yahiro, Catal. Today 22 (1994) 5.

[400] A. Corma, V. Fornes, E. Palonares, Appl. Catal. B 11 (1997) 233.

[401] C. Yokoyama, M. Misono, Catal. Today 22 (1994) 59.

[402] T. Ishihara, M. Kagawa, Y. Mizuhara, Y. Takita, Chem. Lett. (1991) 1063.

[403] Y. Li, T.L. Slager, J.N. Armor, J. Catal. 150 (1994) 388.

[404] H. Hamada, Y. Kintaichi, M. Tabata, M. Sasaki, T. Ito, Chem. Lett. (1991) 2179.

[405] Y. Li, J.N. Armor, J. Catal. 145 (1994) 1.

[406] Y. Nishizaka, M. Misono, Chem. Lett. (1994) 2237.

[407] M. Shelef, Chem. Rev. 95 (1995) 209.

[408] A. Satsuma, K. Yamada, T. Mori, M. Niwa, T. Hattori, Y. Murakami, Catal. Lett. 31 (1995) 367.

[409] I. Halasz, A. Brenner, S.K. Ng, Catal. Lett. 34 (1995) 151.

[410] I. Halasz, A. Brenner, S.K. Ng, Y. Hou, J. Catal. 161 (1996) 359.

[411] J. Szanyi, M.T. Paffett, J. Catal. 164 (1996) 232.

[412] K. Yogo, M. Umeno, H. Watanabe, E. Kikuchi, Catal. Lett. 19 (1993) 131.

[413] G. Centi, S. Perathoner, L. Dall'Olio, Appl. Catal. B 4 (1994) L275.

[414] Y. Li, J.N. Armor, J. Catal. 150 (1994) 376.

[415] Y. Li, J.N. Armor, Appl. Catal. B 3 (1993) 55.

[416] Y. Li, J.N. Armor, Appl. Catal. B 2 (1993) 239.

[417] Y. Li, J.N. Armor, Appl. Catal. 76 (1991) L1.

[418] Y. Li, J.N. Armor, US Patent 5 149 512, 1992.

[419] Y. Li, J.N. Armor, Appl. Catal. B 2 (1993) 71.

[420] E. Kikuchi, K. Yogo, International Forum on Environmental Catalysis '93, Tokyo, 1993.

[421] E. Kikuchi, M. Ogura, I. Terasaki, Y. Goto, J. Catal. 161 (1996) 465.

[422] M. Iwamoto, H. Hamada, Catal. Today 10 (1991) 57.

[423] J.L. d'Itri, W.M.H. Sachtler, Catal. Lett. 15 (1992) 289.

[424] A.P. Walker, Catal. Today 26 (1995) 107.

[425] Y. Li, J.N. Armor, Appl. Catal. B 1 (1992) L31.

[426] K. Yogo, S. Tanaka, M. Ihara, T. Hishiki, E. Kikuchi, Chem. Lett. (1992) 1025.

[427] K. Yogo, M. Ogura, N. Aratani, Y. Sugiura, E. Kikuchi, Abstracts of TOCAT-2, Tokyo, 1994, p. 399.

[428] H. Yasuda, C. Yohoyama, T. Miyamoto, M. Kawamoto, M. Misono, Abstracts of TOCAT-2, Tokyo, 1994, p. 325.

[429] M. Misono, K. Kodo, Chem. Lett. (1991) 1001.

[430] J. Nakatani, H. Hirabayashi, H.K. Shin, K. Ohto, H. Yahiro, N. Mizuno, M. Iwamoto, Abstracts of TOCAT-2, Tokyo, 1994, p. 327.

[431] Y. Nishizaka, M. Misono, Chem. Lett. (1993) 1295.

[432] C. Yokoyama, M. Misono, Bull. Chem. Soc. Jpn. 67 (1994) 557.

[433] S. Katsuta, M. Kumagai, T. Tomura, Jpn. Patent 31 813 211, 1991.

[434] S. Uematsu, M. Hosoya, Jpn. Patent 5 018 237, 1993.

[435] P. Budi, E. Curry-Hyde, R.F. Howe, Catal. Lett. 41 (1996) 47.

[436] A.V. Kucherov, C.P. Hubbard, T.N. Kucherova, M. Shelef, in: H. Chon, S.-K. Ihm, Y.S. Uh (Eds.), Progress in Zeolite and Microporous Materials, Studies in Surface Science and Catalysis, vol. 105, Elsevier, Amsterdam, 1997, p. 1469.

[437] A.Yu. Starkheev, C.W. Lee, S.J. Park, P.J. Chong, Appl. Catal. B 9 (1996) 65.

[438] M.C. Campo, S. De Rossi, G. Ferraris, V. Indovina, Appl. Catal. B 8 (1996) 315.

[439] Z. Charjar, M. Primet, H. Praliaud, M. Chevrier, C. Gauthier, F. Mathis, Appl. Catal. B 4 (1994) 199.

[440] Y. Ukisu, S. Sato, A. Abe, K. Yoshida, Appl. Catal. 2 (1993) 147.

[441] S. Matsumoto, K. Yokota, H. Doi, M. Kimura, K. Sekizawa, S. Kasahura, Catal. Today 22 (1994) 127.

[442] K. Yogo, M. Ihara, I. Terasaki, E. Kikuchi, Appl. Catal. B 2 (1993) L1.

[443] C.J. Lougman, D.E. Resasco, Appl. Catal. B 5 (1995) 351.

[444] C.N. Montreuil, M. Shelef, Appl. Catal. B 1 (1992) L1.

[445] F. Radtke, R.A. Koeppel, A. Baiker, Appl. Catal. 107 (1994) L125.

[446] V.A. Sadykov, G.M. Alikina, R.W. Bunina, A.S. Ivanova, A.Ya. Rozovskii, V.F. Tretyakov, V.V. Lunin, E.V. Lunina, A.N. Kharlanov, V.A. Matyshak, Abstracts of TOCAT-2, Tokyo, Japan, 1994, 9. 315.

[447] T. Inui, S. Kojo, M. Shibata, T. Yoshida, S. Iwamoto, Stud. Surf. Sci. Catal. 69 (1991) 355.

[448] T. Inui, S. Iwamoto, S. Kojo, T. Yoshida, Catal. Lett. 13 (1992) 87.

[449] T. Inui, S. Iwamoto, S. Shimizu, in: R. von Ballmoos et al. (Eds.), Proceedings of the Ninth International Zeolite Conference, vol. II, Butterworths/Heinamann, London, 1992, p. 405.

[450] S. Iwamoto, S. Shimizu, T. Inui, in: J. Weitkamp, H.G. Karge, H. Pfeifer, W. Holderich (Eds.), Zeolites and Related Microporous Materials: State of the Art 1994, Studies in Surface Science and Catalysis, vol. 84, part C, Elsevier, Amsterdam, 1994, p. 1523.

[451] T. Inui, S. Iwamoto, S. Koja, S. Shimizu, T. Hirabayashi, Catal. Today 22 (1994) 41.

[452] S. Iwamoto, M. Okabe, T. Inui, Absrtacts of TOCAT-2, Tokyo, Japan, 1994, p. 325.

[453] T. Inui, in: L. Bonneviot. S. Kaliaguine (Eds.), Zeolites: A refined Tool for Designing Catalytic Sites, Studies in Surface Science and Catalysis, vol. 95, Elsevier, Amsterdam, 1995, p. 1523.

[454] T. Inui, K. Matsuba, Y. Tanaka, Catal. Today 23 (1995) 217.

[455] M. Iwamoto, H. Yahiro, S. Shunda, Y. Yu-u, N. Mizuno, Appl. Catal. 69 (1991) L15.

[456] H. Hirabayashi, H. Yahiro, N. Mizuno, M. Iwamoto, Chem. Lett. (1992) 2235.

[457] H. Hirabayashi, H. Yahiro, N. Mizuno, M. Iwamoto, Shokubai 35 (1993) 402.
[458] M. Shelef, Abstracts of EFCAT-1 Conference, Montpellier, 1993, p. 878.
[459] B. Wichterlova, Z. Sobalik, M. Skokanek, Appl. Catal. A 103 (1993) 269.
[460] J.Y. Lan, G.D. Lei, W.M.H. Sachtler, H.H. Kung, J. Catal. 161 (1996) 43.
[461] F. Radtke, R.A. Koppel, A. Baiker, Catal. Today 26 (1995) 159.
[462] J.N. Armor, T.S. Farris, Appl. Catal. B 4 (1994) L11.
[463] Y. Li, J.N. Armor, Appl. Catal. B 5 (1995) L257.
[464] J.N. Armor, Catal. Today 26 (1995) 147.
[465] K. Yogo, M. Ihara, I. Terasaki, M. Umeno, H. Watanabe, E. Kikuchi, Shokubai 35 (1993) 126.
[466] G. Muramatsu, S. Sumiya, K. Yoshida, A. Abe, Ger. Offen Patent, DE 4 131 954, 1992.
[467] E. Kikuchi, K. Yogo, S. Tanaka, M. Abe, Chem. Lett. (1991) 1063.
[468] B.J. Adelman, T. Beutel, G.D. Lei, W.M.H. Sachtler, J. Catal. 158 (1996) 327.
[469] M. Sasaki, H. Hamada, Y. Kintuichi, T. Ito, Catal. Lett. 15 (1992) 297.
[470] M. Shelef, C.N. Montreuil, H.W. Jen, Catal. Lett. 26 (1994) 277.
[471] J.O. Pentuchi, G. Sill, K.W. Hall, Appl. Catal. B 2 (1993) 303.
[472] F. Cavani, G. Giordano, M. Pedantella, F. Trifiro, in: J. Weitkamp, H.G. Karge, H. Pfeifer, W. Holderich (Eds.), Zeolites and Related Microporous Materials: State of the Art 1994, Studies in Surface Science and Catalysis, vol. 84, part B, Elsevier, Amsterdam, 1994, p. 1425.
[473] V.I. Pârvulescu, L. Frunzå, G. Catanå, R. Russu, V. Pârvulescu, Appl. Catal. A 121 (1995) 69.
[474] C.J. Blower, T.D. Smith, Zeolites 13 (1993) 396.
[475] A.D. Cowan, R. Dumpelmann, N.W. Cant, J. Catal. 151 (1995) 356.
[476] T. Tanaka, T. Okuhara, M. Misono, Appl. Catal. B 4 (1994) L1.
[477] Y. Ukisu, S. Sato, G. Muramatsu, T. Yoshida, Catal. Lett. 11 (1991) 177.
[478] A. Obuchi, A. Ogata, K. Mizuno, A. Ohi, M. Nakamura, H. Ohuchi, J. Chem. Soc., Chem. Commun. (1992) 247.
[479] G.P. Ansell, A.F. Diwell, S.E. Golunski, J.W. Hayes, R.R. Rajaram, T.J. Truex, A.P. Walker, Appl. Catal. B 2 (1993) 81.
[480] G.J. Buckles, G.J. Hutchings, J. Catal. 151 (1995) 33.
[481] N.W. Hayes, R.W. Joyner, E.S. Shpiro, Appl. Catal. B 8 (1996) 343.
[482] C. Yokoyama, M. Misono, J. Catal. 150 (1994) 9.
[483] K.C.C. Kharas, Appl. Catal. B 2 (1993) 207.
[484] N.W. Hayes, W. Grunert, G.J. Hutchings, R.W. Joyner, E.S. Shpiro, J. Chem. Soc., Chem. Commun. (1994) 531.
[485] T. Beuter, B. Adelman, W.M.H. Sachtler, Catal. Lett. 37 (1996) 125.
[486] M. Iwamoto, H. Takeda, Catal. Today 27 (1996) 71.
[487] M. Iwamoto, H. Yahiro, N. Mizuno, Proceedings of the Ninth International Zeolite Conference, vol. II, 1992, p. 397.
[488] F. Witzel, G.A. Sill, W.K. Hall, in: J. Weitkamp, H.G. Karge, H. Pfeifer, W. Holderich (Eds.), Zeolites and Related Microporous Materials: State of the Art 1994, Studies in Surface Science and Catalysis, vol. 84, part C, Elsevier, Amsterdam, 1994, p. 1531.
[489] D.B. Lukyanov, G. Sill, J.L. d'Itri, W.K. Hall, J. Catal. 153 (1995) 265.
[490] F. Pognant, J. Saussey, J.C. LaValley, G. Mabilon, Catal. Today 29 (1996) 93.
[491] R. Burch, P.J. Millington, Appl. Catal. B 2 (1993) 101.
[492] D.J. Liu, H.J. Robota, Appl. Catal. B 4 (1994) 155.
[493] D.J. Liu, H.J. Robota, Catal. Lett. 21 (1993) 291.
[494] K. Matsuba, T. Hattori, M. Okabe, N. Goto, Y. Nakazaki, M. Inoue, T. Inui, Abstracts of 70th Annual Meeting of Catal. Soc., Japan, 1992, p. 188.
[495] G. Zhang, T. Yamaguchi, H. Kawakami, T. Suzuki, Appl. Catal. B 1 (1992) L15.
[496] M. Sasaki, H. Hamada, Y. Kintachi, T. Ito, Catal. Lett. 15 (1992) 297.
[497] M. Inaba, Y. Kintaiki, H. Hamada, Catal. Lett. 36 (1996) 223.
[498] T. Inoue, K. Tomishige, Y. Iwasawa, J. Chem. Soc., Faraday Trans. 92 (1996) 461.
[499] A. Ueda, T. Oshima, M. Haruta, Proceedings of the First World Congress on Environmental Catalysis, Pisa, 1995, p. 343.
[500] R. Burch, T.C. Watling, Appl. Catal. B 11 (1997) 207.
[501] A. Obuchi, A. Ohi, M. Nakamura, A. Ogato, K. Mizuno, H. Ohuchi, Appl. Catal. B 2 (1993) 71.
[502] R. Burch, D. Ottery, Appl. Catal. B 9 (1996) L19.
[503] S. Naito, T. Tanimoto, Chem. Lett. (1993) 1935.
[504] A. Ueda, M. Haruta, Abstracts of 70th Annual Meeting of Catal. Soc., Japan, 1992, p. 321.
[505] T. Torikai, H. Yahiro, N. Mizuno, M. Iwamoto, Catal. Lett. 9 (1991) 91.
[506] H. Hosose, H. Yahiro, N. Mizuno, M. Iwamoto, Chem. Lett. (1991) 1859.
[507] K.A. Bethke, D. Alt, M.C. Kung, Catal. Lett. 25 (1994) 37.
[508] K.A. Bethke, M.C. Kung, B. Yang, M. Slah, D. Alt, C. Li, H.H. Kung, Catal. Today 26 (1995) 169.
[509] M. Tabata, H. Hamada, F. Suganuma, T. Yoshinari, H. Tsuchida, Y. Kintaichi, M. Sasaki, T. Yto, Catal. Lett. 25 (1994) 55.
[510] H. Ukisu, S. Sato, G. Muramatsu, K. Yoshida, Catal. Lett. 16 (1992) 11.
[511] X. Zhang, A.B. Walters, M.A. Vannice, J. Catal. 146 (1994) 568.
[512] R.R. Sikada, R.G. Rinker, Y.L. Wang, W.H. Corcoran, AIChE J. 7 (1961) 658.
[513] M. Shelef, K. Otto, H. Gandhi, Aim. Environ. 3 (1969) 107.
[514] K. Otto, M. Shelef, J. Catal. 29 (1973) 138.
[515] E.R.S. Winter, J. Catal. 22 (1971) 158.
[516] A. Amirnazmi, J.E. Benson, M. Boudart, J. Catal. 30 (1973) 138.
[517] G. Bauerle, S. Wu, K. Nobe, Ind. Eng. Chem. Prod. Res. Dev. 14 (1975) 123.

[518] J. Hightower, D. van Leirsburg, in: R. Klimich, J. Larsen (Eds.), Catalytic Chemistry of Nitrogen Oxides, Plenum Press, London, 1975, p. 63.
[519] T. Yamashita, M.A. Vannice, J. Catal. 163 (1996) 155.
[520] G. Broden, T. Rhodin, C. Brucker, R. Bembow, Z. Hurych, Surf. Sci. 59 (1976) 593.
[521] H. Hamada, Y. Kintaichi, M. Sasaki, T. Ito, Chem. Lett. (1990) 1069.
[522] M. Iwamoto, S. Yokoo, K. Sakai, S. Kagawa, J. Chem. Soc., Faraday Trans. 1 77 (1981) 1629.
[523] M. Iwamoto, H. Furukawa, S. Kagawa, in: L. Guczi, F. Solymosi, P. Tetenyi (Eds.), New Frontiers in Catalysis, Proceedings of the 10th International Congress on Catalysis, Budapest, 1992, Akadémi Kiado, Budapest, 1993, p. 1285.
[524] M. Iwamoto, H. Furukawa, S. Kagawa, in: Y. Murakami, A. Iijima, J.W. Ward (Eds.), New Developments in Zeolite Science and Technology, Studies in Surface Science and Catalysis, vol. 28, Elsevier, Amsterdam, 1986, p. 943.
[525] M. Iwamoto, in: M. Misono, Y. Moro-oka, S. Kimura (Eds.), Future Opportunities in Catalytic and Separation Technology, Studies in Surface Science and Catalysis, vol. 54, Elsevier, Amsterdam, 1990, p. 121.
[526] M. Iwamoto, H. Furukawa, Y. Mina, F. Uemura, S. Mikuriya, S. Kagawa, J. Chem. Soc., Chem. Commun. (1986) 1272.
[527] M. Iwamoto, K. Maruyama, N. Yamazoe, T. Seiyama, J. Chem. Soc., Chem. Commun. (1966) 615.
[528] M. Iwamoto, K. Maruyama, N. Yamazoe, T. Seiyama, J. Phys. Chem. 81 (1977) 622.
[529] Y. Li, W.K. Hall, J. Phys. Chem. 94 (1990) 85.
[530] B. Wichterlova, Z. Sobalik, M. Petras, I. Jirka, V. Bosacek, in: L. Guczi, F. Solymosi, P. Tetenyi (Eds.), New Frontiers in Catalysis, Proceedings of the 10th International Congress on Catalysis, Budapest, 1992, Akadémi Kiado, Budapest, 1993, p. 1649.
[531] F. Steinbach, A. Brunner, H. Muller, A. Drechsler, U. Stan, in: L. Guczi, F. Solymosi, P. Tetenyi (Eds.), New Frontiers in Catalysis, Proceedings of the 10th International Congress on Catalysis, Budapest, 1992, Akadémi Kiado, Budapest, 1993, p. 1299.
[532] G. Centi, S. Perathoner, Appl. Catal. A 132 (1995) 179.
[533] G. Moretti, Catal. Lett. 23 (1994) 135.
[534] V.I. Pârvulescu, P. Oelker, P. Grange, B. Delmon, in: A. Andreev, L. Petrov, Ch. Bonev, G. Kadinov, I. Mitov (Eds.), Proceedings of the Eighth International Symposium on Heterogeneous Catalysis, Varna, 5–9 October 1996, pp. 353–358.
[535] V.I. Pârvulescu, P. Oelker, P. Grange, B. Delmon, to be published, submitted to Catal. Today.
[536] Y. Li, W.K. Hall, J. Catal. 129 (1991) 202.
[537] T. Curtin, P. Grange, B. Delmon, Catal. Today, 35 (1997) 121.
[538] J. Valyon, W.K. Hall, Catal. Lett. 19 (1993) 109.
[539] J. Valyon, W.K. Hall, J. Catal. 143 (1993) 520.
[540] J. Valyon, W.S. Millman, W.K. Hall, Catal. Lett. 24 (1994) 215.
[541] Y.-F. Chang, J.G. McCarthy, J. Catal. 165 (1997) 1.
[542] V.I. Pârvulescu, P. Grange, B. Delmon, to be published.
[543] T. Curtin, P. Grange, B. Delmon, Catal. Today, 36 (1997) 57.
[544] R. Pirone, P. Ciambelli, G. Moretti, G. Russo, Appl. Catal. B 8 (1996) 197.
[545] M. Shelef, Catal. Lett. 15 (1992) 305.
[546] J. Valyon, W.K. Hall, J. Phys. Chem. 97 (1993) 1204.
[547] D.J. Parrillo, D. Dolenec, R.J. Gorte, R.W. McCabe, J. Catal. 142 (1993) 708.
[548] D.J. Parrillo, J.P. Fortney, R.J. Gorte, J. Catal. 153 (1995) 190.
[549] C. Naccache, Y. Ben Taarit, in: F. Ramoa-Ribeiro et al. (Eds.), Zeolites: Science and Technology, NATO ASI Series, Martens Nijkoff Publishers, The Hague, 1984, p. 373.
[550] M.J. Sandoval, A.T. Bell, J. Catal. 144 (1993) 227.
[551] G. Centi, C. Nigro, S. Perathoner, G. Stella, Catal. Today 17 (1993) 159.
[552] M. Iwamoto, H. Yahiro, Y. Mina, S. Kagawa, Chem. Lett. (1989) 213.
[553] M. Iwamoto, H. Yahiro, Y. Torikai, T. Yoshioka, N. Mizuno, Chem. Lett. (1990) 1967.
[554] K. Eranen, N. Kumar, L.E. Lindfors, Appl. Catal. B 4 (1994) 407.
[555] F.S. Xiao, W. Xu, S. Qiu, R. Xu, J. Mater. Sci. 4 (1994) 735.
[556] M. Iwamoto, H. Yahiro, T. Kutsuno, S. Bunyu, S. Kagawa, Bull. Chem. Soc. Jpn. 62 (1989) 583.
[557] S. Kagawa, H. Ogawa, H. Furukawa, Y. Teraoka, Chem. Lett. (1991) 407.
[558] Y. Zhang, M. Flytzani-Stephanopoulos, in: J.N. Armor (Ed.), Environmental Catalysis, American Chemical Society, Washington, DC, 1994, p. 7.
[559] Y. Zhang, T. Sun, A.F. Sarofim, M. Flytzani-Stephanopoulos, in: U.S. Ozkan, (Ed.), Reduction of Nitrogen Oxide Emissions, American Chemical Society, Washington, DC, 1995, p. 133.
[560] Y. Zhang, M. Flytzani-Stephanopoulos, J. Catal. 164 (1996) 131.
[561] A.V. Kucherov, C.P. Hubbard, T.N. Kucherova, M. Shelef, in: H. Chon, S.K. Ihm, Y.S. Uh (Eds.), Progress in Zeolite and Microporous Materials, Studies in Surface Science and Catalysis, vol. 105, Elsevier, Amsterdam, 1997, p. 1469.
[562] V.I. Pârvulescu, P. Grange, B. Delmon, Appl. Catal., B., Environmental, 16 (1998) 1.
[563] P. Oelker, V.I. Pârvulescu, P. Grange, B. Delmon, Book of Abstracts of EuropaCat. II, Maastricht, 3–8 September 1995, p. 315.
[564] P. Oelker, V.I. Pârvulescu, P. Grange, B. Delmon, Book of Abstract of IFEC'95, Tokyo, 1995.
[565] J. Sarkany, J.L. d'Itri, W.M.H. Sachtler, Catal. Lett. 16 (1992) 241.
[566] J. Sarkany, W.M.H. Sachtler, Zeolites 14 (1994) 7.
[567] G.D. Lei, D.J. Adelman, J. Sarkany, W.M.H. Sachtler, Appl. Catal. B 5 (1995) 245.
[568] J. Valyon, W.K. Hall, J. Phys. Chem. 97 (1993) 7054.
[569] R.L. Garten, W.N. Delgass, M. Boudart, J. Catal. 18 (1970) 90.
[570] R.A. DallaBetta, R.L. Garten, M. Boudart, J. Catal. 41 (1976) 40.

[571] E.S. Shpiro, W. Grunert, R.W. Joyner, G.N. Baeva, Catal. Lett. 24 (1994) 159.
[572] W. Grunert, E.S. Shpiro, N.H. Hayes, R.W. Joyner, M.R.H. Siddiqui, G.N. Baeva, J. Phys. Chem. 98 (1994) 10832.
[573] J. Dedecek, B. Wichterlova, J. Phys. Chem. 98 (1994) 5721.
[574] B. Wichterlova, Z. Sobalik, J. Dedecek, Book of Abstracts of EuropaCat. II, Maastricht, 3–8 September 1995, p. 245.
[575] B. Wichterlova, J. Dedecek, A. Vondrova, J. Phys. Chem. 99 (1995) 1065.
[576] J. Dedecek, Z. Sobalik, Z. Tvaruzkova, D. Kaucky, B. Wichterlova, J. Phys. Chem. 99 (1995) 16327.
[577] E. Giamello, D. Murphy, G. Magnacca, C. Mortena, Y. Shioya, T. Nomura, M. Anpo, J. Catal. 136 (1992) 510.
[578] A.V. Kucherov, A.A. Slinkin, S.S. Goryashenko, K.I. Slovetskaja, J. Catal. 118 (1989) 459.
[579] P.A. Jacobs, W. DeWilde, R. Schoonheydt, J.B. Uytterhoeven, H. Beyer, J. Chem. Soc., Faraday Trans. 1 72 (1976) 1221.
[580] P.A. Jacobs, H. Beyer, J. Phys. Chem. 83 (1979) 1174.
[581] M. Anpo, T. Nomura, T. Kitao, E. Giamello, D. Murphy, M. Che, M.A. Fox, Res. Chem. Intermed. 15 (1991) 225.
[582] C. Naccache, M. Che, Y. BenTaarit, Chem. Phys. Lett. 13 (1972) 109.
[583] M. Anderson, L. Kevan, J. Phys. Chem. 91 (1987) 4174.
[584] R.A. Schoonheydt, Catal. Rev.-Sci. Eng. 35 (1993) 129.
[585] A.V. Kucherov, A.A. Slinkin, D.A. Kondratev, T.N. Bondarenko, A.M. Rubinstein, Kh.M. Minachev, Zeolites 5 (1985) 320.
[586] A.V. Kucherov, A.A. Slinkin, Zeolites 6 (1986) 175.
[587] S. deTavernier, R.A. Schoonheydt, Zeolites 11 (1991) 155.
[588] M. Anpo, M. Matsuoka, Y. Shioya, H. Yamashita, E. Giamello, C. Morterra, M. Che, H.H. Patterson, S. Weber, S. Ouellette, M.A. Fox, J. Phys. Chem. 98 (1994) 5744.
[589] A.V. Kucherov, T.N. Kucherova, A.A. Slinkin, Catal. Lett. 10 (1991) 289.
[590] T. Tanabe, T. Iijima, A. Koiwai, J. Mizuno, K. Yokota, A. Isogai, Appl. Catal. B 6 (1995) 145.
[591] A.V. Kucherov, A.A. Slinkin, D.A. Kondratev, T.N. Bondarenko, A.M. Rubinstein, Kh.M. Minachev, Kinet. Katal. 26 (1985) 353.
[592] A.V. Kucherov, J.L. Gerlock, H.W. Jen, M. Shelef, Zeolites 15 (1995) 15.
[593] A.V. Kucherov, J.L. Gerlock, H.W. Jen, M. Shelef, J. Catal. 152 (1995) 63.
[594] A.V. Kucherov, C. Hubbard, M. Shelef, J. Catal. 157 (1995) 603.
[595] A.V. Kucherov, K.I. Slovetskaya, S.S. Goryaschenko, E.G. Aleshin, A.A. Slinkin, Microporous Mater. 7 (1996) 27.
[596] S.L. Larsen, A. Aylor, A.T. Bell, J.A. Reimer, J. Phys. Chem. 98 (1994) 11533.
[597] G.L. Wooley, L.B. Alemany, R.M. Dessau, A.W. Chester, Zeolites 6 (1986) 14.
[598] K.C.C. Kharas, D.-J. Liu, H.J. Robota, Catal. Today 26 (1995) 129.
[599] H. Hamada, N. Matsubayashi, H. Shimada, Y. Kintaichi, T. Ito, A. Nishijima, Catal. Lett. 5 (1990) 189.
[600] D.-J. Liu, H.J. Robota, Prepr. Div. Petrol. Chem., Am. Chem. Soc. 38 (1993) 742.
[601] D.-J. Liu, H.J. Robota, Prepr. Div. Petrol. Chem., Am. Chem. Soc. 39 (1994) 107.
[602] D.-J. Liu, H.J. Robota, Prepr. Div. Petrol. Chem., Am. Chem. Soc. 39 (1994) 175.
[603] D.-J. Liu, H.J. Robota, in: U.S. Ozkan, S.K. Agarwal, G. Marcelin (Eds.), Reduction of Nitrogen Oxide Emissions, ACS Symposium Series, vol. 587, 1995, p. 147.
[604] M. Narayana, S. Contarini, L. Kevan, J. Catal. 94 (1985) 370.
[605] L.P. Haack, M. Shelef, in: J.N. Armor (Ed.), Environmental Catalysis, American Chemical Society, Washington, DC, 1994, p. 66.
[606] J.G. Fripiat, F. Berger-Andre, J. Andre, E.G. Deroune, Zeolites 3 (1983) 306.
[607] J.G. Fripiat, E.G. Deroune, Zeolites 5 (1985) 165.
[608] A. Miyamoto, M. Kubo, in: J.C. Jansen, M. Stocker, H.G. Karge, J. Weitkamp (Eds.), Advanced Zeolite Science and Applications, Studies in Surface Science and Catalysis, vol. 85, Elsevier, Amsterdam, 1994, p. 117.
[609] A. Miyamoto, H. Himei, E. Maruya, M. Katagiri, R. Vetrivel, M. Kubo, in: H. Hattori, M. Misono, Y. Ono (Eds.), Acid–Base Catalysis II, Studies in Surface Science and Catalysis, vol. 90, Elsevier, Amsterdam, 1994, p. 217.
[610] A. Miyamoto, H. Himei, Y. Oka, E. Maruya, M. Katagiri, R. Vetrivel, M. Kubo, Catal. Today 22 (1994) 87.
[611] M. Yamadaye, H. Himei, T. Kanougi, Y. Ouomi, M. Kubo, A. Stirling, R. Vetrivel, E. Brodawik, A. Miyamoto in: H. Chon, S.-K. Ihm, Y.S. Uh (Eds.), Progress in Zeolite and Microporous Materials, Studies in Surface Science and Catalysis, vol. 105, Elsevier, Amsterdam, 1997, p. 1485.
[612] M. Iwamoto, H. Yahiro, N. Mizuno, Nippon Kagaku Kaishi (1991) 574.
[613] D.C. Sayle, C.R.A. Catlow, M.A. Perrin, P. Nortier, J. Chem. Soc., Chem. Commun. (1995) 945.
[614] D.C. Sayle, C.R.A. Catlow, J.D. Gale, M.A. Perrin, P. Nortier, J. Phys. Chem. 101 (1997) 3331.
[615] D.C. Sayle, C.R.A. Catlow, M.A. Perrin, P. Nortier, J. Mater. Chem. 7 (1997) 1635.
[616] D.C. Sayle, C.R.A. Catlow, M.A. Perrin, P. Nortier, J. Mater. Chem. 7 (1997) 1917.
[617] Y. Yokomichi, T. Nakayama, O. Okada, Y. Yokoi, I. Takahashi, H. Uchida, H. Ishikawa, R. Yamaguchi, H. Matsui, T. Yamabe, Catal. Today 29 (1996) 155.
[618] M. Iwamoto, H. Yahiro, N. Mizuno, W.-X. Zhang, Y. Mino, H. Furukawa, S. Kagawa, J. Phys. Chem. 96 (1992) 9360.
[619] J. Valyon, W.K. Hall, in: L. Guczi, F. Solymosi, P. Tetenyi (Eds.), New Frontiers in Catalysis, Proceedings of the 10th International Congress on Catalysis, Budapest, 1992, Akadémi Kiado, Budapest, 1993, p. 1339.
[620] D.J.C. Yates, Catal. Rev. 2 (1968) 113.
[621] Y. Fu, Y. Tian, P. Lin, J. Catal. 132 (1992) 85.
[622] G. Centi, S. Perathoner, Y. Shioya, M. Anpo, Res. Chem. Intermed. 17 (1992) 125.
[623] G. Centi, S. Perathoner, Y. Shioya, M. Anpo, Catal. Today 17 (1993) 159.

[624] C. Marquez-Alvarez, G.S. McDougall, A. Guerrero-Ruiz, I. Rodriguez-Ramos, Appl. Surf. Sci. 78 (1994) 477.
[625] W.K. Hall, J. Valyon, Catal. Lett. 15 (1992) 311.
[626] J. Valyon, W.K. Hall, J. Phys. Chem. 97 (1993) 520.
[627] A.W. Aylor, S.C. Larsen, J.A. Reimer, A.T. Bell, J. Catal. 157 (1995) 592.
[628] V.I. Pârvulescu, P. Grange, B. Delmon et al., J. Phys. Chem. B 101 (1997) 6933.
[629] P. Ciambelli, E. Garufi, R. Pirone, G. Russo, F. Santagata, Appl. Catal. B 8 (1996) 333.
[630] T. Cheung, S.K. Bhargava, M. Hobday, K. Foger, J. Catal. 158 (1996) 301.
[631] Y. Teraoka, H. Fukuda, S. Kagawa, Chem. Lett. (1990) 1.
[632] H. Yasuda, N. Mizuno, M. Misono, J. Chem. Soc., Chem. Commun. (1990) 1094.
[633] L. Forni, C. Oliva, F.P. Vatti, N.A. Sinitsina, S.V. Sorochkin, A.V. Moevard, A.V. Vishniakov, J. Chem. Soc., Faraday Trans. 1 88 (1992) 1041.
[634] Z. Zhao, X. Yang, Y. Wu, Appl. Catal. B 8 (1996) 281.
[635] S. Shin, Y. Hatakeyame, K. Ogawa, K. Shimomura, Mat. Res. Bull. 14 (1975) 133.
[636] H. Shimada, S. Miyama, H. Kuroda, Chem. Lett. (1988) 1797.
[637] A. Ogata, A. Obuchi, K. Mizuno, A. Ohi, H. Ohuchi, J. Catal. 144 (1993) 452.
[638] J. Lin, A.T.S. Wee, K. Lee Tan, K.G. Neoh, W.K. Teo, Inorg. Chem. 32 (1993) 5522.
[639] H. Komiyama, F. Ohue, T. Kanai, A. Hayashi, Y. Yamaguchi, M. Funakoshi, H. Inoue, Kagaku Kogaku 47 (1983) 41.
[640] S. Pancharatnam, R.A. Huggins, D. Mason, J. Electrochem. Soc. 127 (1975) 869.
[641] T.M. Gur, R.A. Huggins, J. Electrochem. Soc. 129 (1979) 1067.
[642] B.G. Ong, C.G. Chiang, D.M. Mason, Sol. St. Ionics 314 (1981) 447.
[643] B.C. Nguyen, T.A. Lin, D.M. Mason, J. Electrochem. Soc. 133 (1986) 1804.
[644] D.C. Cicero, L.A. Jan, Sep. Sci. Technol. 25 (1990) 1455.
[645] K. Tomishige et al., Chem. Lett. (1994) 34.